AD-A071 715 AIR FORCE FLIGHT DYNAMICS LAB WRIGHT-PATTERSON AFB OH F/G 1/3
SKIN AND SPAR INTERFACE PROGRAM (SASIP).(U)
MAY 79 A GONSISKA, R T ACHARD

UNCLASSIFIED AFFDL-TR-79-3054 NL

1 OF 2
AD A071715

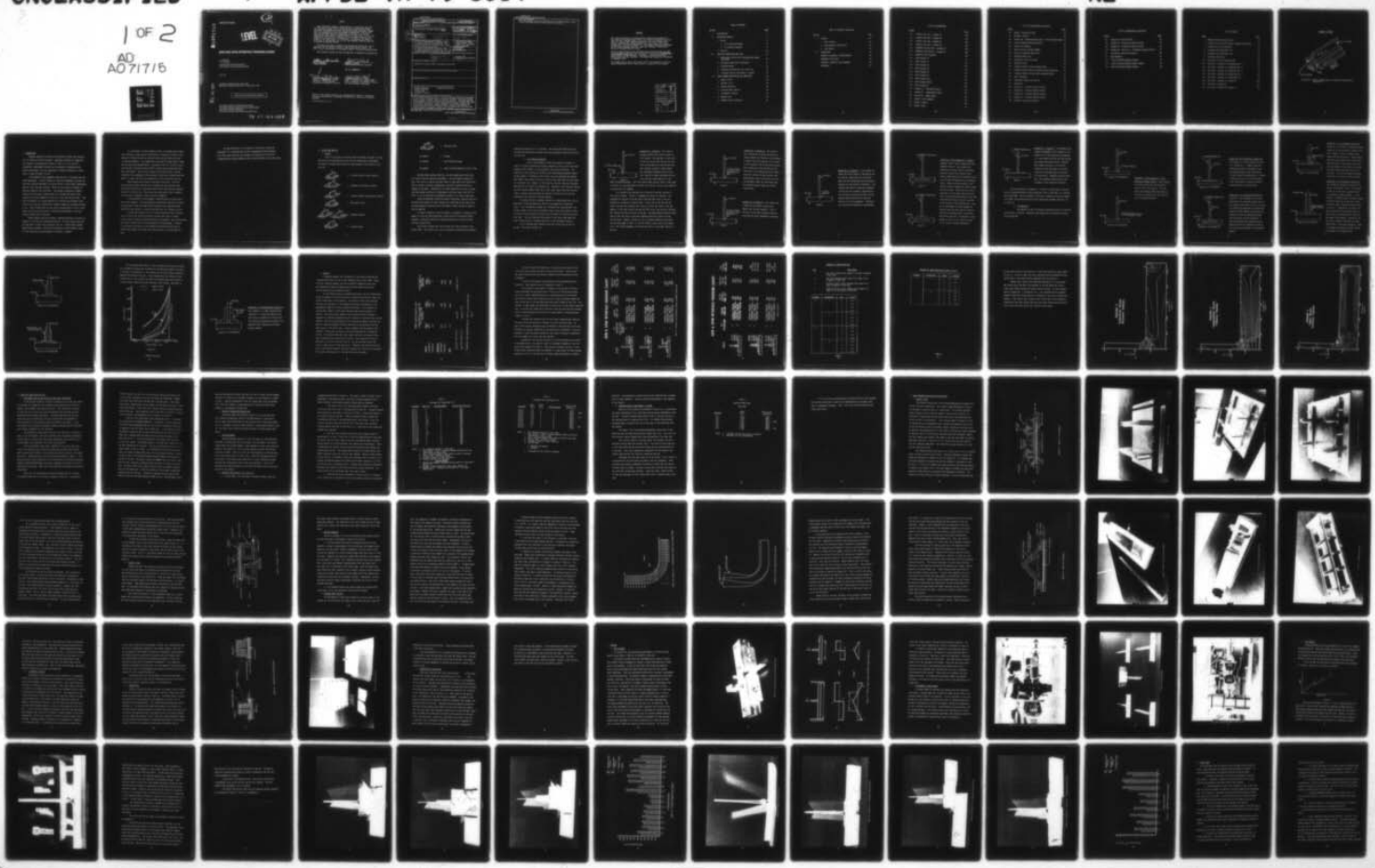

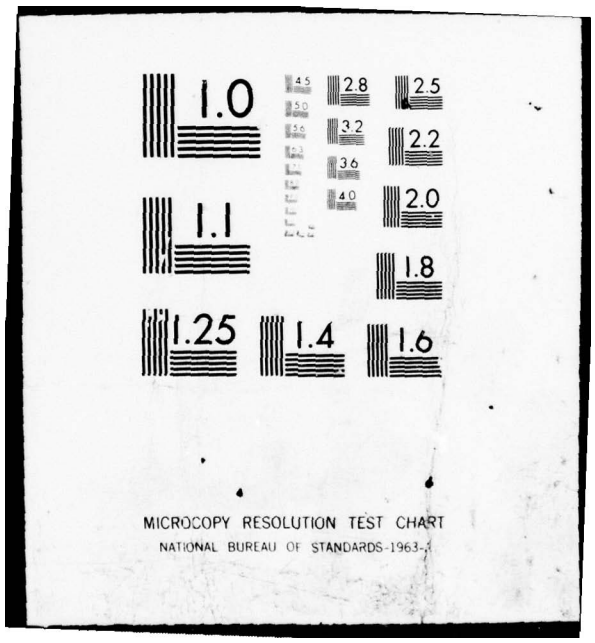
1.0
1.1
1.25
1.4
1.6
1.8
2.0
2.2
2.5
2.8
3.2
3.6
4.0
4.5
5.0
5.6
MICROCOPY RESOLUTION TEST CHART
NATIONAL BUREAU OF STANDARDS-1963-A

AFFDL-TR-79-3054

LEVEL II

SKIN AND SPAR INTERFACE PROGRAM (SASIP)

A. GONSISKA
R. T. ACHARD
STRUCTURAL CONCEPTS BRANCH
STRUCTURES AND DYNAMICS DIVISION

May 1979

TECHNICAL REPORT AFFDL-TR-79-3054
Final Report for Period 20 June 1975 – 29 September 1978

Approved for public release; distribution unlimited.

AIR FORCE FLIGHT DYNAMICS LABORATORY
AIR FORCE WRIGHT AERONAUTICAL LABORATORIES
AIR FORCE SYSTEMS COMMAND
WRIGHT-PATTERSON AIR FORCE BASE, OHIO 45433

NOTICE

When Government drawings, specifications, or other data are used for any purpose other than in connection with a definitely related Government procurement operation, the United States Government thereby incurs no responsibility nor any obligation whatsoever; and the fact that the Government may have formulated, furnished, or in any way supplied the said drawings, specifications, or other data, is not to be regarded by implication or otherwise as in any manner licensing the holder or any other person or corporation, or conveying any rights or permission to manufacture, use, or sell any patented invention that may in any way be related thereto.

This report has been reviewed by the Information Office (IO) and is releasable to the National Technical Information Service (NTIS). At NTIS, it will be available to the general public, including foreign nations.

This technical report has been reviewed and is approved for publication.

Allen Gonsiska
ALLEN GONSISKA
Project Engineer

Robert T. Achard
ROBERT T. ACHARD
Manufacturing and Test Engineer

FOR THE COMMANDER

FRANCIS J. JANIK, JR., Chief
Structural Concepts Branch
Structures and Dynamics Division

RALPH L. KUSTER, JR., Colonel, USAF
Chief, Structures and Dynamics Division
AF Flight Dynamics Laboratory

Copies of this report should not be returned unless return is required by security considerations, contractual obligations, or notice on a specific document.

AIR FORCE/56780/5 July 1979 — 140

Unclassified

SECURITY CLASSIFICATION OF THIS PAGE *(When Data Entered)*

REPORT DOCUMENTATION PAGE

READ INSTRUCTIONS BEFORE COMPLETING FORM

1. REPORT NUMBER: AFFDL-TR-79-3054	2. GOVT ACCESSION NO.
3. RECIPIENT'S CATALOG NUMBER	
4. TITLE *(and Subtitle)*: Skin and Spar Interface Program (SASIP).	5. TYPE OF REPORT & PERIOD COVERED: Final Technical Report - 20 June 1975 - 29 Sep 1978
6. PERFORMING ORG. REPORT NUMBER	
7. AUTHOR(s): Allen R. Gonsiska, Richard T. Achard	8. CONTRACT OR GRANT NUMBER(s): 17 03 / 16 2401
9. PERFORMING ORGANIZATION NAME AND ADDRESS: Air Force Flight Dynamics Laboratory (FBSA), AF Wright Aeronautical Laboratories, AFSC, Wright-Patterson Air Force Base, Ohio 45433	10. PROGRAM ELEMENT, PROJECT, TASK AREA & WORK UNIT NUMBERS: Program Element 62222F, Project 2401, Task 240103, Work Unit 24010320
11. CONTROLLING OFFICE NAME AND ADDRESS: Air Force Flight Dynamics Laboratory (FB), AF Wright Aeronautical Laboratories, AFSC, Wright-Patterson Air Force Base, Ohio 45433	12. REPORT DATE: May 1979 / 13. NUMBER OF PAGES
14. MONITORING AGENCY NAME & ADDRESS *(if different from Controlling Office)*: 12 131p	15. SECURITY CLASS. *(of this report)*: Unclassified / 15a. DECLASSIFICATION/DOWNGRADING SCHEDULE

16. DISTRIBUTION STATEMENT *(of this Report)*

Approved for public release; distribution unlimited.

17. DISTRIBUTION STATEMENT *(of the abstract entered in Block 20, if different from Report)*

18. SUPPLEMENTARY NOTES

19. KEY WORDS *(Continue on reverse side if necessary and identify by block number)*

Advanced Composites
Integral Skin/Spar
Aircraft Wing
Elastomeric Tooling
Composite Fabrication

20. ABSTRACT *(Continue on reverse side if necessary and identify by block number)*

This program had two basic goals. First was the investigation of the effects of fuel pressure (flatwise tension) loads and chordwise (transverse tension) loads on several integral composite skin/spar concepts. The second goal was the development of suitable tooling which could be used to produce these types of structural components. Several concepts were designed, produced, and tested under the required loading conditions. Results indicated that a) integral composite skin/spar concepts could be manufactured using hard autoclave tooling or elastomeric tooling and b) concepts could be designed to

Over

DD FORM 1 JAN 73 1473 EDITION OF 1 NOV 65 IS OBSOLETE

Unclassified

SECURITY CLASSIFICATION OF THIS PAGE *(When Data Entered)*

012 070

Block 20 Continued
carry the required loads, provided some type of coupling device is used to help distribute the loads from the spar to the skin.

FOREWORD

This report describes an in-house effort conducted by personnel of the Structural Concepts Branch (FBS), Structures and Dynamics Division (FB), Air Force Flight Dynamics Laboratory, Air Force Wright Aeronautical Laboratories, Wright-Patterson Air Force Base, Ohio, under Project 2401, "Structural Mechanics", Task 240103, "Advanced Structures for Military Aerospace Vehicles", Work Unit 24010320, "Preliminary Design of Advanced Wing Structures."

The work reported herein was performed during the period 20 June 1975 to 29 September 1978 under the direction of the authors, Allen Gonsiska (AFFDL/FBSA), Project Engineer, and Robert T. Achard (AFFDL/FBSC), Manufacturing and Test Engineer. The report was released by the authors in September 1978.

The authors wish to thank the entire staff of the Composites Facility Group (AFFDL/FBSC) for all their effort in support of this program.

TABLE OF CONTENTS

TABLE OF CONTENTS (Continued)

LIST OF ILLUSTRATIONS

LIST OF ILLUSTRATIONS (Continued)

LIST OF ILLUSTRATIONS (Continued)

LIST OF TABLES

GLOSSARY OF TERMS

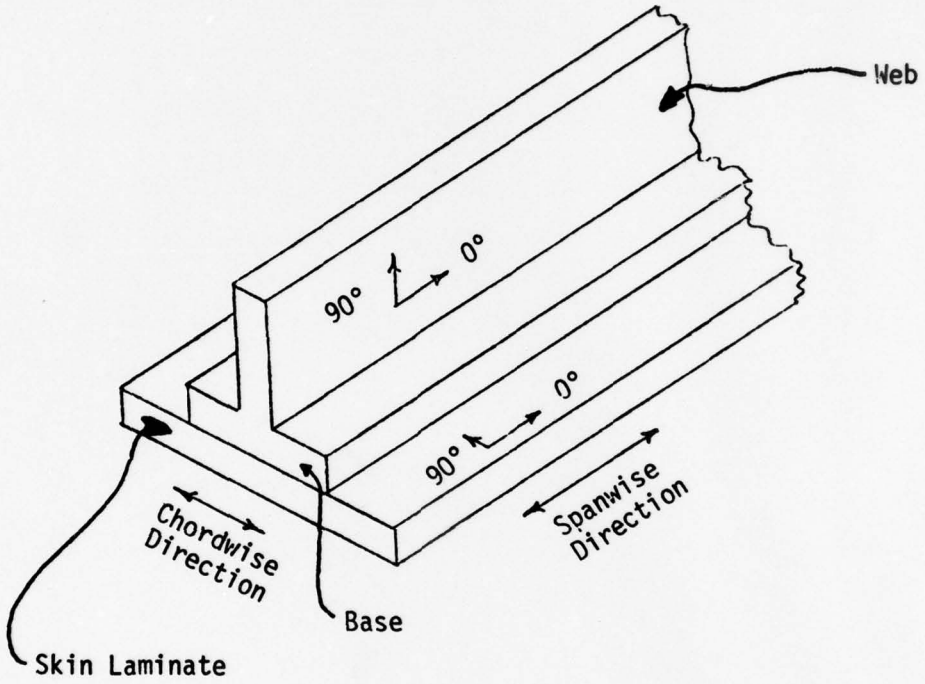

Tee Section - Entire specimen which is basically shaped like an inverted "T".

I INTRODUCTION

Advanced composite structures are beginning to make their presence felt in military aircraft airframes. Empennage structures of composites are already in the production versions of the F-14, F-15, and F-16. Furthermore, development programs are now underway to demonstrate the weight, performance, and cost advantages of advanced composites in other areas of these and other aircraft.

A few composite wing components have been built, and others are now under development. A major drawback to these wing components has been the fact that they were designed to be quite similar to their metal counterparts. However, there has been proposed a family of new structural concepts for advanced composite wing structures. The concepts proposed are integral wing-skin-to-wing-spar concepts which will eliminate the need to have separate structural elements for wing skins, spar caps and spar webs. They have the potential to provide extensive cost savings and increased reliability, even over the "conventional" advanced composite structures designed so far. They eliminate the cost and stress concentrations of bolts in the lower wing skin and also result in significant improvements in the fuel sealant capabilities of the wing.

These integral spar/skin concepts, although promising, do involve an element of risk over the conventional designs. For this reason, they have not been used in actual wing structures thus far. Before these concepts become widely accepted, a detailed investigation of their behavior under all load conditions and environmental conditions is needed.

As a forerunner to these extensive tests, an in-house test program was initiated to study some of the effects of variations in terms of the method of forming the spar cap and spar web by using either skin plies or separate elements. This program was envisioned to study effects rather than to obtain the optimum design. Therefore, with this in mind, various Skin and Spar Interface Program (SASIP) concepts were designed and specimens constructed. These various concepts were modifications, with the exception of the embedded titanium concept, to the basic concept where the upper, or inner, skin plies are wrapped up at 90° to form the spar web.

These concepts were tested in two major directions. The first direction was flatwise tension which simulated the fuel pressure load. The second direction was transverse tension which simulates the chordwise tension in the wing skin. These tests were performed on small component tee sections as opposed to large structural assemblies.

A limited amount of environmental conditioning was accomplished on two of the concepts. This environmental conditioning consisted of soaking the specimens at 180°F and 92% relative humidity until specimen weight equilibrium was achieved. Selected specimens were also thermally cycled.

A second major feature of this in-house program was the investigation of some of the tooling required to produce this type of concept. Various types of tooling, ranging from hard to elastomeric, were investigated. Each type of tooling has its own advantages and disadvantages. However, it was shown, that after all the problems associated with each type of tooling and concept are solved, high quality parts can be obtained with each.

The data generated in this program is sufficient to form the groundwork for a more detailed and more comprehensive design program. This effort does show that the concepts are feasible and if carried through detailed design probably could be used favorably in aircraft wings.

II DESIGN AND ANALYSIS

1. DESIGN

Prior to any design or analysis being performed, the types of loads which were to be encountered by this type of concept were investigated. The types of loadings which should be investigated in any program of this type are:

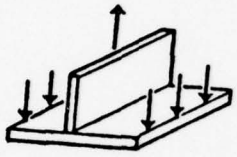

a. Flatwise Tension (Fuel Pressure)

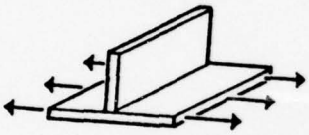

b. Chordwise (Transverse) Tension

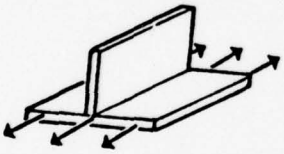

c. Primary Bending (Longitudinal) Tension

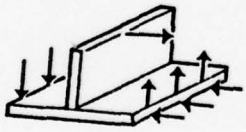

d. Web Lateral Load

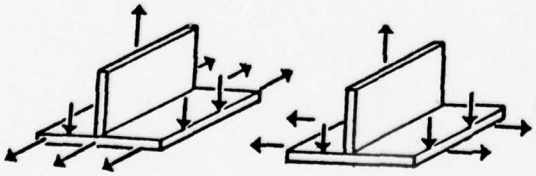

e. Combined Loading

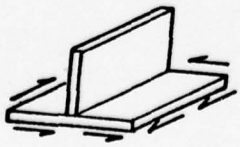

f. In-plane Shear

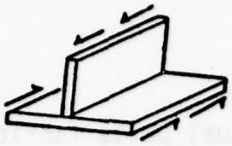

g. Spar/skin Shear

No example h. Fatigue

No example i. Fuel Pressure Fatigue

No example j. Impact (Foreign Object) at base of tee

Besides these loading conditions, the environment which this joint will have to survive should be considered. This environment consists of fuel, JP-4, JP-5, or any of the other types of fuels which can currently be used in military aircraft, condensation, and other residuals which are trapped in the tanks. Combining all of these potentially corrosive liquids with the extreme variations in temperature, which may range from -65°F to 270°F, it can be seen that environmental testing is of a major importance.

These environmental conditions become increasingly important when one considers that several of these concepts are controlled by the items which are most adversely affected by the environment, namely the matrix material and the adhesive.

In order to determine realistic design requirements in regards to the number of plies and the orientation of these plies for the various SASIP concepts, a baseline aircraft was selected along with a location on that baseline aircraft wing.

Two aircraft, namely the F-111 and the F-16, were involved in this design study. The initial work, such as preliminary tooling and preliminary

designs were based on an F-111 design. The actual parts fabrication and testing were performed on concepts which were designed to meet the criteria for the F-16.

a. F-111 Baseline Designs

Since a large amount of data was currently available on the F-111 aircraft (studies were being conducted on this aircraft for other programs within AFFDL), it was selected as the original baseline. The selection of the location on the wing to be investigated presented another unique problem. A location at the root of the wing contained the highest skin loads in the plane of the skin, while on the other hand the fuel loads are relatively low. However, at the wing tip, the fuel loads are extremely high but the skin loads are extremely low. Therefore, since the main concern was the flatwise tension loads due to fuel loads rather than high in-plane loads, a station which was about two thirds of the way out the wing was selected as the location for design purposes.

The design for this location resulted in a design which had a 40 ply base and a 10 ply web made up of 60% 0° plies (spanwise) and 40% $\pm$45° plies. As an alternative, another ply orientation was selected which contained a number of 90° plies (chordwise) close to the skin surface to help in carrying the fuel pressure loads and to also help in carrying the chordwise loads. The fuel pressure loads result in the skins, both upper and lower, being placed in a bending condition in the chordwise direction.

A set of designs were selected using this 40 ply base and the 10 ply web. The select designs are:

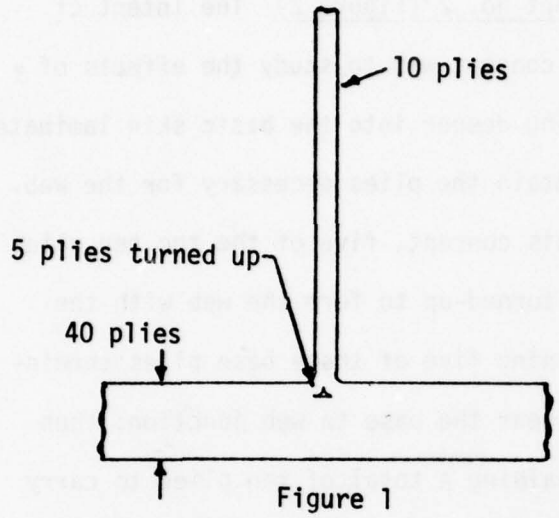

Figure 1

Concept No. 1 (Figure 1) This type of concept portrays the original intent of this program. The spar web is truly part of the skin plies since the top five skin plies are turned-up to form the spar web. This concept, although it does reduce the continuous chordwise plies by five, still results in more continuous plies to carry the skin loads than any of the other following concepts. The first double angle tooling, which is described in Section III, was developed to produce this concept, and was later modified to accept the F-16 concepts.

This concept also displayed one of the basic problems involved in this type of design: the web is unsymmetrical about its midplane. The unsymmetrical aspects of the web result when the $\pm$45° plies in the skin laminate are turned-up to form the web. On one side of the web the +45° plies, from the skin laminate, will turn-up to form +45° plies in the web. However, on the other side of the web the +45° plies, from the skin laminate, will turn-up to form -45° plies in the web. The same problem naturally holds true for the -45° plies in the skin laminate which also turn-up to form the web plies. However, the web is still a balanced laminate since there are the same number of $\pm$45°, 0°, and 90° lamina on each side of the center-line. The slight unsymmetry in the web did result in very small twists in the web.

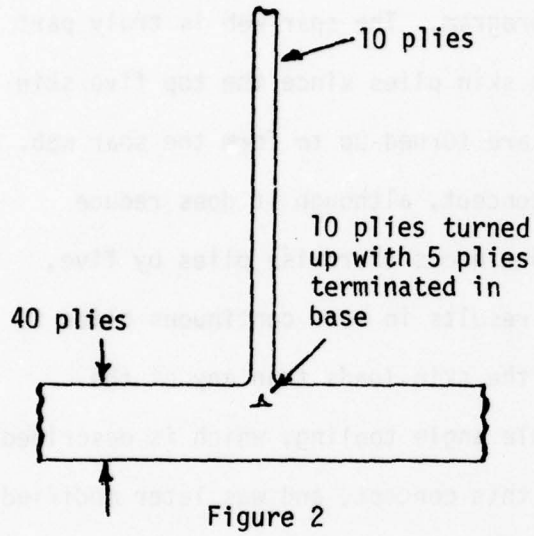

Figure 2

Concept No. 2 (Figure 2) The intent of this concept was to study the effects of digging deeper into the basic skin laminate to obtain the plies necessary for the web. In this concept, five of the top ten plies were turned-up to form the web with the remaining five of these base plies terminated near the base to web junction; thus maintaining a total of ten plies to carry the chordwise loads, but the effect upon the flatwise tension loads was of main concern here.

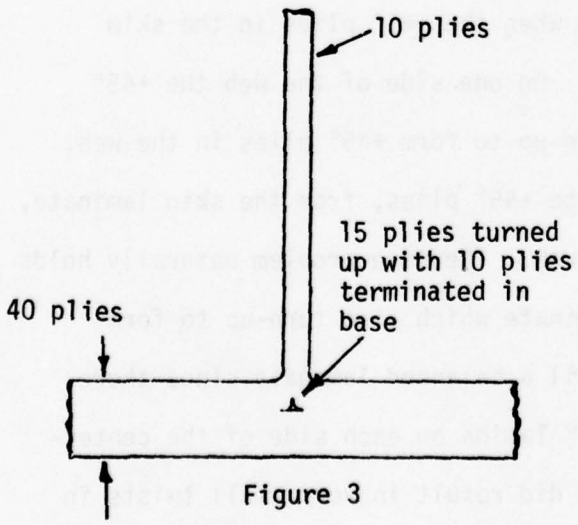

Figure 3

Concept No. 3 (Figure 3) This concept was a study of the effects of going even deeper into the base laminate. Five of the top 15 plies were turned-up with the remaining ten plies terminated in the base.

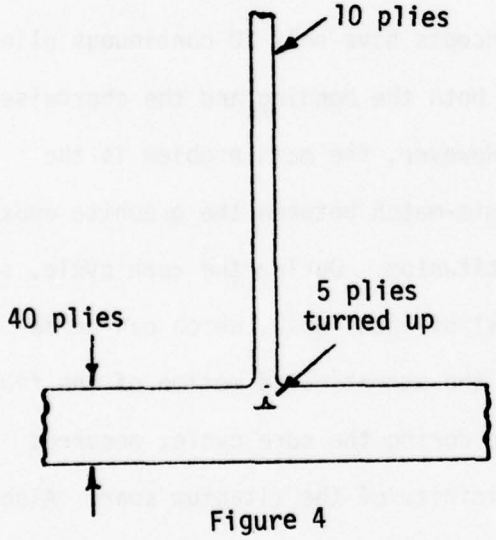

Figure 4

Concept No. 4 (Figure 4) In an attempt to reduce the strain levels in the base of the tee section, additional skin plies were added and the orientations were drastically changed over the baseline orientation. The laminate described in Figure C4 of Appendix C would not have produced a theoretically good laminate, but was consistent with the program purpose which was to study the effects of various parameters. Therefore, this lamination schedule was investigated.

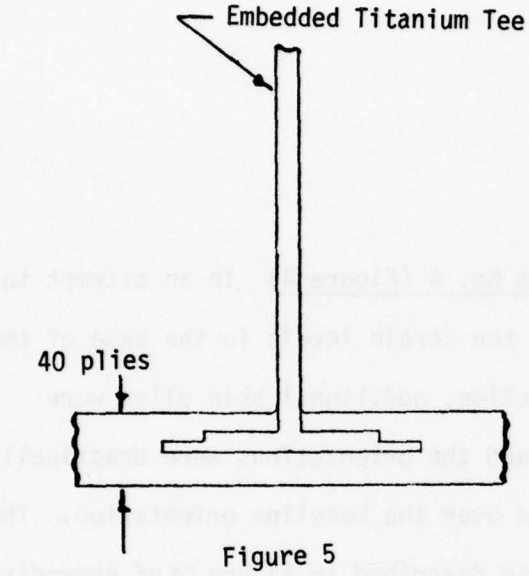

Figure 5

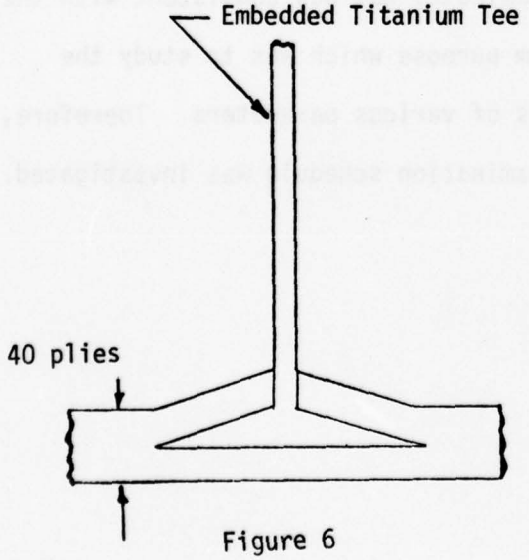

Figure 6

Concept No. 5 and Concept No. 6 (Figures 5 and 6) Both of these concepts deal with embedded titanium. Both concepts are essentially the same, the only difference being the shape of the titanium insert. These concepts have only 20 continuous plies to carry both the bending and the chordwise loads. However, the main problem is the thermal mis-match between the graphite epoxy and the titanium. During the cure cycle, a great deal of local wash, which can be defined as the uncontrolled motion of the fiber direction during the cure cycle, occurred in the vicinity of the titanium spar. Also, due to the thermal mis-match between the graphite epoxy and the titanium, stresses were built-up between these two materials during the cure cycle. During NDI, a large number of voids are also typically found in this type of concept (Reference 1).

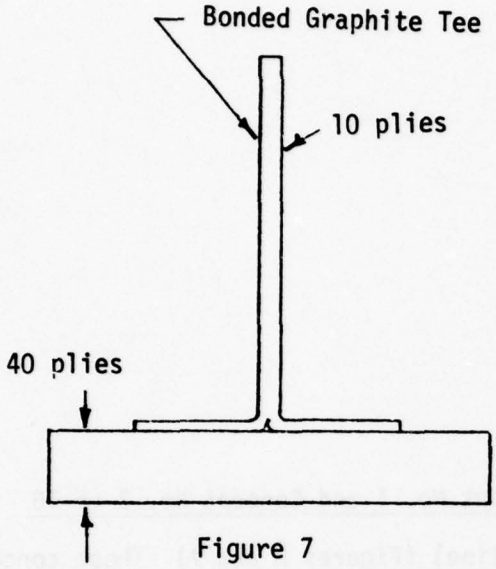

Figure 7

Concept No. 7 (Figure 7) The bonded-on tee concept represented in this drawing is the opposite end of the spectrum from Concepts 1, 2, and 3 where the plies to form the tee were taken from within the skin laminate. This concept utilizes all of the skin laminate to carry the loads in the skin rather than interrupt some of the plies to form the tee. Therefore, based on this fact, this concept should be one of the strongest in the transverse direction.

With the exception of Concept No. 1, which was fabricated for the purpose of uncovering possible tooling problems, none of the other F-111 designs were fabricated. Due to a change in direction, dictated by relevant programs with AFFDL, the design baseline for this program was changed from the F-111 to the F-16.

b. F-16 Baseline

The designs for the F-16 baseline required 56 plies in the skin and 28 plies in the web. Therefore, the concepts were re-worked to satisfy the new baseline.

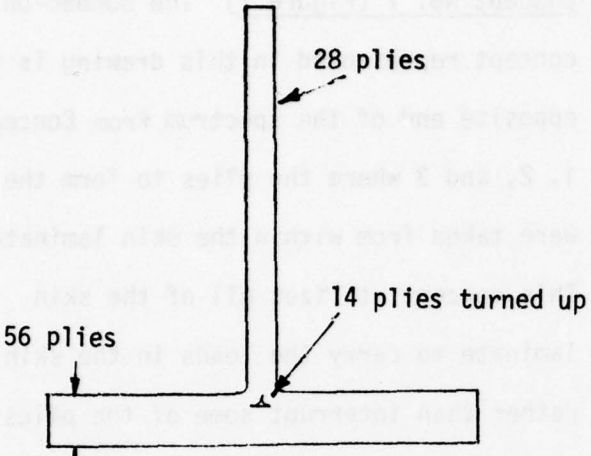

Figure 8 (F-16 Baseline)

Concept No. 1 and Concept No. 2 (F-16 Baseline) (Figures 8 and 9) These concepts are direct transitions from Concept No. 1 and 2 of the F-111 baseline. The drawbacks and advantages which were observed on the F-111 concepts still hold true for the F-16 baseline concepts.

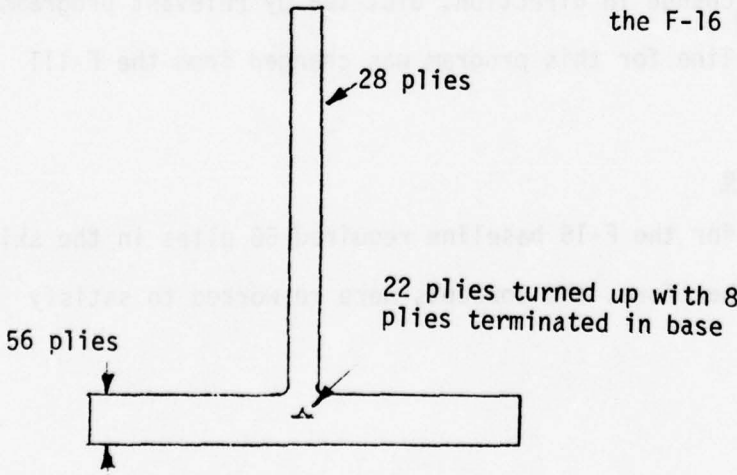

Figure 9 (F-16 Baseline)

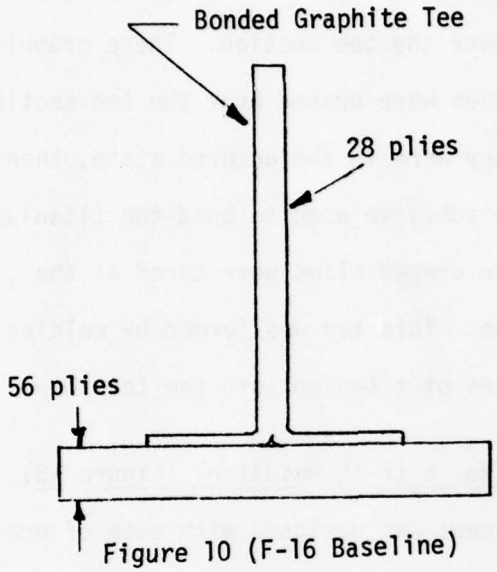

Figure 10 (F-16 Baseline)

Concept No. 3 (F-16 Baseline) (Figure 10)

This concept is a direct transition of the F-111 Concept No. 7. However, when this concept was actually constructed, it was not produced exactly as per the drawing in order to ease the manufacturing. Instead of making the tee as a co-cured assembly, it was fabricated by secondarily bonding precured angles to a precured base.

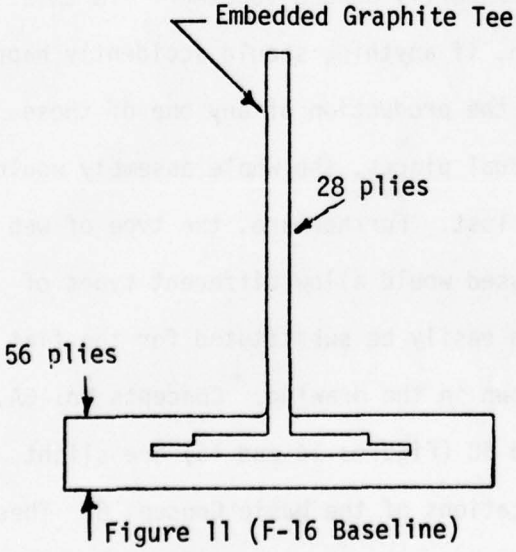

Figure 11 (F-16 Baseline)

Concept No. 4 (F-16 Baseline) (Figure 11)

Concept No. 4 was intended to be a direct substitution of a precured graphite tee for the stepped titanium tee in the F-111 design. This concept was conceived to eliminate the thermal mis-match between the graphite and titanium, but was not constructed, based upon the results from the Concept No. 2 tests, which showed that terminating plies within the basic skin laminate in order to form the spar web resulted in a much weaker concept.

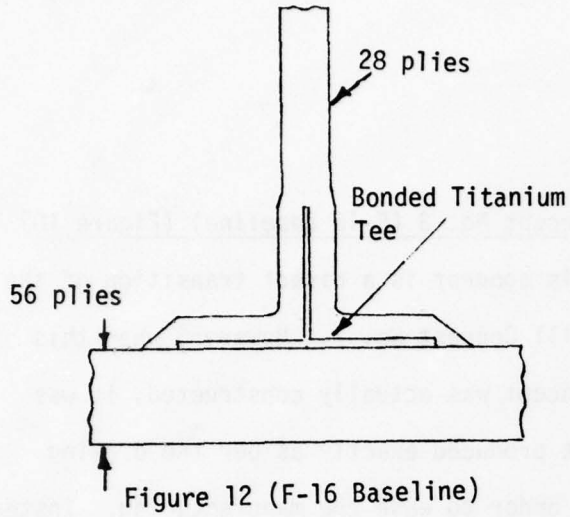

Figure 12 (F-16 Baseline)

Concept No. 5 (F-16 Baseline) (Figure 12)

Concept No. 5 involved a titanium tee section bonded on to a pre-cured base laminate along with a number of plies of graphite epoxy draped over the tee section. These graphite epoxy plies were draped over the tee section while they were in the uncured state, then both the adhesive used to bond the titanium and these draped plies were cured at the same time. This tee was formed by welding two pieces of titanium into the tee shape.

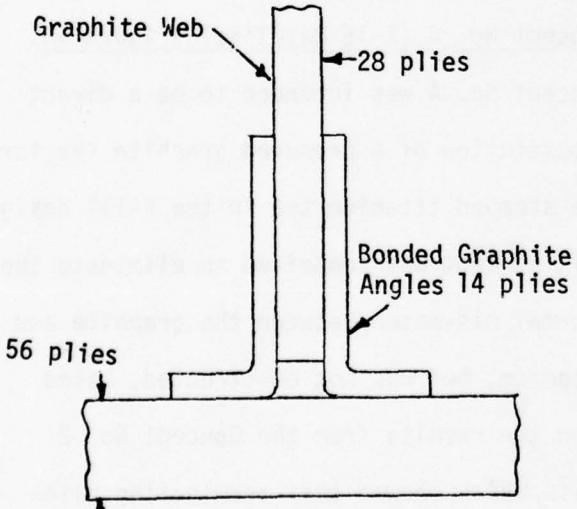

Figure 13 (F-16 Baseline)

Concept No. 6 (F-16 Baseline) (Figure 13)

This concept was designed with ease of production and assembly in mind. This concept is made up of four basic components which are secondarily bonded together. In this fashion, if anything should accidently happen during the production of any one of these individual pieces, the whole assembly would not be lost. Furthermore, the type of web being used would allow different types of webs to easily be substituted for the flat web shown in the drawing. Concepts No. 6A, 6B, and 6C (Figures 14 and 15) are slight modifications of the basic Concept 6. These are attempts at reducing the peel stresses at the edge of the bonded-on tee.

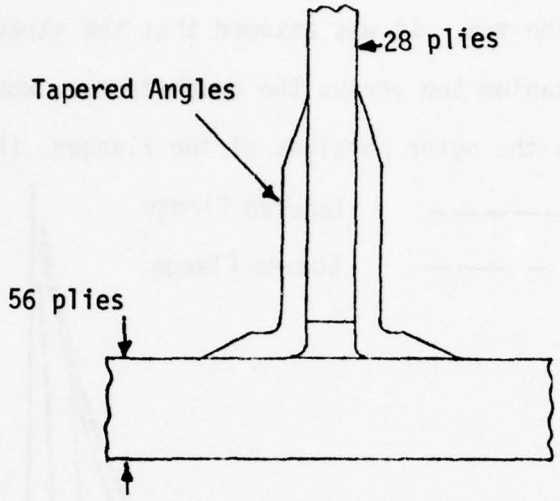

Figure 14 (F-16 Baseline)

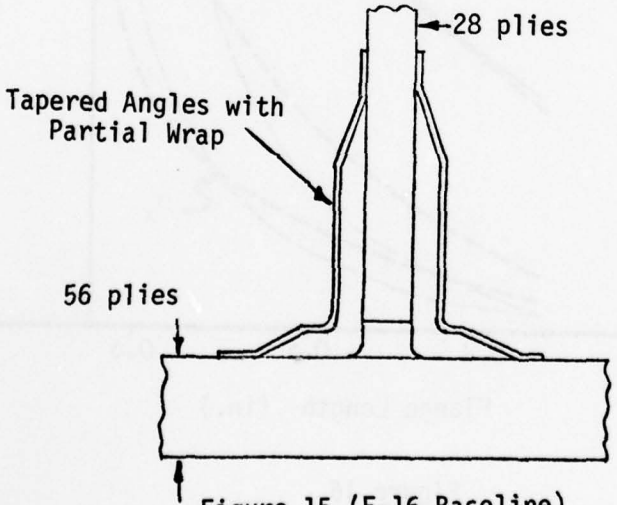

Figure 15 (F-16 Baseline)

As can be seen from Figure 16, which represents the bondline stresses for a bonded-on titanium tee as opposed to the bonded-on graphite tee which is the case for Concept No. 6, the stresses can be significantly reduced by tapering the flange of the tee. It was assumed that the stresses of both systems, that is the titanium tee versus the graphite tee, would behave in a similar manner towards the outer portions of the flanges. (Reference 3)

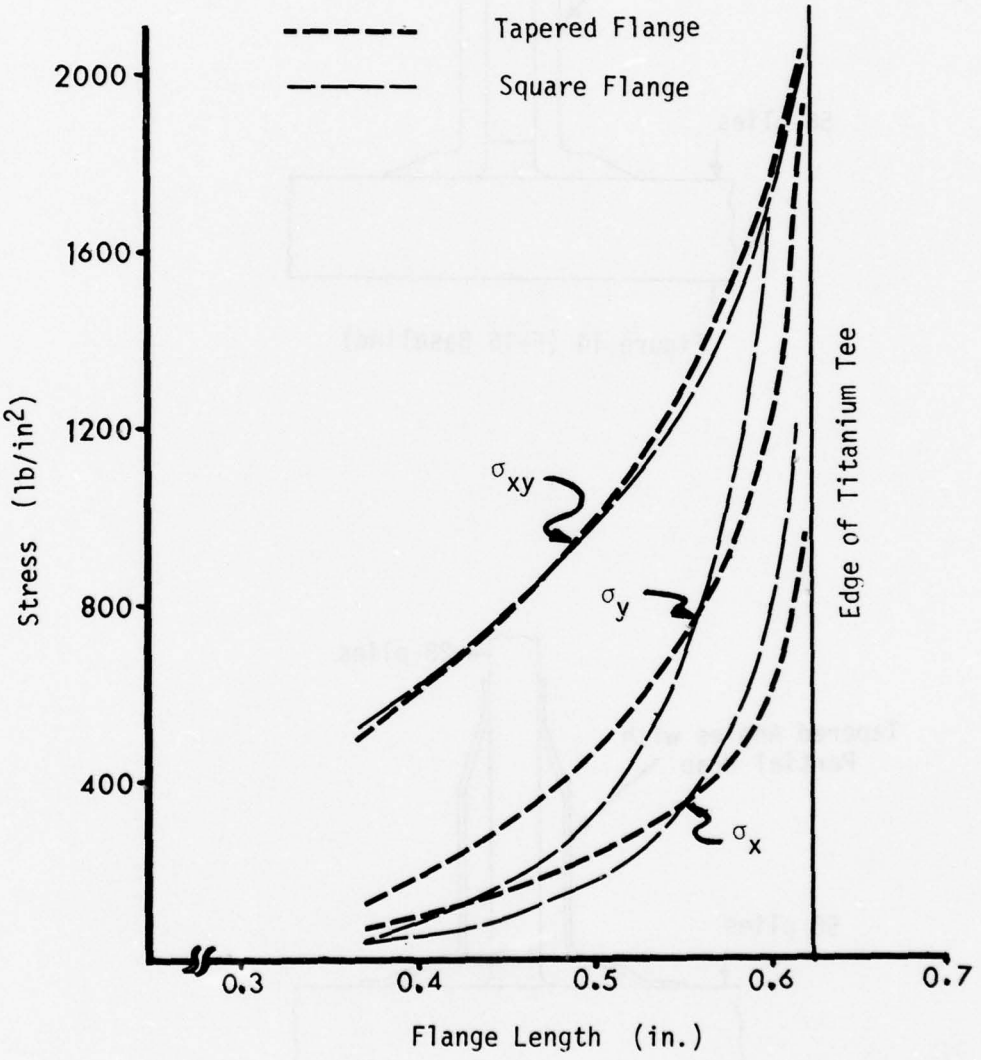

Figure 16

Bondline Stresses

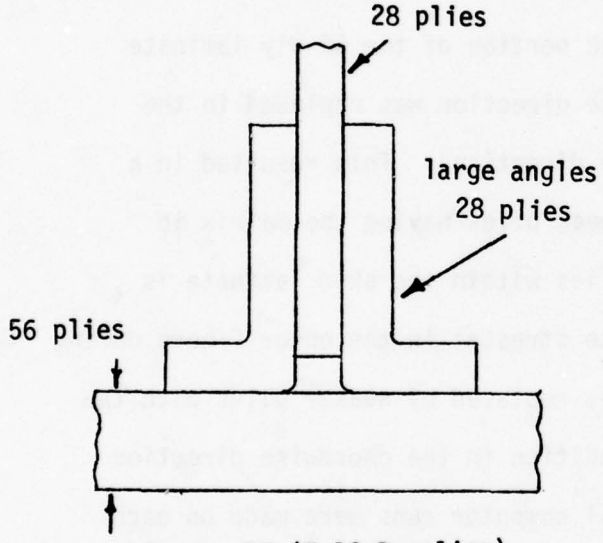

Figure 17 (F-16 Baseline)

Concept No. 7 (F-16 Baseline) (Figure 17)

This concept is a slight variation from Concept No. 6 in that the angles are 28 plies thick as opposed to 14 plies thick. This concept was designed to achieve less bending in the flange during flatwise tension loading.

2. Analysis

A computer program, SQ-5 (Reference 2), was used to generate the strength predictions for the various laminates used in this study. Along with this computer program, two sets of material properties were used, one representing design allowables and the other predicting failure. These allowables are presented in Table 1.

For the flatwise tension strength predictions, the skin laminate was placed in bending as would be the actual condition which the skin would see during loading due to fuel pressure. The portion of the 56 ply laminate which was not continuous in the chordwise direction was replaced in the mathematical model by 0° plies (spanwise direction). This resulted in a correct total number of plies with the weak plies having the matrix in tension. The correct total number of plies within the skin laminate is important to simulate reasonably accurate stresses in the outer fibers during bending. Having the non-continuous plies replaced by weaker plies with the matrix in tension simulates the weak condition in the chordwise direction which occurs in the fillet area. Several computer runs were made on each laminate. During each run the ply with the minimum margin of safety was failed. It should be noted that even though individual plies were failed, total laminate failure had not yet occurred. Total laminate failure was defined as a failure of the 90° plies or, for the laminates with no 90° plies, a shear failure in the $\pm$45° plies. Therefore, the failed plies were given a new material property with zero strength and a new SQ-5 run was made. This process continued until a defined failure was achieved.

NARMCO 5208/T300 GRAPHITE EPOXY

	DESIGN PROPERTIES @ ROOM TEMP FOR F-16 WING DESIGN (ULTIMATE)		FAILURE PREDICTION PROPERTIES (ROOM TEMP)
TENSION	STRESS ksi	STRAIN μ in./in.	STRAIN μ in./in.
Longitudinal	83.2	4000	9762
Transverse	9.3	6344	*
COMPRESSION			
Longitudinal	83.2	-4000	13200
Transverse	16.2	-11000	13230
SHEAR	9.4	18000	19000

$E_{11}=20.8 \times 10^6$ lb./in.^{2} $\quad \nu_{12}=0.30$ $\quad \rho=0.058$ lb./in.^{3}

$E_{22}=1.46 \times 10^6$ lb./in.^{2} $\quad G_{12}=0.56 \times 10^6$

* Transverse strain properties were not used for failure predictions.

Table 1

Two sets of material properties, as used during the design of the F-16, were used to obtain design and failure predictions. Table 2 shows the values obtained using the design allowables and the predicted failure allowables.

A similar SQ-5 analysis was performed for the transverse tension direction. These results are also presented in Table 2.

As discussed in more detail in Chapter V, the testing of flatwise tension specimens was performed using a fixture which forced the specimen to act as a simply supported beam with a concentrated load at the center. The spacing of these simple supports was set so that the bending moment and shear at the base of the web would match the actual loading on the F-16. This spacing, or gage length, was determined to be 2.67 in. for the simply supported case. A similar test condition at the base of the web could also be produced using a fixed-fixed beam simulation with a gage length, or distance between clamps, of 5.33 in.

A concern was expressed that for the simply supported test condition the test section did not have a constant EI across its entire span. The small fillet section essentially has a different EI than the rest of the span. Therefore, an analysis (Reference 3) was performed to see whether it would be necessary to vary the support spacing for each type of concept to compensate for this change in EI across the test specimen.

Essentially, this analysis looked at a fixed-fixed beam with variable EI characteristics. The analysis itself is presented in Appendix A and the results are presented in Table 3. These results represent the error in predicted failure load which would be obtained if a gage length (distance between supports) of 2.67 in. was used for all simply supported concepts as opposed

SKIN & SPAR INTERFACE PROGRAM (SASIP)

DESIGN	PLY ORIENTATION	LOADING CONDITION	DESIGN ALLOWABLE LOAD (LBS)	PREDICTED FAILURE LOAD (LBS)	TEST FAILURE LOAD (LBS)
	REFER TO DETAIL DRAWINGS IN APPENDIX C				
 14 PLIES TURNED-UP	2	FLATWISE TENSION	294	533	542
		TRANSVERSE TENSION	2698	2828	6152
	3	FLATWISE TENSION	172	574	489
		TRANSVERSE TENSION	2828	3621	7353
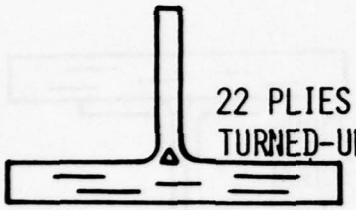 22 PLIES TURNED-UP	2	FLATWISE TENSION	137	337	254
		TRANSVERSE TENSION	1673	2536	4698
	3	FLATWISE TENSION	94	313	330
		TRANSVERSE TENSION	1858	2455	5145
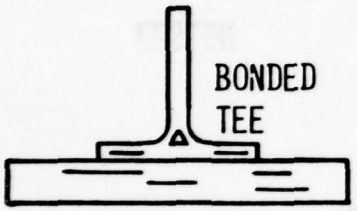 BONDED TEE	2	FLATWISE TENSION	666	1073	774
		TRANSVERSE TENSION	4267	5559	8779
	3	FLATWISE TENSION	508	1683	879
		TRANSVERSE TENSION	6422	8425	11679

Table 2 - Flatwise and Transverse Tension Strength Predictions

SKIN & SPAR INTERFACE PROGRAM (SASIP)

DESIGN	PLY ORIENTATION	LOADING CONDITION	DESIGN ALLOWABLE LOAD (LBS)	PREDICTED FAILURE LOAD (LBS)	TEST FAILURE LOAD (LBS)
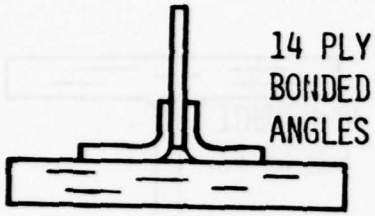 14 PLY BONDED ANGLES	1	FLATWISE TENSION	508	1683	940
		TRANSVERSE TENSION	4267	5559	9830
	2	FLATWISE TENSION	666	1073	669
		TRANSVERSE TENSION	6422	8425	8574
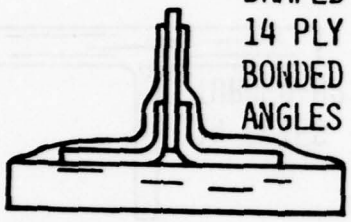 DRAPED 14 PLY BONDED ANGLES	1	FLATWISE TENSION	474	1571	879
		TRANSVERSE TENSION	3636	7626	NOT TESTED
	2	FLATWISE TENSION	546	1008	NOT TESTED
		TRANSVERSE TENSION	3846	4875	NOT TESTED
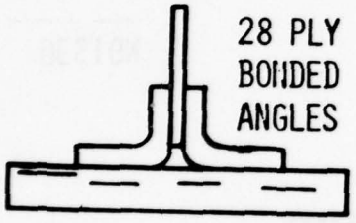 28 PLY BONDED ANGLES	1	FLATWISE TENSION	416	1376	NOT TESTED
		TRANSVERSE TENSION	4267	5559	NOT TESTED
	2	FLATWISE TENSION	468	929	555
		TRANSVERSE TENSION	6422	8425	NOT TESTED

Table 2 (Con't)

VARIABLE EI ERROR PREDICTION

Case	Description
1	Full skin laminate with change in EI under triangular fillet area.
2	Full skin laminate with change in EI under 1/2 of triangular fillet area.
3	Failed 0° plies in skin laminate with change in EI under triangular fillet area.
4	Failed 0° plies in skin laminate with change in EI under 1/2 of triangular fillet area.

Concept	Orientation	Case	% Error
1	1	1	4.0
		2	-1.6
		3	6.0
		4	-0.6
	2	1	2.7
		2	-2.2
		3	5.6
		4	-0.8
2	1	1	4.3
		2	-1.5
		3	6.5
		4	-0.4
	2	1	3.0
		2	-2.1
		3	6.5
		4	-0.4

TABLE 3

VARIABLE EI ERROR PREDICTION (Table 3 Con't)

Concept	Orientation	Case	% Error
3	1	1	3.2
		2	-2.0
		3	4.7
		4	-1.3
	2	1	2.2
		2	-2.5
		3	4.6
		4	-1.3

TABLE 3

to the actual points of inflection of a fixed-fixed beam with a gage length of 5.33 in. As can be seen, the error resulting from not changing the test section span is very small and was neglected from this point on.

Another small analysis was performed (Reference 3) to investigate the strain levels and their distributions in the area where the initial cracks were forming during the flatwise tension testing. A finite element model of Concept No. 1, Orientation No. 1, was developed and the computer program "PLSTR-Plane Stress Analysis" (Reference 4) was used to perform the analysis. The contour plots (Figure 18 thru Figure 20) of the transverse, longitudinal and shear strains show the high strain levels which were occurring in the fillet area during the flatwise tension tests.

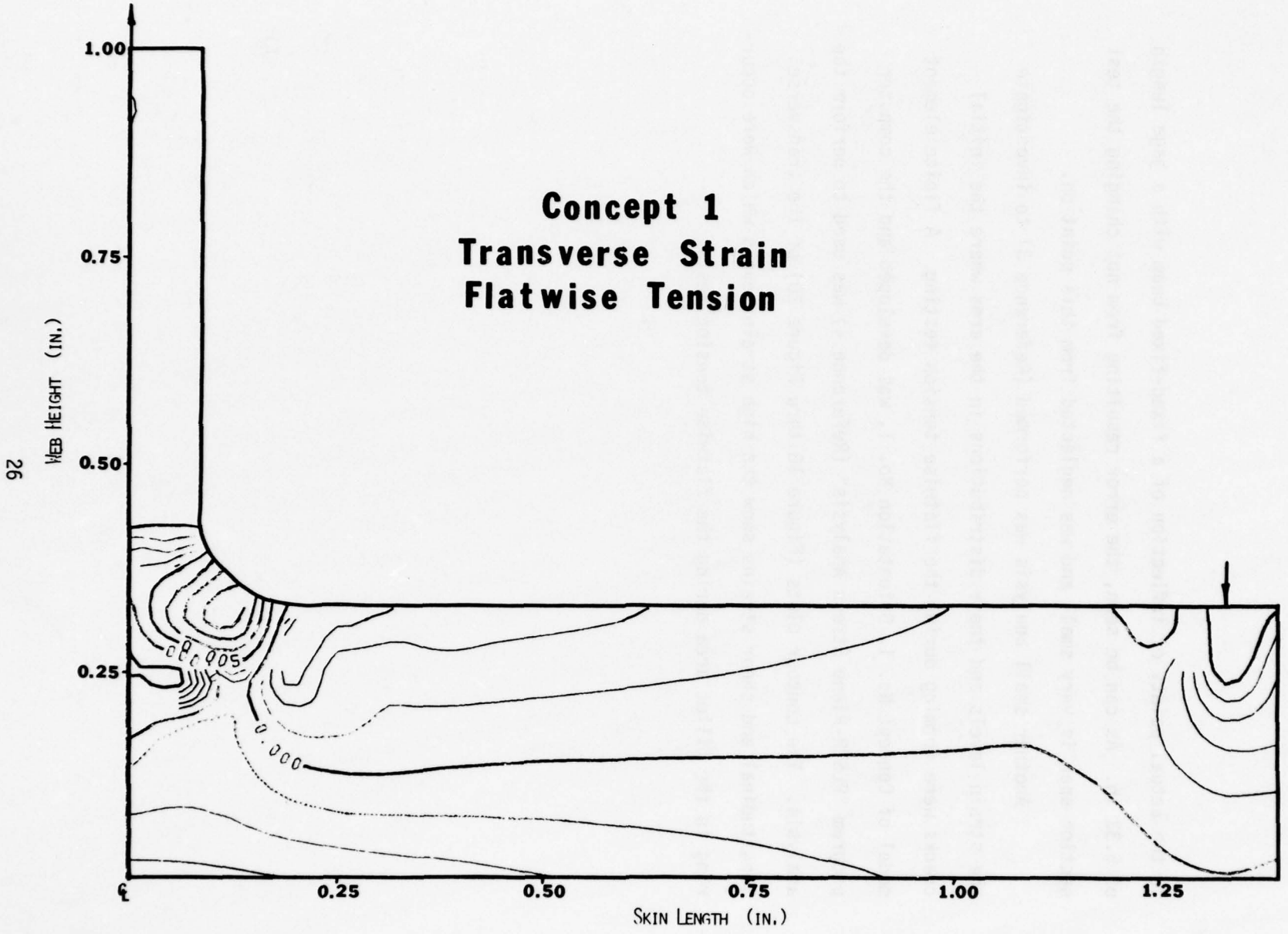
Concept 1
Transverse Strain
Flatwise Tension
1.00
0.75
0.50
0.25
Web Height (in.)
0.005
0.000
0.25
0.50
0.75
1.00
1.25
Skin Length (in.)

Figure 18

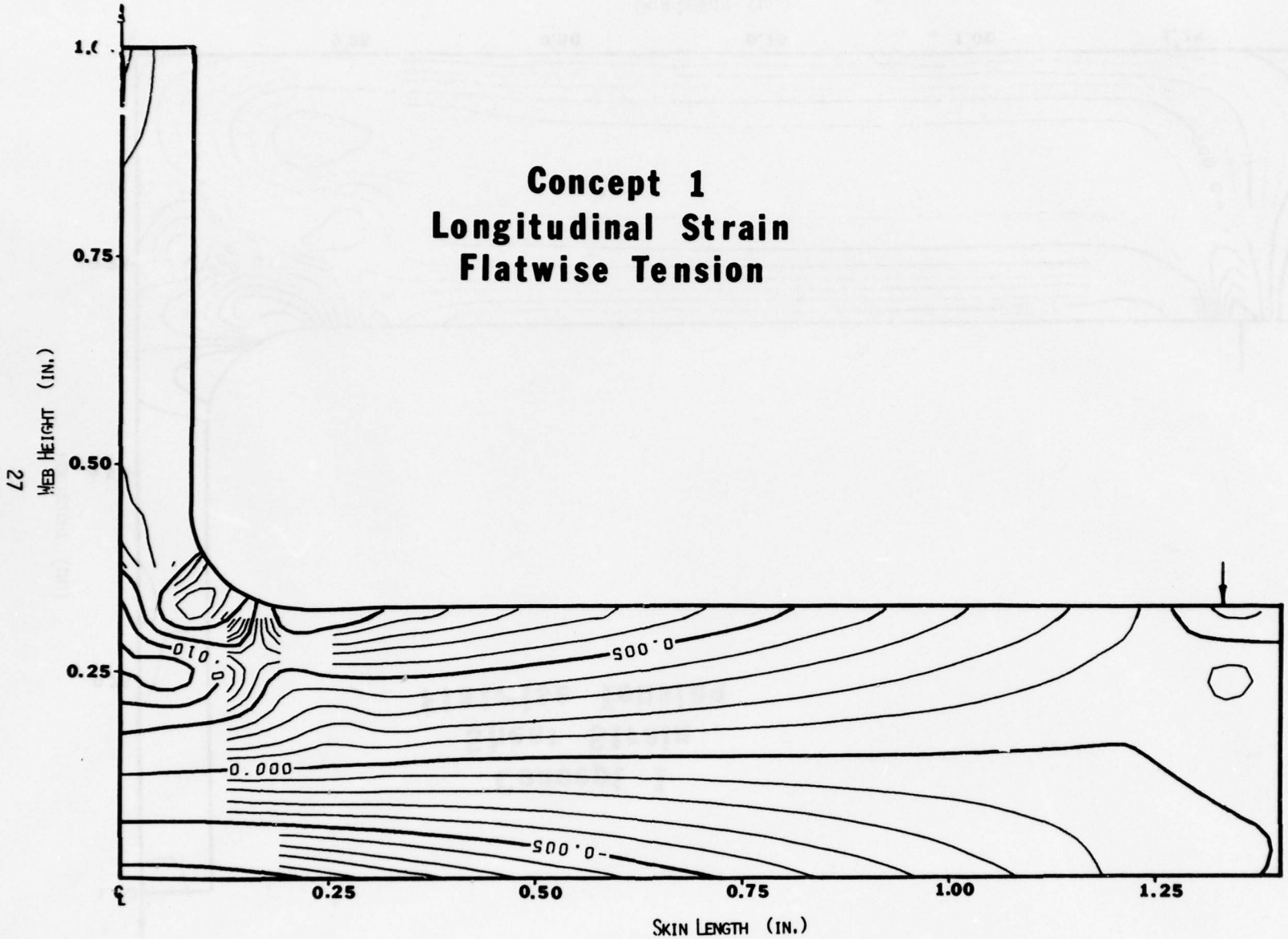
Concept 1
Longitudinal Strain
Flatwise Tension
1.0
0.75
0.50
0.25
WEB HEIGHT (IN.)
0.010
0.005
0.000
-0.005
0.25
0.50
0.75
1.00
1.25
SKIN LENGTH (IN.)

Figure 19

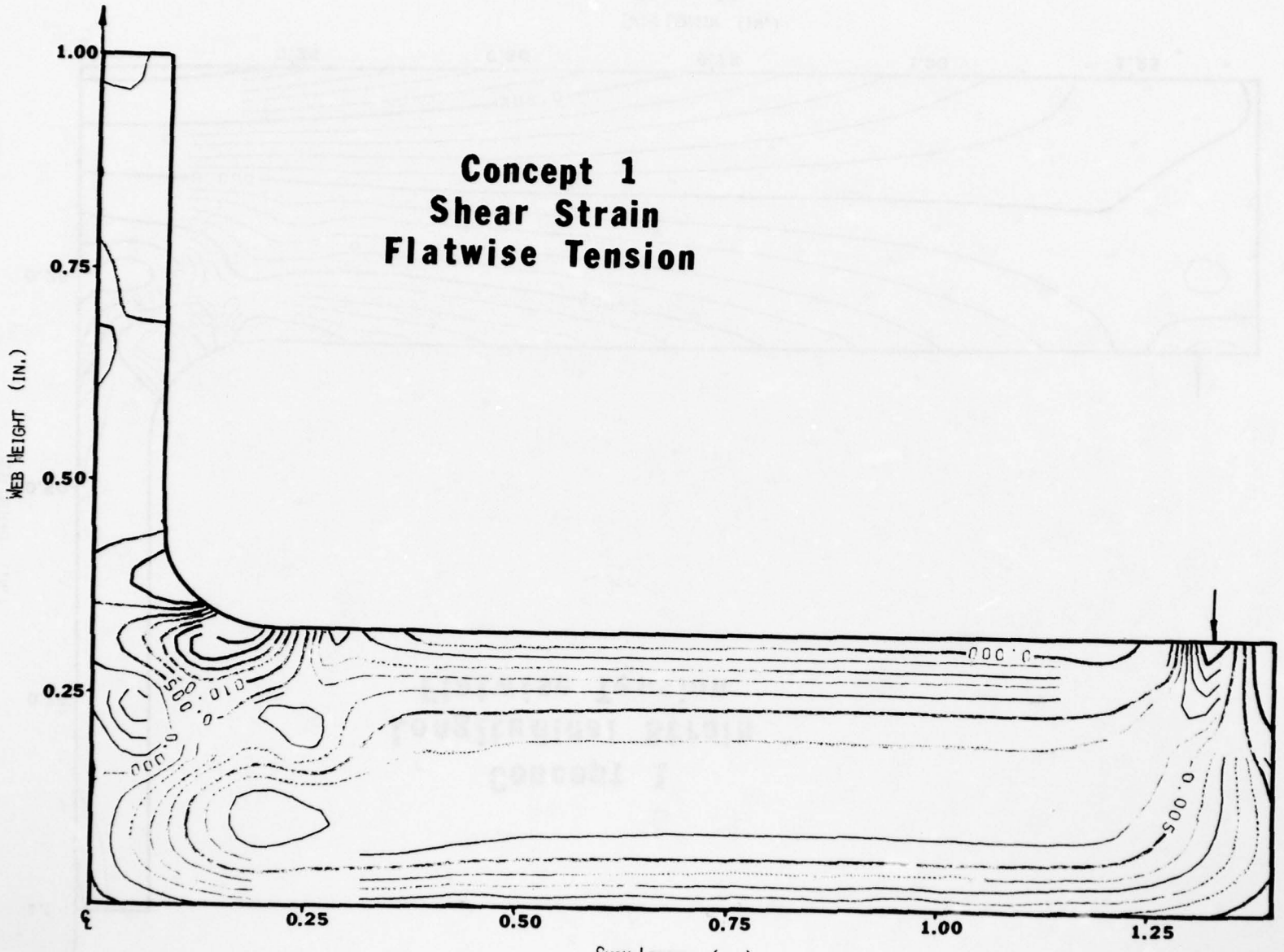
Concept 1
Shear Strain
Flatwise Tension
1.00
0.75
0.50
0.25
WEB HEIGHT (IN.)
0.000
-0.005
-0.010
-0.005
-0.000
℄
0.25
0.50
0.75
1.00
1.25
SKIN LENGTH (IN.)

Figure 20

III PROTOTYPE FABRICATION AND TEST

1. PRELIMINARY TOOLING AND PROTOTYPE SPAR PANEL FABRICATION

At the program inception, the basic concept for curing the spar panels was designed for commonality with standard vacuum bag/autoclave curing procedures, with bleeders being used during cure. This approach was selected to allow the use of cure cycles and bleed methods that have been verified through extensive industry experience. Pressures experienced by the part during the cure cycle were designed to be controllable and comparable to those achieved by a flat laminate being cured under a caul plate. It was anticipated that the material properties thereby produced would be consistent with industry standards for flat laminates.

Two preliminary T-spar panels (having a six inch base, 5 inch web or stem, and 32 inch length in the spar direction) were fabricated to determine various aspects of fabrication and tooling technology, and to obtain data on failure modes, test techniques, and fillet area materials.

The two preliminary spar panels, denoted IS-1 and IS-2, were fabricated in an autoclave using nylon film vacuum bags and sheet metal tooling that included steel (0.060 in. thick) angle caul plates on top of a flat sheet metal base. These panels were laid up to the design shown in Figure 1. This design involved a 40 ply base with a 10 ply web having the following lamination sequence ($\pm$45/0/$\pm$45/$\mp$45/0/$\mp$45); the web was composed of two sets of the five upper plies of the base. After cure, the panels were sectioned into individual T-specimens.

Panel IS-1 was fabricated from Hercules 3501/AS using 0° oriented dry graphite fibers to fill the small triangular fillet area. The Hercules

3501/AS material was used for this preliminary tooling test panel since it was readily available at the time the panel was fabricated. Bleeder plies were used, both below the base and in the web areas. This panel, upon curing, demonstrated a slight dimple, on the order of 20 mils, in the base below the web. Other than this, the panel was well formed along the base and the web. Base thicknesses were on the order of 0.0052 in. per ply and the web had a corresponding per ply thickness of 0.0058 in.

Panel IS-2 was fabricated to the same design as IS-1. This panel was constructed using NARMCO 5208/T300. In addition, the root areas were filled with pre-impregnated material laid in the 0° (spanwise) direction, as compared to the dry fibers used in panel IS-1. In an attempt to reduce the amount of dimpling the root was overstuffed with the filler material After cure, dimpling below the web was still present and tended to be [illegible] than that for IS-1. This was attributed to the greater flow characteri[illegible] of the resin system. The bleeder material in the web areas tended to wrink[illegible] and form imperfections in the web. This was also found to be true but to a lesser degree in the IS-1 panel. The overstuffing of the root caused the angle caul plates to bend during cure in an angle opening fashion, causing a taper to form in the web with decreasing web thickness from the base to the top of the web. The greater flow of the NARMCO resin over that of the Hercules resin resulted in extensive wash and resin rich areas in the root area. The web at the root was nearly twice as thick as the web thickness above the thickened area. Extensive wrinkling of the bleeder caused deep troughs in parts of the web. Thickness in the web over the central half above the root area was approximately 0.0049 in./ply. The thickness of the

base was substantially thinner than that for the IS-1 panel with an average thickness of 0.0046 in./ply (nominal thickness for this material is 0.0052 in./ply). Rotation and bending of the caul angles due to the overstuffed root filler also tended to cause depressions in the base on both sides adjacent to the web/base intersection.

2. PROTOTYPE FABRICATION CONCLUSIONS

Based upon these two preliminary panels, it was concluded that (a) bleeders and separators should be avoided adjacent to angle tools, (b) the lower flow 3501/AS material was superior from a fabrication standpoint, (c) methods to restrict edge bleeding of the web were essential, and (d) rigid angle tools should be employed instead of flexible sheet metal angles.

3. SPECIMEN NAMING

The two prototype panels (IS-1 and IS-2) were cut into individual specimens to develop data on failure modes, test techniques, root design, coupon widths and cutting methods. Each specimen cut from a spar panel was named for the panel (e.g., IS-1) and the specimen location from the end originally trimmed. Thus, IS-1-5 was the fifth specimen cut from the spar panel starting end after an initial trim. After the prototype portion of the program, T-spar panels were named with an S and a consecutive number denoting the chronological order of the cure operations. Thus, S-3-2 designated the second specimen cut from the third panel cured in the major portion of the program.

4. PROTOTYPE TEST RESULTS (IS-1 and IS-2)

a. Failure Mode - All tests were in flatwise tension using the

clamped-mode described in Section V. Test data is shown in Tables 4 and 5. Regardless of the specimen width, base span (distance between grips) or other variables, the following general failure mode was observed:

The initial failure was characterized by vertical splitting of the web plies and filler in the upper part of the root. Filament fracture often occurred in the center of one of the fillets. Cracks then spread in the vertical plane of the web. Finally, ultimate failure resulted from interlaminar splitting in the base below one of the fillets. A key conclusion from these tests was that the root filler must have transverse strength greater than that of the resin (i.e., transverse or two dimensional strength was required).

b. One inch wide specimens tested with spans between clamps of approximately 1/2 inch, 2 inch, and 3.5 inch all demonstrated the same mode of failure, but with lower loads as the span and bending moment increased. Various methods of cutting specimens into coupons were investigated. These included band saw cutting, band saw cutting followed by hand sanding, and diamond wheel cutting. The diamond wheel produced a polished surface with higher strengths since crack starters were removed. Based on these results, and the delivery of equipment, future test specimens were cut using a 14 in. diameter impregnated-diamond high speed cut-off wheel mounted in a cut-off machine that had a translating table. Specimens were backed with disposable hardboard and clamped to avoid vibration during cutting operations. The cutting operation was performed under flood water coolant.

c. Ultimate failure was preceded by initial cracking. To develop visual information on the mode of failure slow loading rates were considered

Table 4

Prototype Test Data/Panel IS-1

Specimen	Span (in.)	Cutting Method	Failure Load (lb./in.)
IS-1-1	2	1	600
IS-1-2	2	1	820
IS-1-3	2	1	640
IS-1-4	2	1	548
IS-1-5	0.5	2	590
IS-1-6	2	2	384
IS-1-7	3.5	2	338
IS-1-8	3.5	2	350
IS-1-9	0.5	1	794
IS-1-10	0.5	1	675
IS-1-11	2	1	627
IS-1-12	2	1	567
IS-1-13	2	1	573
IS-1-14	3.5	1	386
IS-1-15	3.5	1	482
IS-1-17	2	1	590
IS-1-19	2	3	854
IS-1-20	2	3	750
IS-1-23	3	3	526
IS-1-24	2	3	823
IS-1-25	3	3	501

Notes:
1. All specimens nominally 1 inch wide
2. Gage length = 2 inch = distance between Instron grips and intersection of web to base
3. Span = distance between inner edges of grips on the base
4. Failure load = lb/inch of width
5. Specimens loaded at 0.005 inches/min
6. Cutting code and load averages:

Cutting Method

1 - Bandsaw and Sanding - Average Failure Load for 2 inch span = 621 lb./in.
2 - Bandsaw - Failure Load for 2 inch span = 384 lb./in.
3 - Diamond Cutoff - Average Failure Load for 2 inch span = 809 lb./in.

Table 5

Prototype Test Data/Panel IS-2

Specimen	Span (in.)	Width (in.)	Cutting Method	Failure Load (lb./in.)	
IS-2-1	3.5	2	1	187	
IS-2-2	3.5	2	1	230	228*
IS-2-3	3.5	2	1	266	
IS-2-4	3.5	1	2	216	
IS-2-5	3.5	1	2	295	279
IS-2-6	3.5	1	2	245	
IS-2-7	3.5	1	2	268	
IS-2-8	3.5	1	2	340	
IS-2-9	3.5	1	2	311	
IS-2-10	2	1	2	348	362
IS-2-11	2	1	2	375	

Notes:
1. All specimens nominally 1 inch wide
2. Gage length = 2 inch = distance between Instron grips and intersection of web to base
3. Span = distance between inner edges of grips on the base
4. Failure load = lb./inch of width
5. Specimens loaded at 0.005 inches/min.
6. Cutting code:

   1 - Bandsaw and Sanding
   2 - Bandsaw

7. * Averages are for values in brackets

essential. The progressive cracking could be well observed with a loading rate of 0.005 inches/min. This was selected and employed in the remainder of the program.

5. PROTOTYPE ARTICLE FROM DOUBLE T FIXTURE

Details on this fixture are presented in Section IV. A preliminary spar panel (designated P) was cured from over-age Narmco 5208/T300 to proof the tool. The panel laminate design had 40 plies in the base 10 plies in the stem and used a 0° prepreg root filler. It differed from the other prototype panels by having a 90° ply in the stem, at the fourth ply from the outside.

The Double T tool incorporated developments from earlier trials where web tops and sides were sealed to reduce resin flow. This, plus the hard tooling, greatly reduced resin flow and dimpling in the root area.

Test results (Table 6) indicated rather low strength, but with a different failure mode from previous tests. The initial failure mode was a flat crack below the web and directly above the top continuous 90° ply in the base. This crack subsequently propagated into the adjacent base regions below the 90° ply, that also formed one stem ply.

Specimens from this panel were cut to two widths (1 and 2 inches) to correspond with the grip widths available on the test equipment. These specimens were tested to determine the effects of width upon the running flatwise tensile strength. No major running load variations were noted for the particular failure mode observed. Based upon these limited results, all the test specimens for this program were cut to a nominal width of one inch.

Table 6

Specimen Width Check

Test Data

Specimen	Width (in.)	Failure Load (lb./in.)	
P-1	1.001	382	
P-2	1.010	294	
P-3	1.011	351	
P-4	1.011	307	362*
P-5	1.019	414	
P-6	1.007	326	
P-8	2.004	354	349
P-9	1.915	344	

Notes: 1. * Averages are for the values in brackets
2. Specimens cut with diamond wheel

A 1/2 inch trim was removed before cutting the initial test specimen. The low test value seen in Table 5 was representative of low edge values seen in contemporary programs. Thus, a 3/4 inch trim was established for future spar panels.

IV MAJOR PROGRAM FABRICATION AND INSPECTION

1. DOUBLE T TOOL

The primary fixture used in this program embodied the findings from the IS-1 and IS-2 fabrication. This fixture, named the Double-T Fixture, was designed to form two spars on a single base. The fixture included a central channel section which was pinned to allow vertical motion (i.e., horizontally constrained) and two angle pieces which could move both vertically as well as horizontally. This fixture, shown in Figures 23 to 26, was considered to be advantageous over a single spar approach since lay up of the web and base plies was straight forward, location of the roots could be precise, and perpendicularity of the stems to the base was readily obtained. In addition, the 12 inch long (spar direction) tool was reasonably compact. The inner channel was pinned at the center of the two outer edges to provide horizontal constraint. Each pin fit in a vertical slot that was machined into the respective edge dams. This fixed the horizontal positions of the two spar webs during cure.

The aluminum tooling cauls were 1/2 in. thick, with a 1/8 in. machined radius on the male side of the fillets. Stops were employed to assure the proper web thickness of 0.00525 in. per ply (Figure 23). All bleeders were positioned underneath the base plies with no bleeders or separators in the web plies. A total of 13 bleeders were used, which was less than the nominal 3 prepreg to one bleeder ratio. The lower number of bleeders was used since substantial edge bleed was anticipated (and subsequently occurred). Pre-bleeding of the web plies was initially employed. This was discontinued due

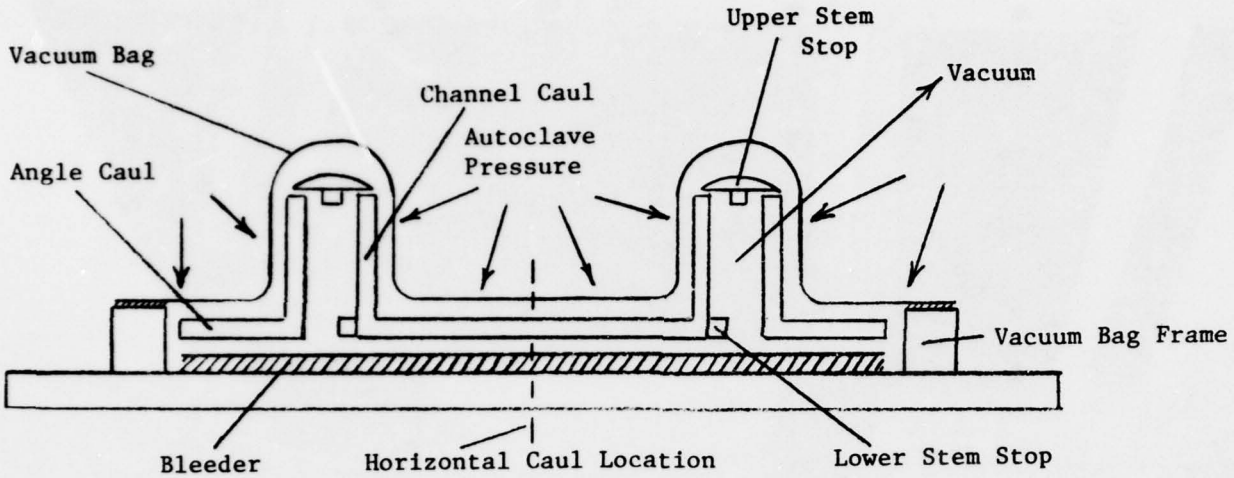

Figure 23. Double T Tool Schematic

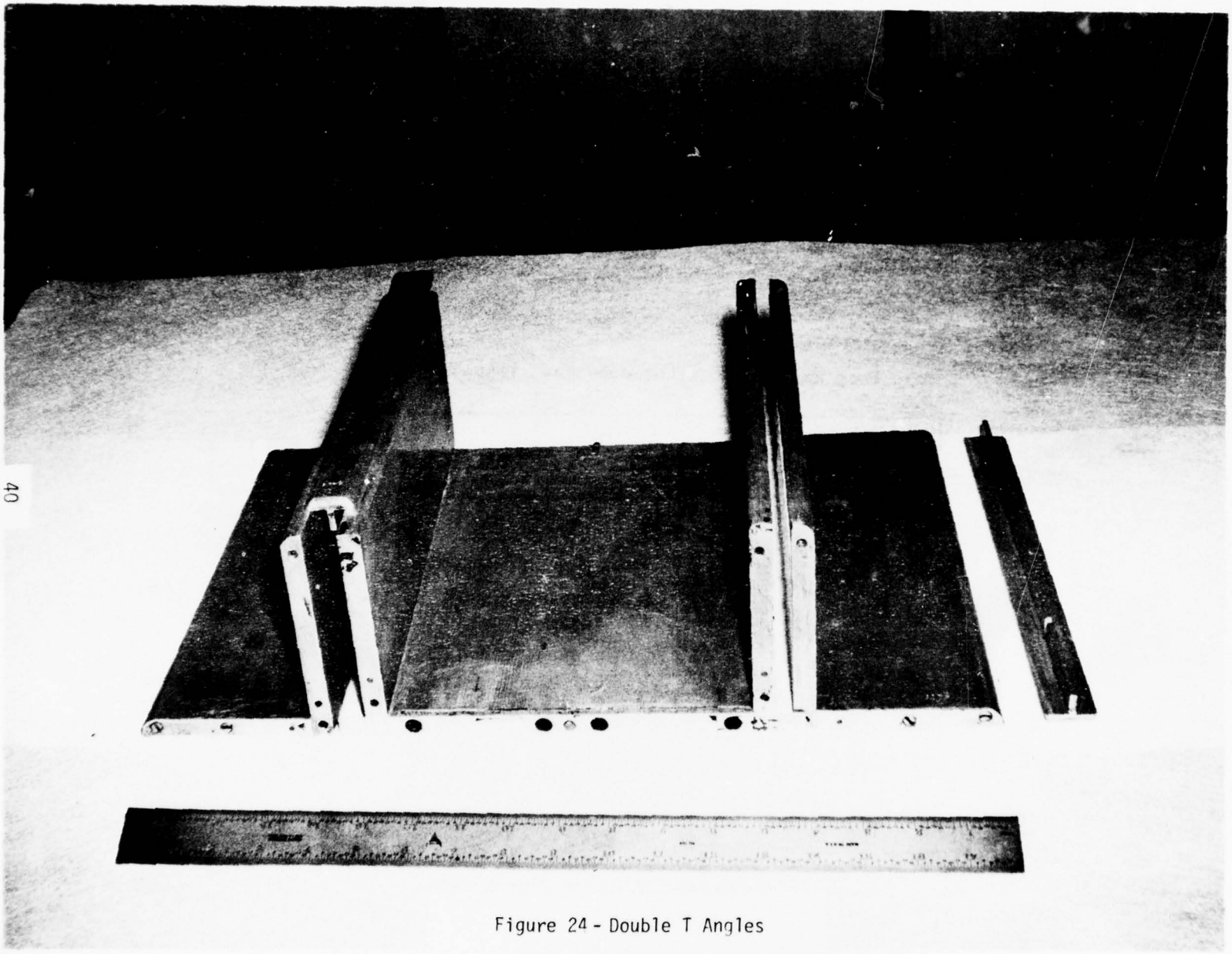

Figure 24 - Double T Angles

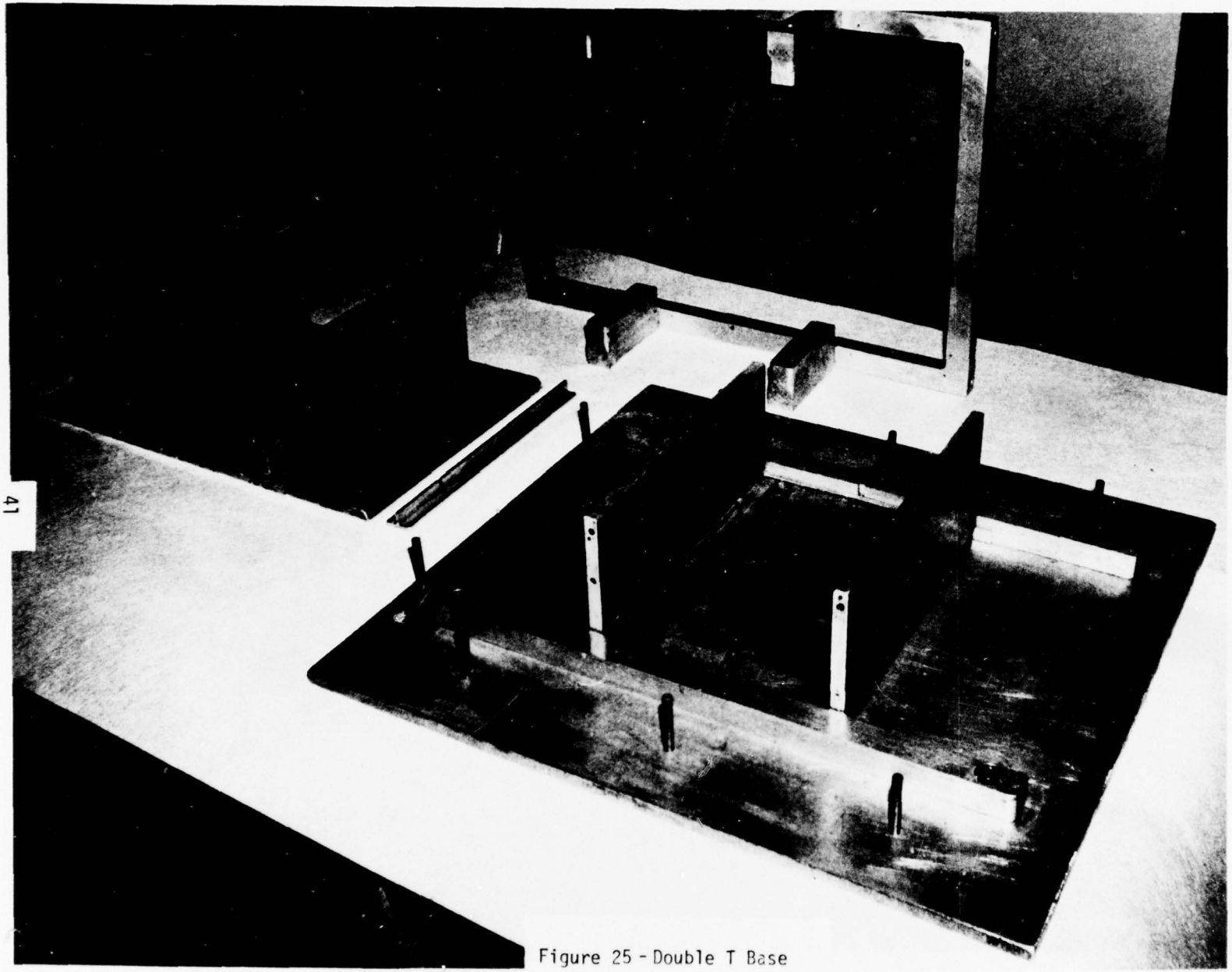

Figure 25 - Double T Base

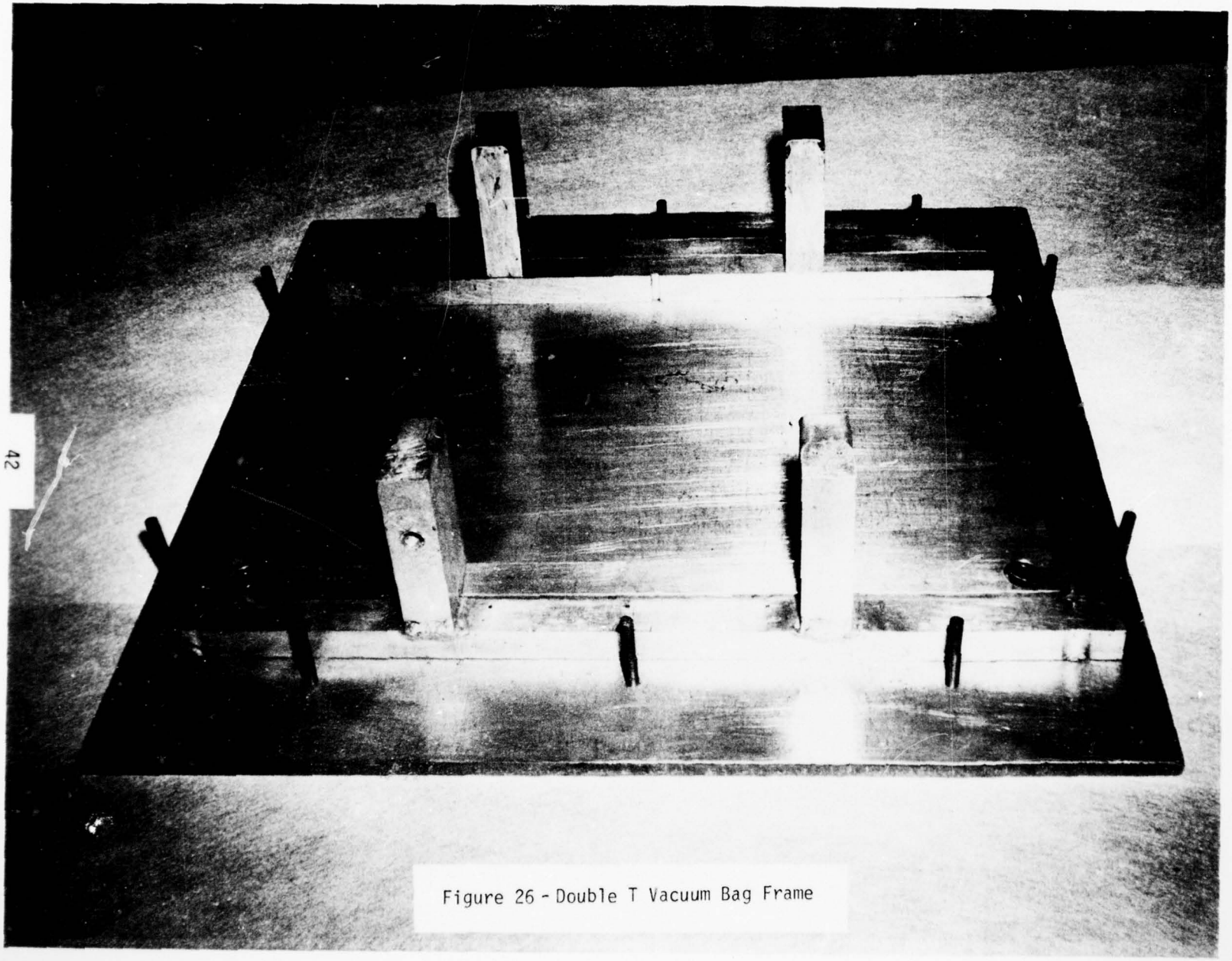

Figure 26 - Double T Vacuum Bag Frame

to the low resin contents experienced with the 5208 material.

Early attempts with this tool concept involved the use of a nylon vacuum bag with vacuum bag sealant. These attempts led to a number of vacuum bag failures during the cure where either the sealant moved or the bags failed by bridging. Subsequently, a frame was placed around the tool so that the bag and sealant were virtually at the upper level of the horizontal legs of the tool angles. Also, the frame had extensions at each end of the vertical members (web). Thus, the bag or film was applied and sealed with one degree of drape. This method was also prone to failure in the bag area. However, the failure was determined to be caused in part by the fact that the vacuum bags being used on the program were stored in an atmosphere with very low humidity, on the order of 5-15% relative humidity. Thus, the bags were quite brittle and did not conform where bridging occurred. In addition, nylon bags with conventional bag sealant techniques proved to be rather cumbersome to remove and clean.

An alternative to the nylon bags was employed. This involved the use of highly elastic silicone bags which were mechanically fastened to the outer frame through continuous flat bars and screws. Calendered silicone stock No. 1453, manufactured by Mosites Rubber Company, Inc., Fort Worth, TX was used. This method eventually proved successful. However, the first bag used degraded after its initial run by the action of the epoxy and hardener system. That is, the bag rubber tended to crumble and split in some areas. To protect the rubber from amine attack from the uncured epoxy prepreg, Mosites No. 10139 coating was employed. This was release-coated

to limit epoxy sticking and peeling of the coating. These bags performed well although some of the coating had to be repaired after each use. Ultimate life was limited to approximately four to six runs due to tearing of the highly compressed bag around the fastener holes. Otherwise, this method was judged successful and the bulk of the spars fabricated under this program were fabricated in this manner.

In both the nylon and silicone bag fixtures, vacuum was drawn from the bag through a port in one of the stems of the frame (Figure 23). It was necessary to install resin traps outside the fixture at this vacuum junction to reduce the amount of resin drawn into the vacuum lines of the autoclave system. That is, a substantial amount of resin was drawn directly towards the vacuum port from the port edges and not through the bleeder material.

2. UPRIGHT T TOOL

Towards the end of the program an alternate fixture was developed to allow vacuum and bleed to be directed out the planform of the base. The configuration of this fixture had the "T" section in a normal letter fashion with the base on top (Figure 27). Bleed was upward into the bleeder plies and vacuum was drawn on the outside of the bleed plies, in a conventional manner. Edge bleed could be readily controlled by tape and edge dams. As developed from the double spar tool, bleeder and separators which were undesirable adjacent to the web were not employed.

The fixture consisted of a fixed rectangular member and a similar member that translated with pressure and compaction. A nylon vacuum bag was used to apply pressure for part compaction across the top of the tee.

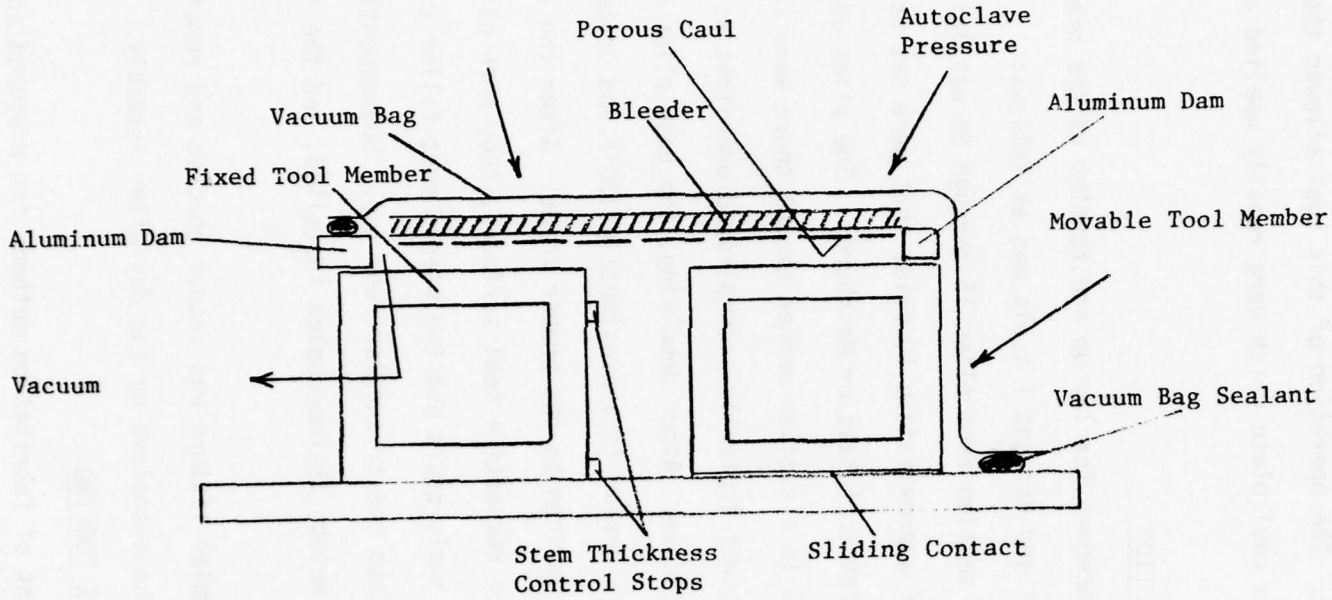

Figure 27. Upright T Fixture

The movable square member incorporated stops in the web region to assure proper web thickness. The operation of this tool allowed the use of bleed material and a porous caul plate which were readily applied on top of the piece.

3. PREPREG FORMATION

The basic procedure for lay up and forming of the prepreg material for both the Double T and Upright T tools was as follows:

a. The base section from plies 15 through 56 was laid up and debulked in groups of approximately 10 plies that were set between porous separators and vent fabric (glass or Mochburg). The plies used to form the web were debulked in a similar manner except there were seven (7) plies per group. Debulking was typically accomplished overnight at room temperature and under full vacuum. After debulking, the base plies were assembled. Next, angle plies were heated to approximately 130°F and draped over a warm angle tool to form them to the proper shape. After the angle plies were formed into their respective tool surfaces, they were placed together along with the metal angle cauls and the staged root-filler adhesive was inserted and forced into the triangular root gap. Subsequently, the base and angle plies were mated, thermocouples installed, and the tool final assembly performed.

b. The assembled fixture was vacuum checked and remained under vacuum until run in the autoclave on the day after assembly.

4. PRECURED ANGLE TOOLING

The development of fabrication methods for precured angles in this program was initiated after the integral spar studies were well under way.

Thus, the drawbacks of bleeders and potential wrinkling of separators on the inside of the angles were known. Preliminary efforts involved the use of bleeders and vacuum bag techniques, with bleeders on the outside of the uncured angle plies. Angles were initially formed over 90° male aluminum angles without the use of female tools or cauls. The results were not satisfactory since a pinching motion occurred which tended to wash the outer plies away from the vertex region. Subsequently, the use of a thin metal slip caul over the bleeder plies was attempted. A similar washing motion of bleeder and composite was observed unless the caul had a radius pre-formed to match the outer radius of the composite plus bleeder. In addition, wrinkling of the bleeder and a creasing of the composite were randomly observed, when bleeder was used. The preliminary efforts also determined that the angles, fabricated from 5208 resin, were low in resin content with per ply thicknesses generally below 0.0048 in. Although bleed could have been reduced by changing the cure procedures, it was decided to maintain a consistent cure for all parts of the program. To correct these situations, angles were formed over a male tool with the thin metal slip caul bent to a matched radius and positioned directly in contact with the composite plies. Both tool surfaces were release coated and a nylon peel ply was cured as the outermost ply of the composite (to cover the bond surface). Such angles demonstrated a higher resin content and were generally well formed. However, there was a tendency for taper in the legs of the angles with the angles becoming thinner away from the vertex where edge wash was extensive (even with dams in place). Also, the composite thickness in the fillet area tended to be different from that in the angle legs.

Another problem area which appeared during the initial attempts at manufacturing a 90° angle was that the cured angles were less than 90°, e.g., 87°-89°. As a result, when the components of Concept 6 were assembled by bonding, cracks were formed in the fillet area of the tees since the pressure from the bonding fixtures forced the angles to be 90°. These specimens failed at very low loads because of this problem.

To fabricate 90° angles it was necessary to cure each angle over a tool which was at an angle greater than 90°. By essentially an empirical approach using trial and error for our particular laminate, the proper included angle of the tool was found to be 92°.

In addition, an analysis using finite elements (Reference 3) was performed. Models were constructed to represent different laminate stacking sequences and different radii. A typical model for the particular laminate and radius under consideration in Concept 6 is shown in Figure 28. This model was loaded by means of a 100°F thermal drop from a 172°F reference temperature. This 172°F reference temperature was selected to provide the 100°F thermal drop down to room temperature. The deflected shape is presented in Figure 29. It should be noted that the actual displacement of the nodes in both the X and Y directions, was multiplied by a factor of 100 for clarity. The actual angular displacement, as determined by the finite element model is 0.097°. There is a large discrepancy between the empirical solution and the theoretical solution. However, it should be noted that the most important parameter in the theoretical analysis, namely the values of the coefficient of thermal expansion at the various temperatures, had to be assumed since it was unknown. Therefore, this finite

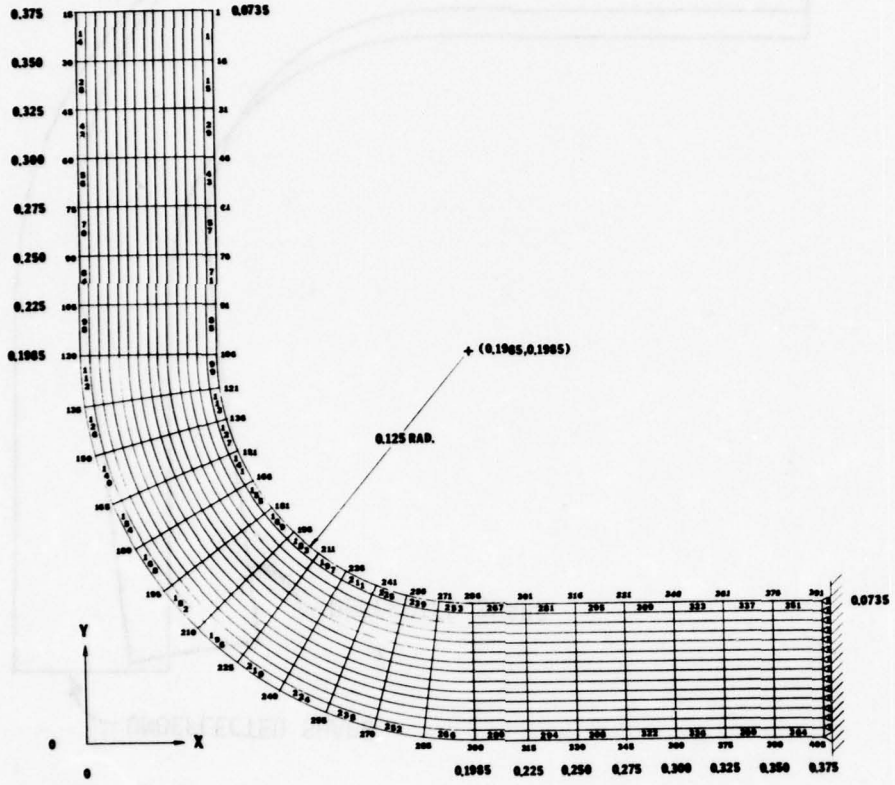

Figure 28 - Concept No. 6, Graphite/Epoxy Angle-Finite Element Model

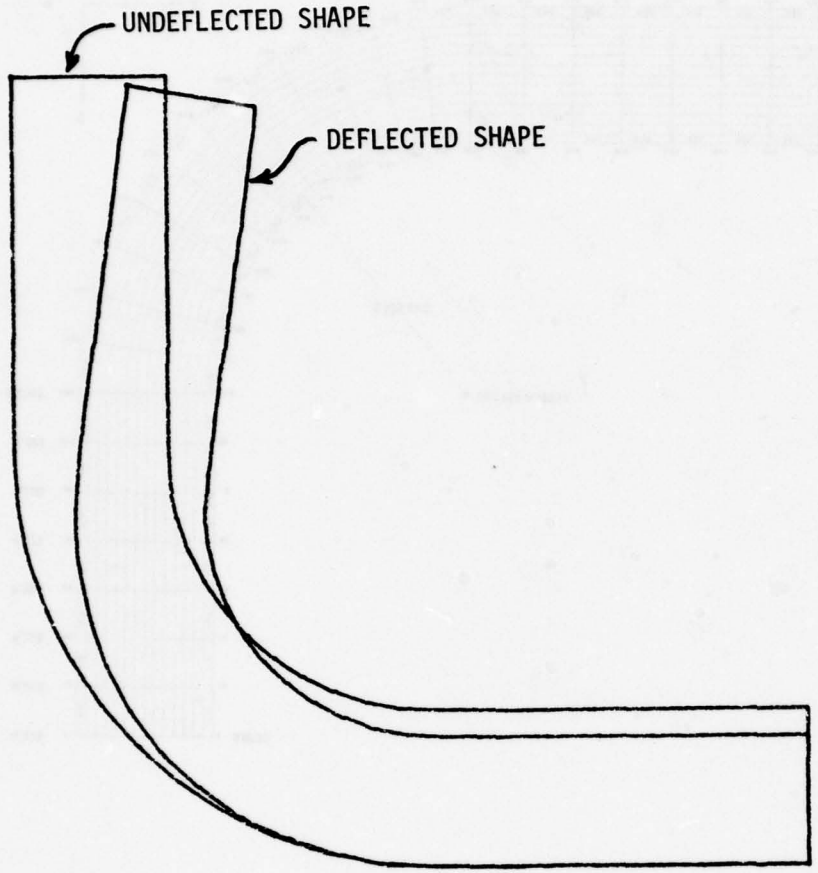

Figure 29 - Finite Element Deflection Diagram

element analysis only gave a trend as opposed to an exact answer. This finite element analysis also showed that the change in the included angle is dependent upon the radius of the fillet, the laminate thickness, and the stacking sequence.

Since angles were to be bonded on their outer surfaces, it was decided to modify fabrication procedures by using a female tool machined to a 92° angle. Commercially available angle extrusions were used for this purpose, with the extrusions having a thickness of approximately 1/2 inch. The compaction and formation of the part using the female angles was by a rubber male tool member, similar to that shown in Figure 30. However, the curing trials with this concept were conducted using a vacuum bag and autoclave pressure - not the self contained tool of Figure 30. Parts were not pre-bled. Rubber mandrels with a 92° angle were cast to match the inner surfaces of the cured angles. These mandrels were subsequently judged unacceptable since they did not force the root area of the angle in towards the female tool. That is, the fillet radius was greater than that of the female tool, and a cavity existed between the composite part and the female tool which eventually accepted resin being expelled from the composite. Attempts to rectify this situation involved the use of sharper male angle tools (85°) which helped the situation, and the use of hard rubber portions of the male tool in the vertex region to act as an intensifier.

Angles used for the test specimens in this program included both those formed on male tools and those formed on female tools with the 85°

male blocks. All angles had a superficial appearance of being well formed, with the root areas being approximately the same thickness as the leg thickness. However, it was recognized that the compaction in the root area was less than desired due to the incomplete compaction on the outer radius of the fillet, and possibly microcracks or voids existing in the area. Use of a microscope to detect such voids often uncovered what appeared to be small cracks running between plies. Thus, the critical failure area in those angles; i.e., the fillet, was of doubtful integrity.

The final tooling for forming angles was a 92° female tool with a male inner angle formed to intensify the compaction at the root or vertex of the composite part. Compaction was initially applied by means of a vacuum bag with autoclave augmentation. However, to reduce the autoclave expense and scheduling problems, self pressurized tools were developed (Figures 30 and 33). The fixtures contained a silicone rubber diaphragm (Mosites No. 1453) which was pressurized from beneath and, thereby, exerted pressure on the male rubber tool. These fixtures worked satisfactorily with no bladder failures occurring. To assure root compaction for small radii angles, the fixtures have been adapted as matched metal tooling in a follow-on program. Another innovation accomplished after this program was the use of sheet metal caul sheets which can be inserted between the composite and the heavy female tool angle, and which are bent to radii larger than the major tool angle. These can be readily inserted to form larger radius angles.

The actual preparation of the Gr/Ep prepreg subassemblies was similar to that performed using the Double T tooling. After laying plies

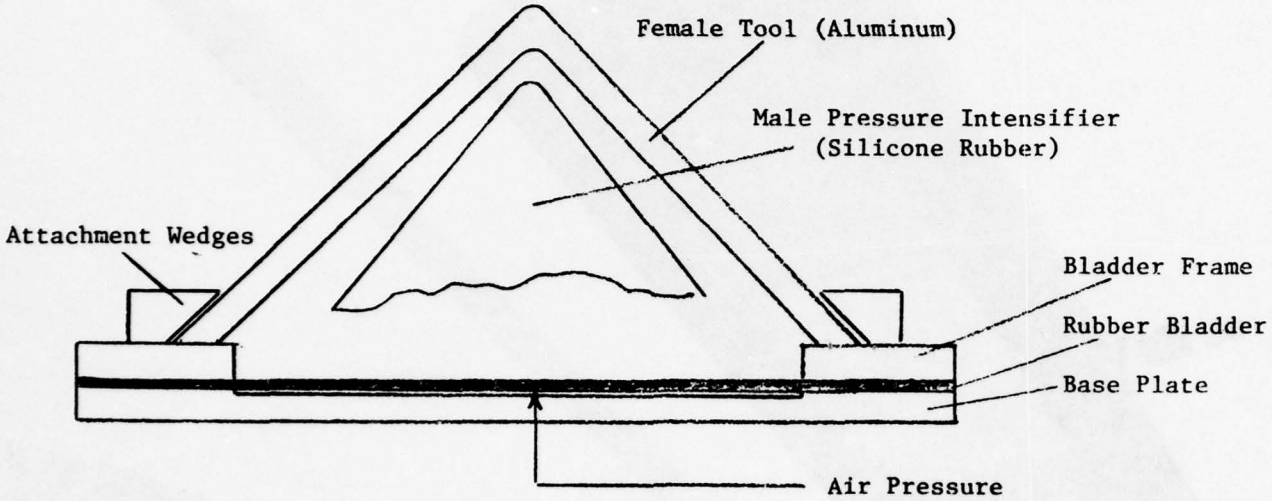

Figure 30. Angle Tool Schematic

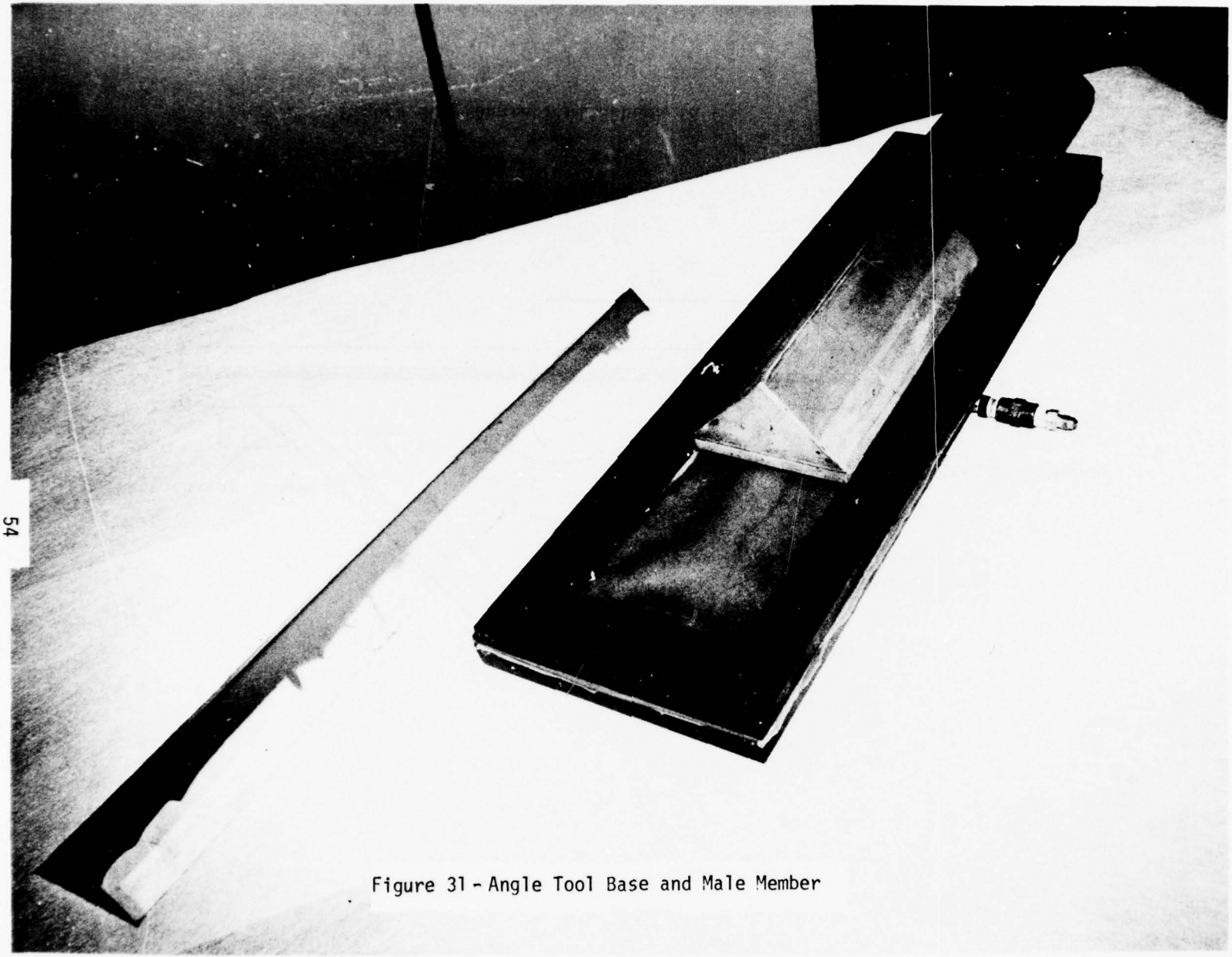

Figure 31 - Angle Tool Base and Male Member

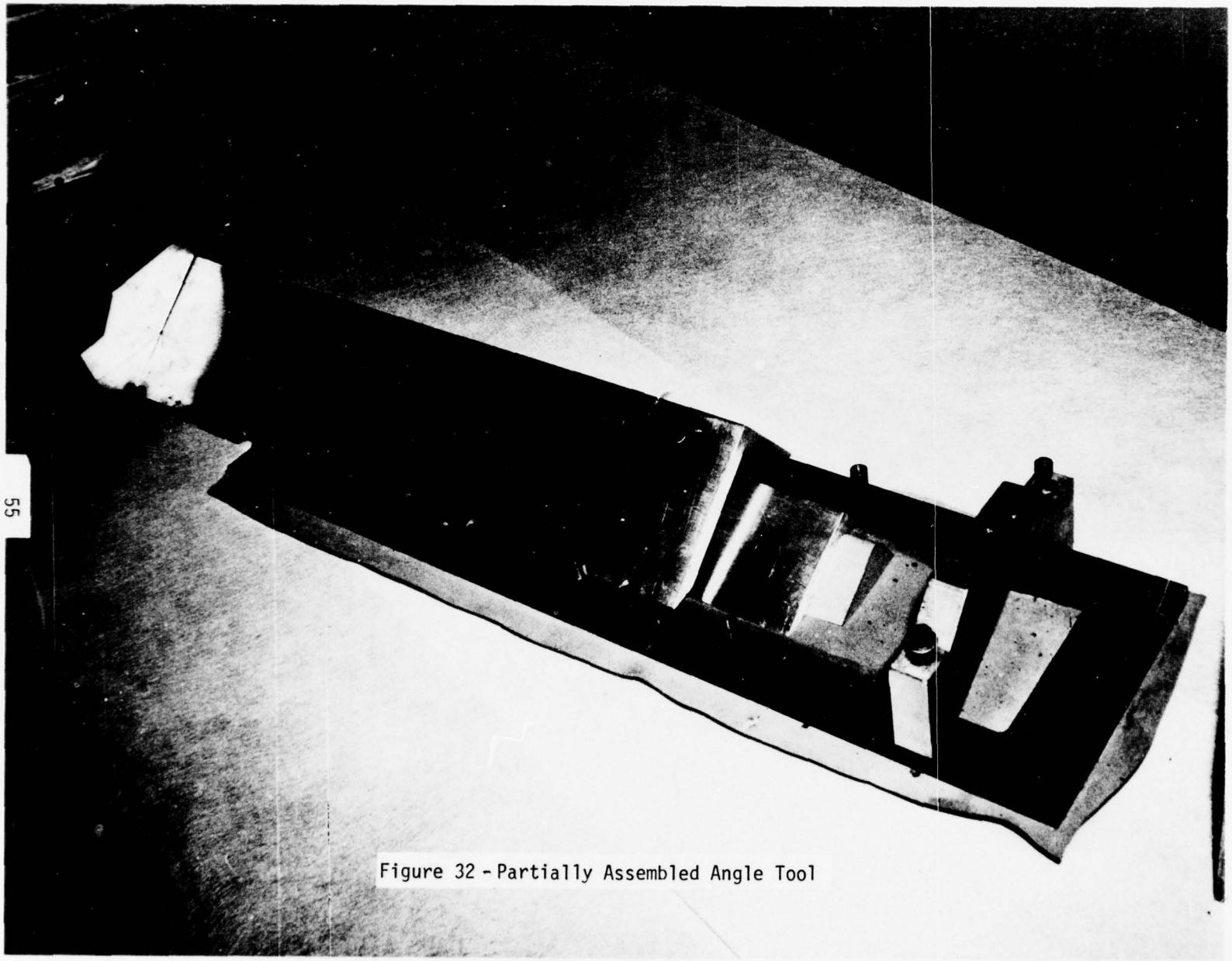

Figure 32 - Partially Assembled Angle Tool

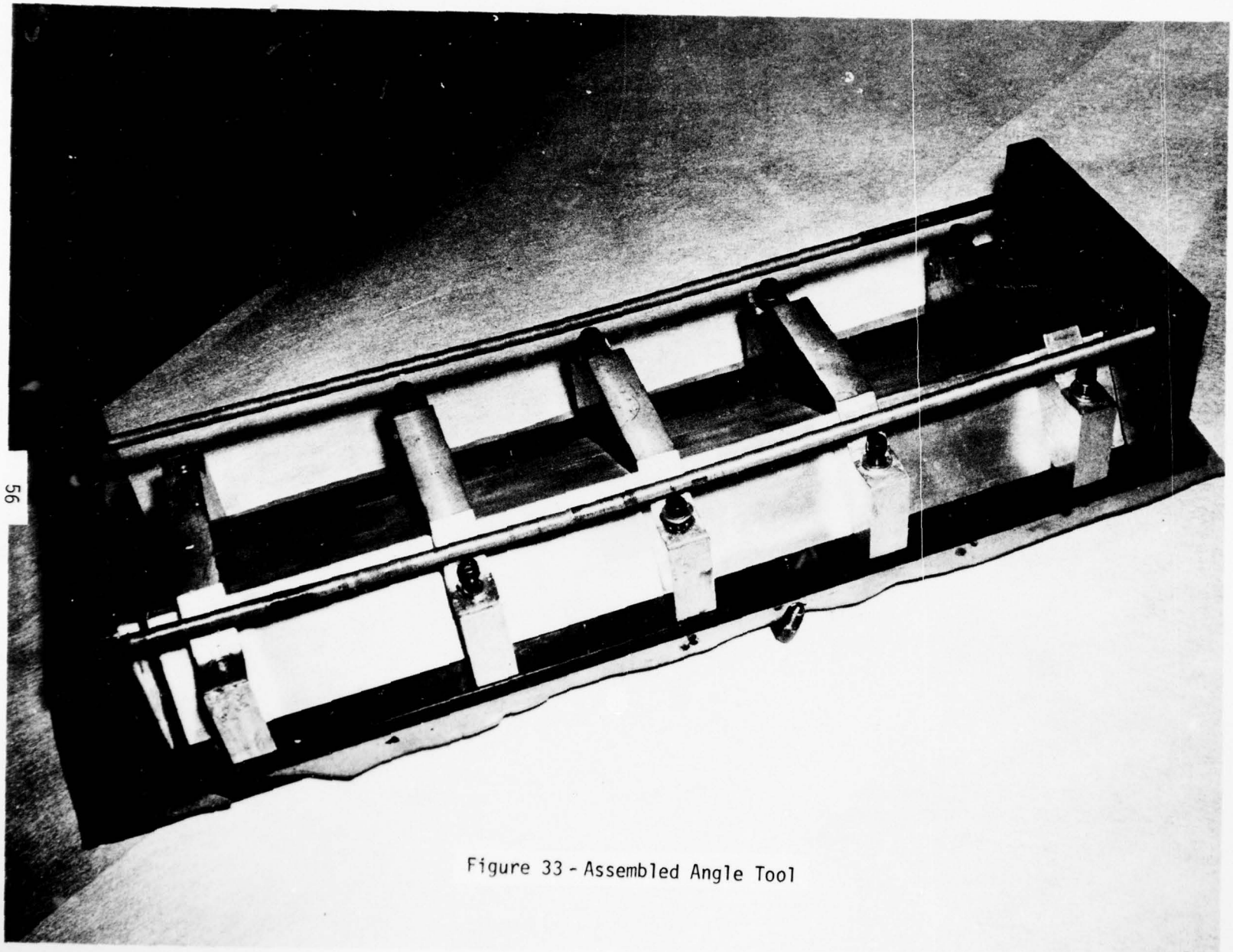

Figure 33 - Assembled Angle Tool

in the flat, they were draped over a male angle tool (130°F) and debulked overnight at room temperature. Cork dams were installed around the composite prepreg directly on the female tool. Angles formed were neither pre-bled nor did they use bleeder during the cure. Even with this arrangement, the resin content of the angles was typically on the order of 27% by weight, which was characteristic for the high bleed material used, and was even more pronounced for these small parts where edge area was large relative to planform area. That is, even with edge dams, appreciable material flowed out by an edge bleed mechanism.

5. ELASTOMERIC TOOLING

Concurrently with the autoclave curing approaches, an independent effort was initiated to determine the practicality of fabricating T specimens using elastomeric tooling and oven heating. A box frame fixture was available for immediate use on the program. This frame, shown on the left in Figure 34, was adapted by inserting two large elastomeric blocks adjacent to the web and an elastomeric block on the base. The preparation of the fixture consisted of inserting the unit in an oven and allowing the expansion characteristics of the rubber to provide compressive forces and, thereby, consolidation of the part. Two such parts were fabricated using available woven graphite material to check out the applicability of this tool. It was noted that compaction pressure on the first spar fabricated was inadequate due to the small thickness of rubber adjacent to the stems. Subsequently, the tool was increased in width and thicker rubber pieces inserted. Although compaction improved, it was judged still inadequate for fabricating spars. To provide positive pressure the concept shown

on the right (Figure 34) was considered. However, this concept would only be valid if a hydrostatic condition in the rubber existed. Since this is not assured it was decided to construct an elastomeric fixture wherein the pressure could be controlled and assured using air bladders which were substituted for the two side expansion elastomers in Figure 34. Discussion of this work is presented in Reference 5. The concept was eventually developed to provide both a low cost method of fabricating spars and was also used in the development and screening of potential root filler concepts for this program (Reference 5).

The general utility of the elastomeric fixture was well demonstrated from preliminary tests and was subsequently used for the curing of large fillet radius T specimens (report is in preparation).

6. BONDING TOOL

Bonding of pre-cured angles and stems for Concepts 3 and 6 (Figures 10 and 13) was performed using an available rigid box, fitted with a diaphragm and pressurized as shown in Figure 35. The medium used to transmit the pressure from the diaphragm to the adherends was a bed of 1/4 in. diameter hollow aluminum beads. This concept had previously been used in Reference 6. The large ductile beads were probably less effective in providing lateral pressure (normal to the web) than a truly fluid bed, such as would be approached by small, hard spheres with low friction surfaces. In fact, compaction pressure in the fillet areas seemed inadequate, based upon the observed thick bondline in specimens fabricated for this program. Towards the end of the program the pressurized elastomeric tool of

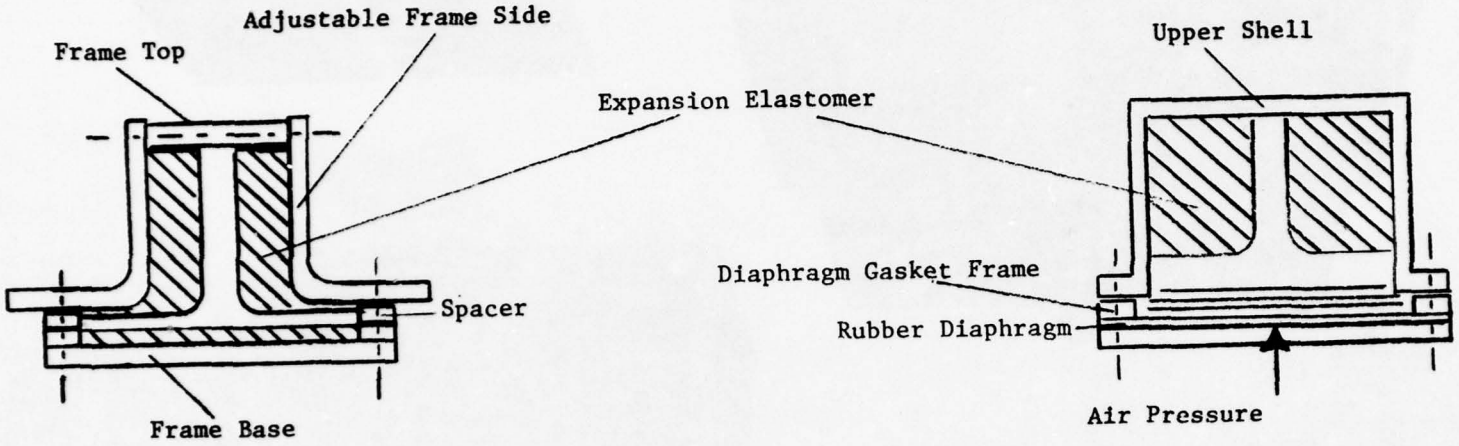

Figure 34. Elastomeric Tooling Fixtures

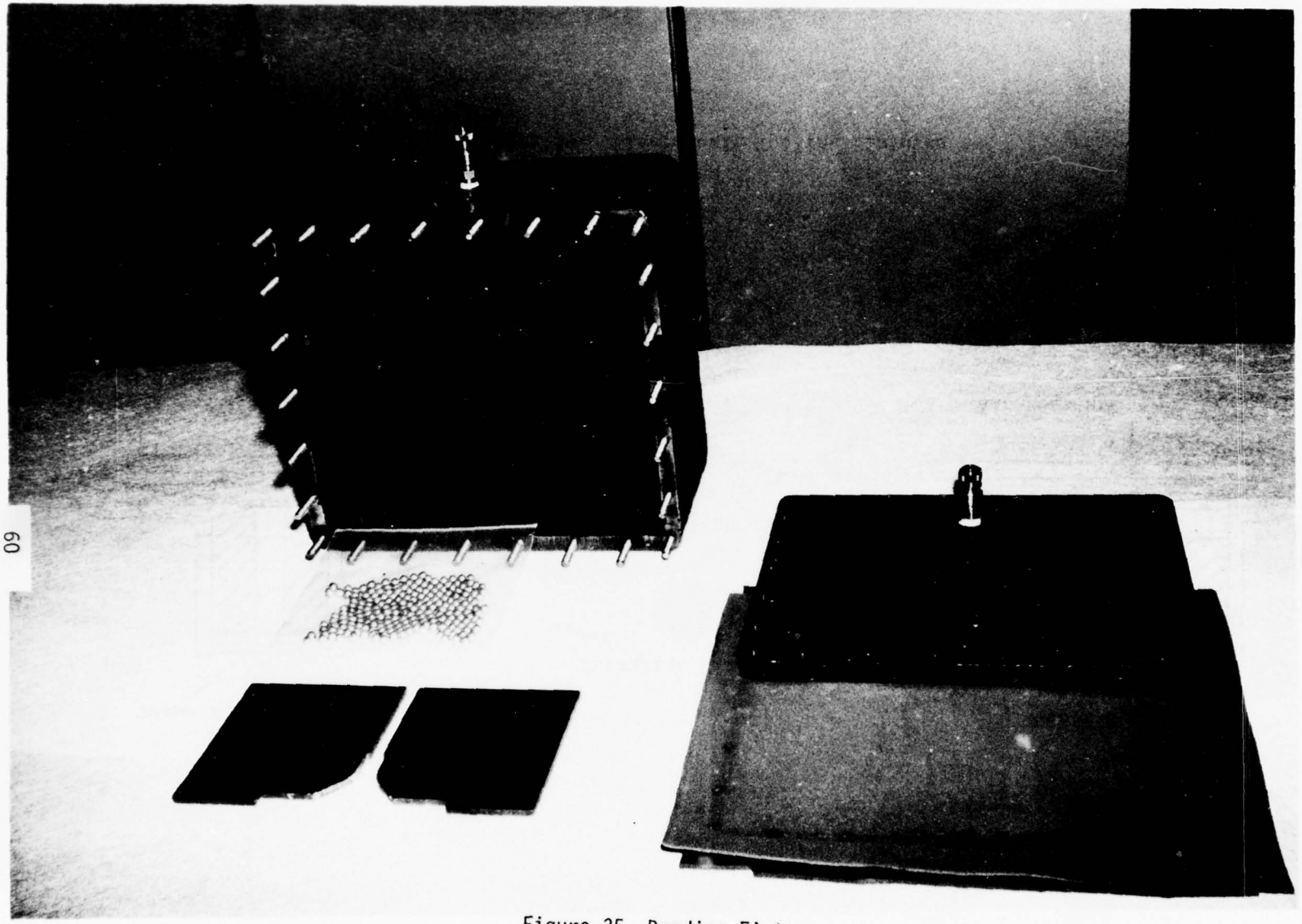

Figure 35 - Bonding Fixture

Reference 5 was used to bond angles. These specimens had uniform bond lines with low porosity.

The stem components of all specimens were pinned prior to bonding to vertically locate the two angles and inner web (where used). This was accomplished by two drilled holes at each end of the spar. Horizontal location of the web components to the base was by metal locators, two at each spar end.

7. NONDESTRUCTIVE INSPECTION

After each autoclave cure and fixture disassembly, specimens were observed for surface condition, perpendicularity of the web to base, adhesive and resin bleed, and any resin rich or resin starved appearance of the surfaces. Specimens were dimensionally checked, using micrometers for cover and web thicknesses. Subsequently, the spar panel was delivered to the NDI group within the Air Force Materials Laboratory for ultrasonic C-scan inspection of the flat areas; i.e., views normal to the web and base. No inspection of the root area was attempted. Acceptability was based on matching the attenuation relative to standards from assumed, well compacted areas of each spar. Specimens that were eventually tested for inclusion as data samples were found to be void free using this method. After the spar panels were returned from NDI and cut into individual specimens, the edges were viewed with the naked eye for porosity in the root, fillet, and base areas. Generally, some porosity was seen in the root. In addition, the cut surfaces of specimens were visually inspected for water weeping (from the flood coolant used in cutting) to determine if

any cracks or pores were present. A few specimens were randomly selected for inspection under microscope to qualitatively determine the extent of porosity or interlaminar cracks around the root area. Generally, it was noted that some voids were present in the fillet areas. The high resin content root areas had a high void content. However, since failures were never in the root this was not considered a problem.

V TESTING

1. TEST FIXTURES

All testing for this program was performed on an Instron testing machine using either a 1,000 lb. or 20,000 lb. load cell.

The flatwise tension tests were performed using a special fixture. The original fixture attempted to simulate a fixed-fixed beam with a single load at the mid-span. It was felt that this fixed-fixed end condition would closely approximate the actual conditions which the test section would experience. There are considerable difficulties involved in performing a fixed-fixed beam test. The hardest problem is simulating the fixed-fixed boundary conditions. Using the clamp-up system shown in Figure 36 there was difficulty experienced in alignment, clamp-up tension consistency from test to test, and lengthy time delays between running simple flatwise tension tests. After comparing the shear and moment diagrams of the fixed-fixed beam (Figure 37) with those of a simply supported beam, it can be seen that if the length of the test section (section between supports) is reduced by 1/2 from the fixed-fixed beam to the simply supported beam, the bending moments and shear across the span, will be equivalent. The other major advantages to using the simply supported test fixture are the ease of test set-up and the high degree of repeatability from one test to the next. The fixture was designed so that the distance between supports could be adjusted and it also had centering adjustments for the specimen. Another major advantage to the simply supported test fixture was the fact that no special tabbing was required during the testing. For the fixed-

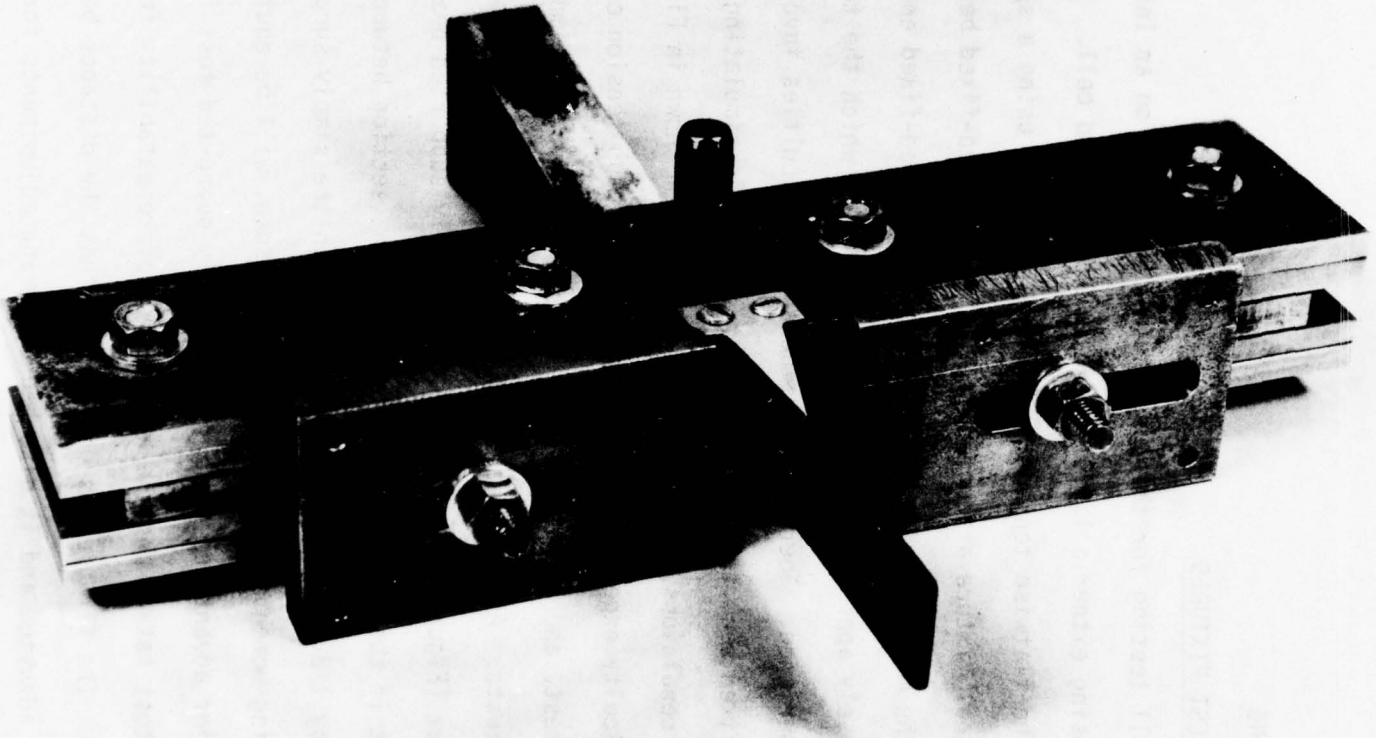

Figure 36 - Flatwise Tension Fixture/Clamped Edges

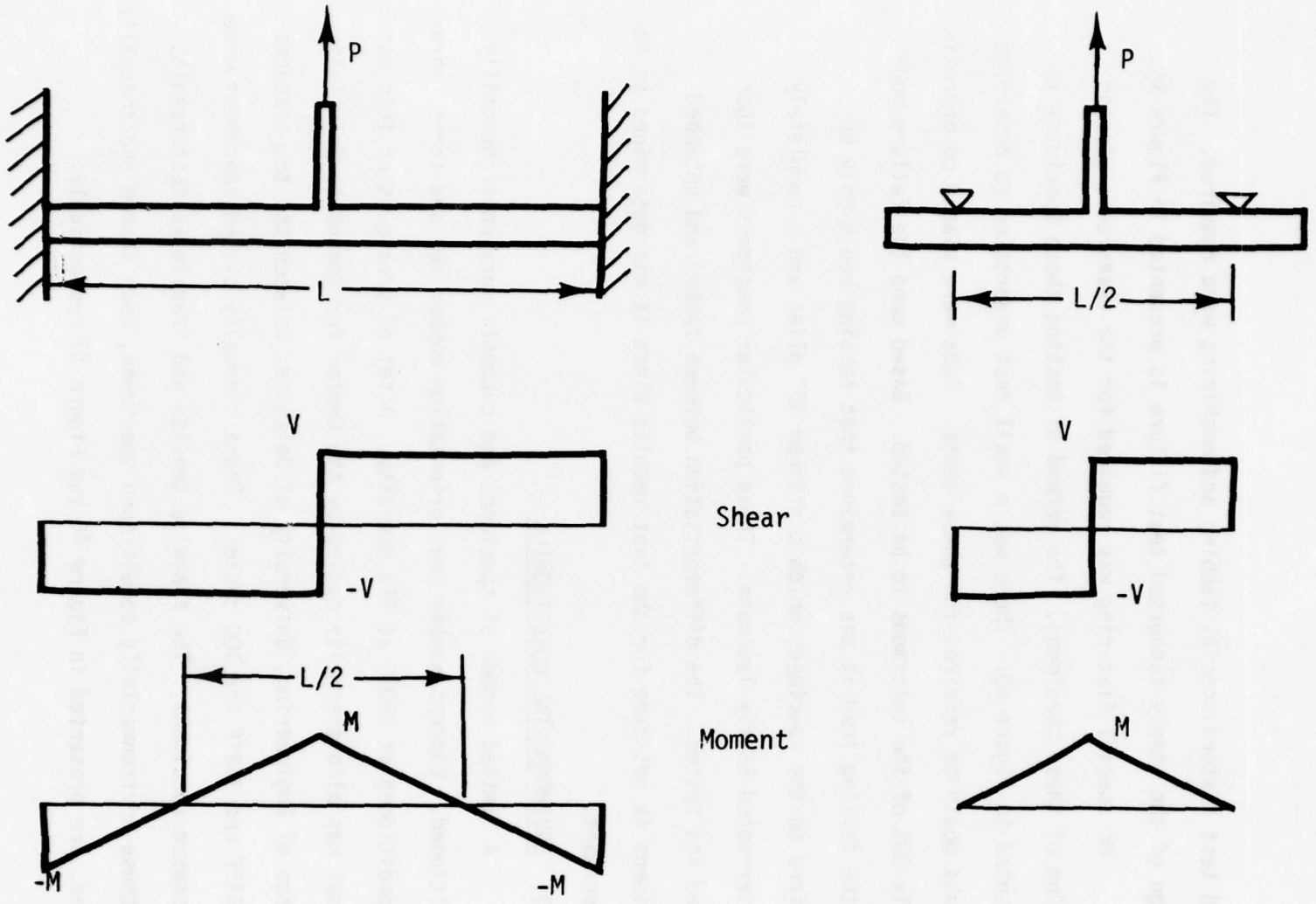

Figure 37 - Flatwise Tension Shear and Moment Diagram Comparison

fixed test fixture special tabbing and machining were required. The design of the simply supported test fixture is presented in Figure 38.

No special fixturing was required for the transverse tension testing of these specimens. The method of testing these specimens is presented in Figure 40. There was a small test undertaken to determine if tabs would be required for these tests. Tabs were placed on approximately 30% of the specimens to be tested. Based upon the failure mode and the failing load it was determined that tabbing would only be required on the specimens which contained 90° plies and a completely uninterrupted 56 ply laminate. These particular specimens were then tabbed and tested. The differentiation between tabbed and untabbed specimens is not made for the test results since it was determined to be unimportant.

2. ENVIRONMENTAL CONDITIONING

A limited number of specimens and concepts were environmentally conditioned. Concept number one, orientation number two and three, were preconditioned at 180°F at 91% humidity. A set of specimens of this same concept was also thermally cycled by the Center for Composite Materials, College of Engineering, University of Delaware, between the temperatures of -41°F and 318°F for 100 cycles. These thermally cycled specimens were not soaked specimens. The flatwise tension and transverse test results for these environmentally conditioned specimens, both soaked and thermally cycled, are presented in Figure 46 and Figure 51 respectively.

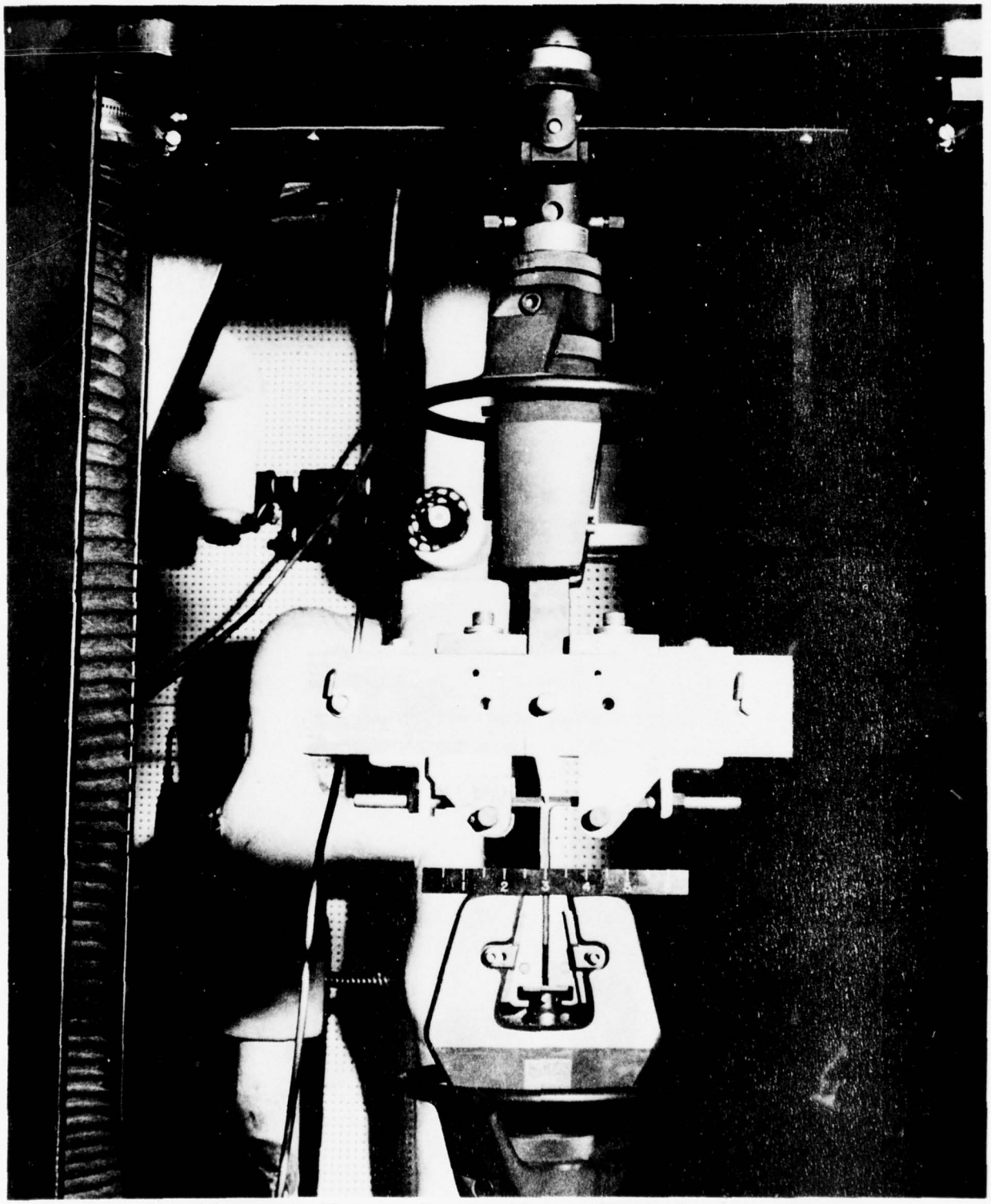

Figure 38 - Flatwise Tension Fixture/Simply Supported Edges

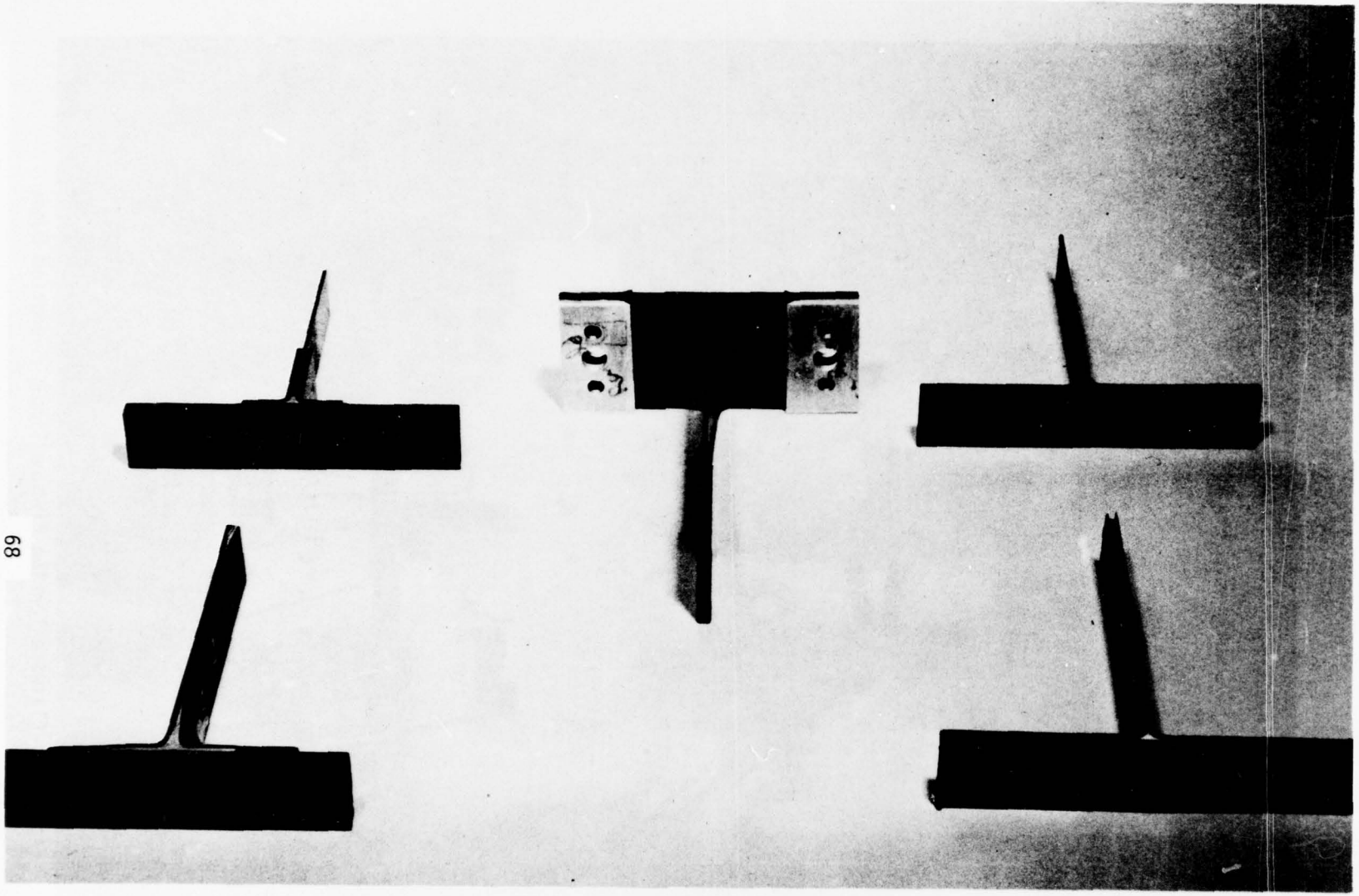

Figure 39 - SASIP Specimens

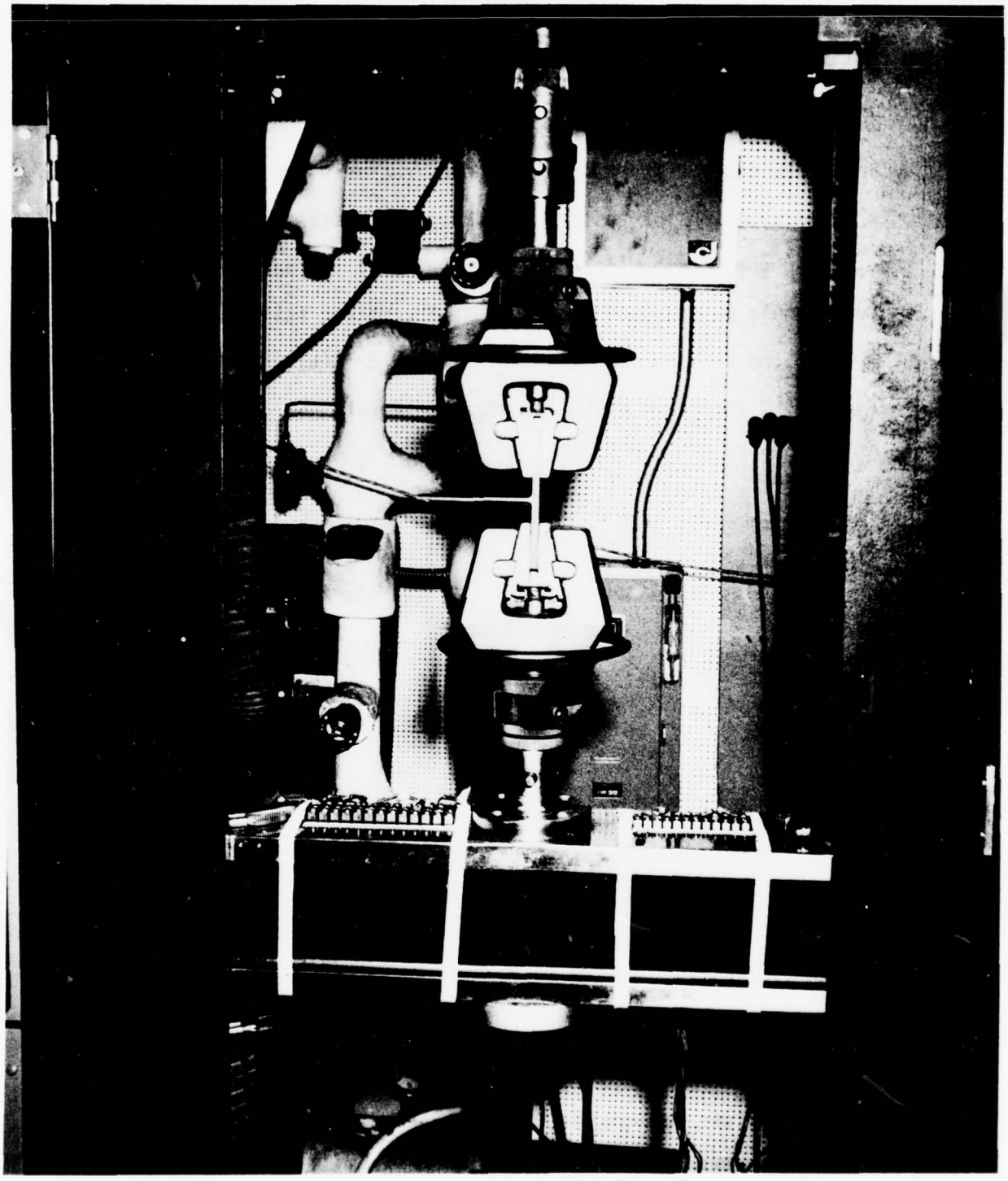

Figure 40 - Transverse Tension Test Set-up

3. TEST RESULTS

Flatwise tension tests were performed on all of the F-16 concepts defined previously. There were common characteristics of a large majority of the flatwise tension tests which should be discussed briefly. Since the loading rate of the Instron was set at 0.01 in./sec., any individual failures could be seen and observed until complete failure occurred.

As can be seen from the typical load deflection curve presented in Figure 41, there are a few points of interest.

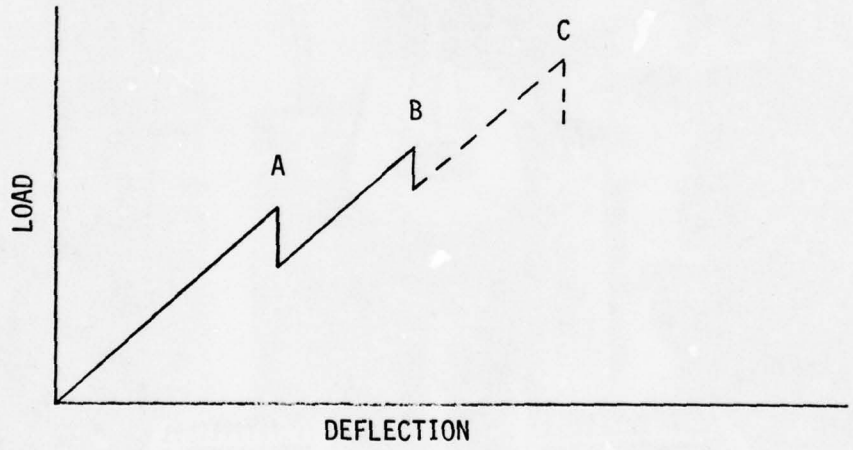

Figure 41

First to be considered is point A. Prior to reaching point A on the curve, as the load was increased the composite specimen typically made slight snapping sounds which were audible but which did not show up on the plot as distinct variations from the curve. However, at point A, a distinct failure occurred in the radius of the fillet area as shown in Figure 42. This failure generally occurred in an interlaminar fashion

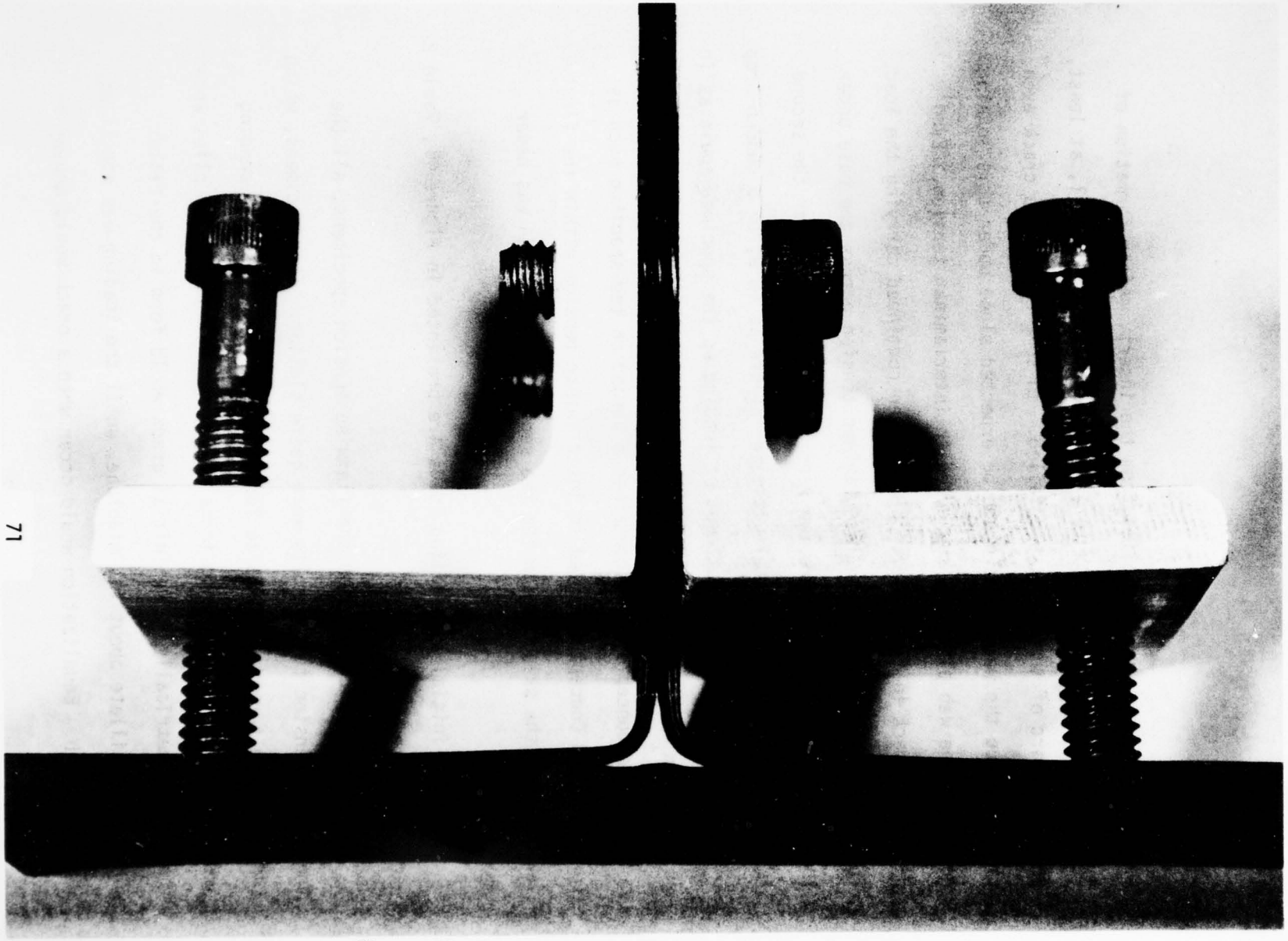

Figure 42 - Concept No. 1, Flatwise Tension Failure

within the first couple of plies from the insert. After formation of this crack, it had a tendency to grow in each direction until, at least, the entire arc of the fillet had failed. In some cases, the crack even progressed up the web. This would be expected since under this loading condition the web plies are subjected to interlaminar tension. Even with this crack in the fillet, the specimen continued carrying the load. The next failure occurred in interlaminar tension across the base under the fillet insert. There are two versions of this curve for the second failure. It is either a total ultimate failure as in B, or a sudden drop in the loading and then an attempt at loading up the specimen again as in curve C. In most cases, it did not exceed the final failure of curve B.

The concepts which contained a bonded-on tee specimen such as Concept 3 and Concept 6 failed in interlaminar tension within the first few plies of the skin beneath the tee section. Concept 6A was never fabricated.

The initial and failing loads are presented in Figure 46, Table 2 and Appendix B.

As was the case with the flatwise tension specimens, all the transverse tension test results were quite similar. The specimens, which contained the turned-up plies to form the web, were placed in bending during the transverse tension tests since the continuous skin plies were loaded unsymmetrically. The initial crack would form in the fillet. The web would oscillate about its midplane, until the loading was equalized across the web. Equalization would occur when a crack would appear in

the opposite fillet and along the centerline of the web. Failures of these skin laminates would then be a result of bending in the skin due to the unsymmetrical loading.

In the case of the bonded-on tee's, the initial failures were a disbonding of one leg of the tee from the skin laminate. The skin laminate then proceeded to fail in tension.

The initial and failing loads for the transverse tension condition are presented in Figure 51, Table 2, and Appendix B.

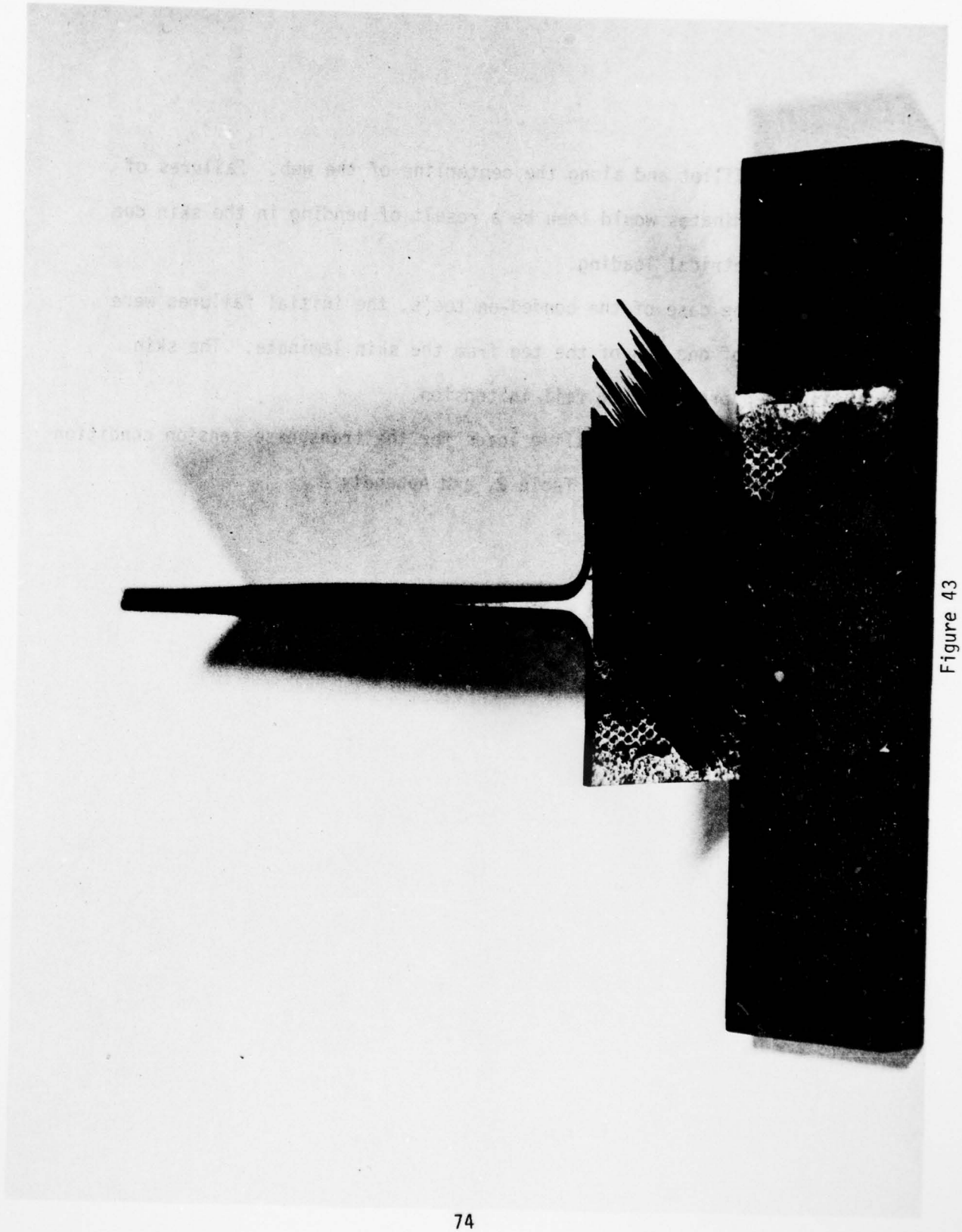

Figure 43

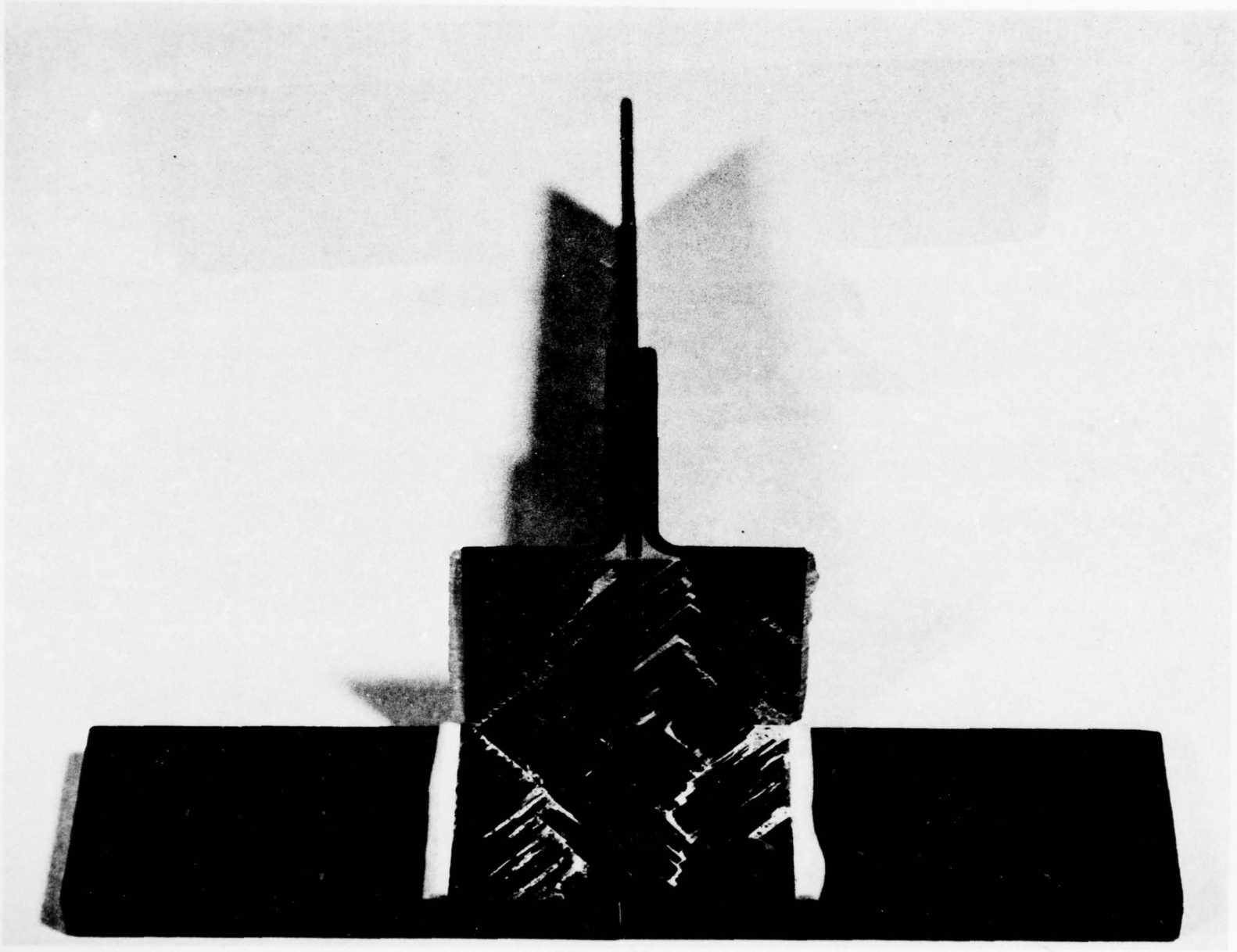

Figure 44

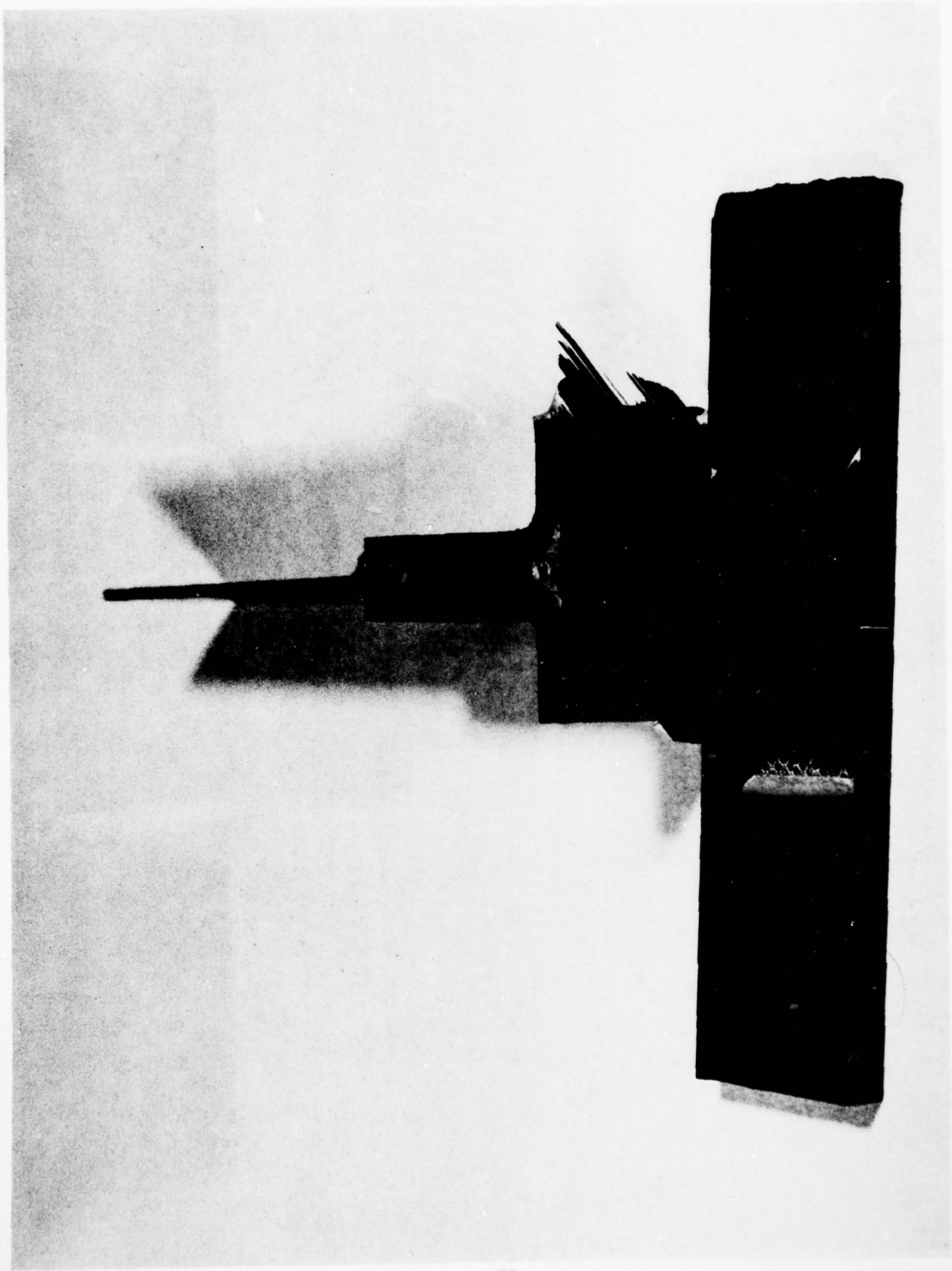

Figure 45

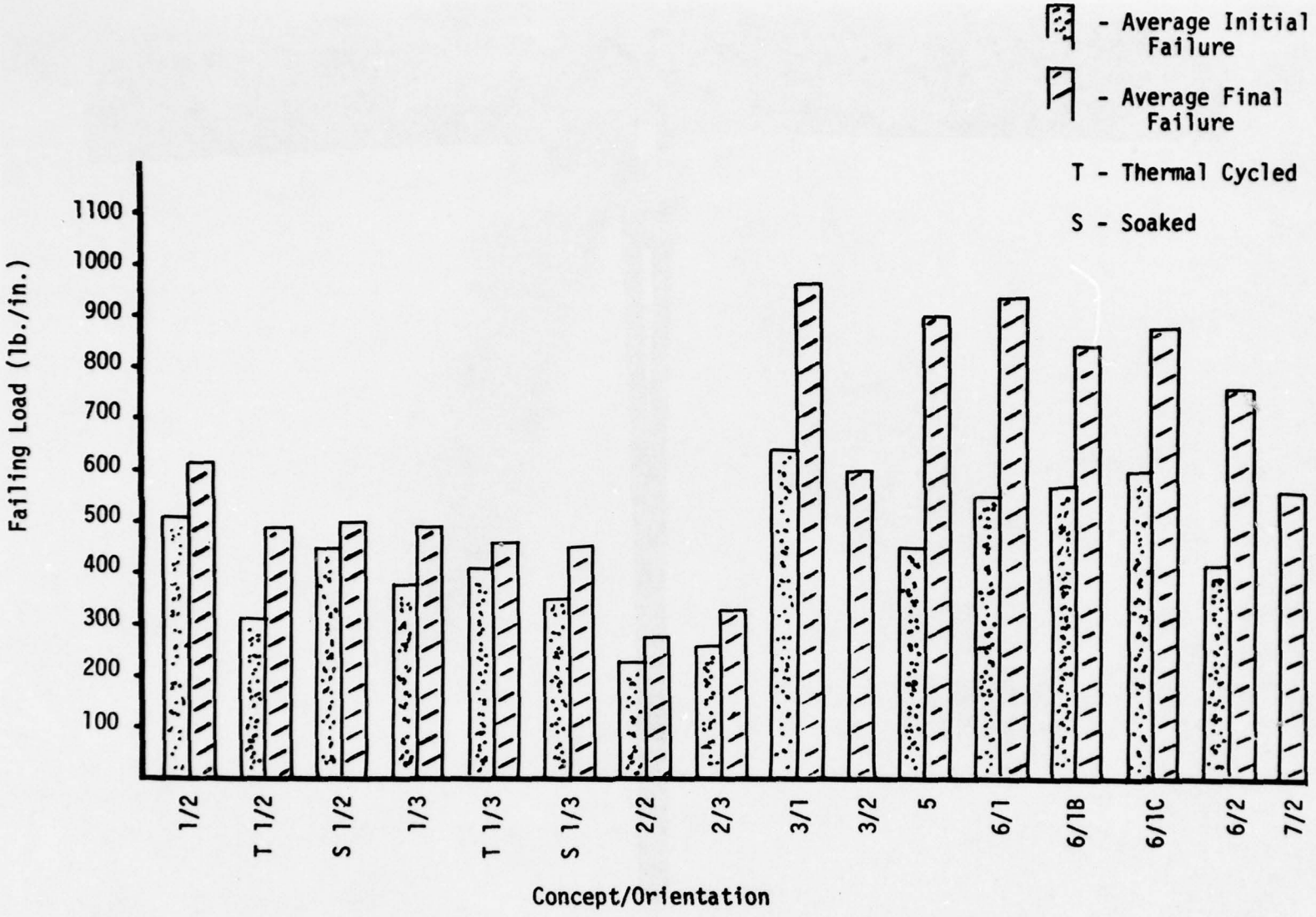

Figure 46 - FLATWISE TENSION TEST RESULTS

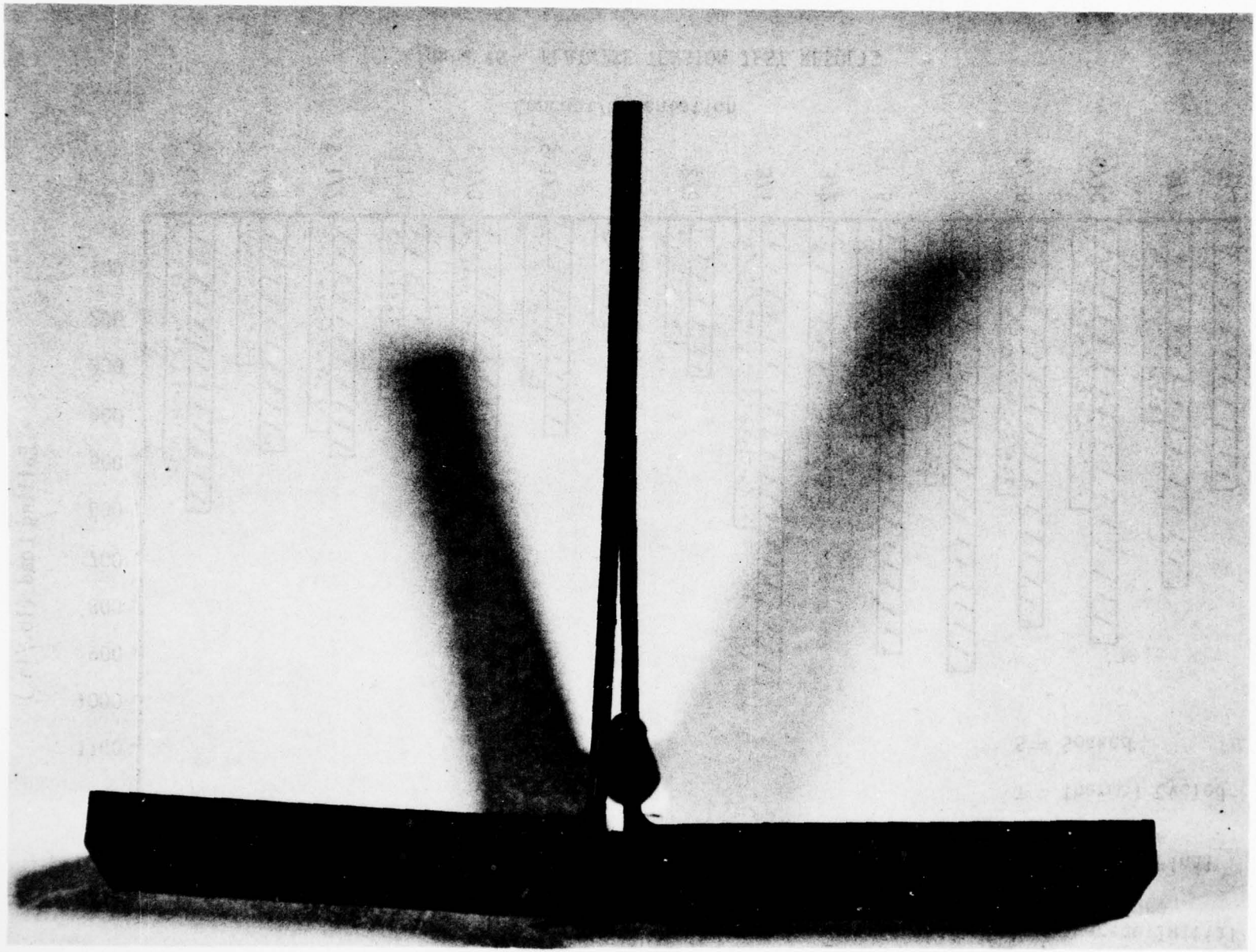

Figure 47 - Transverse Tension Failure

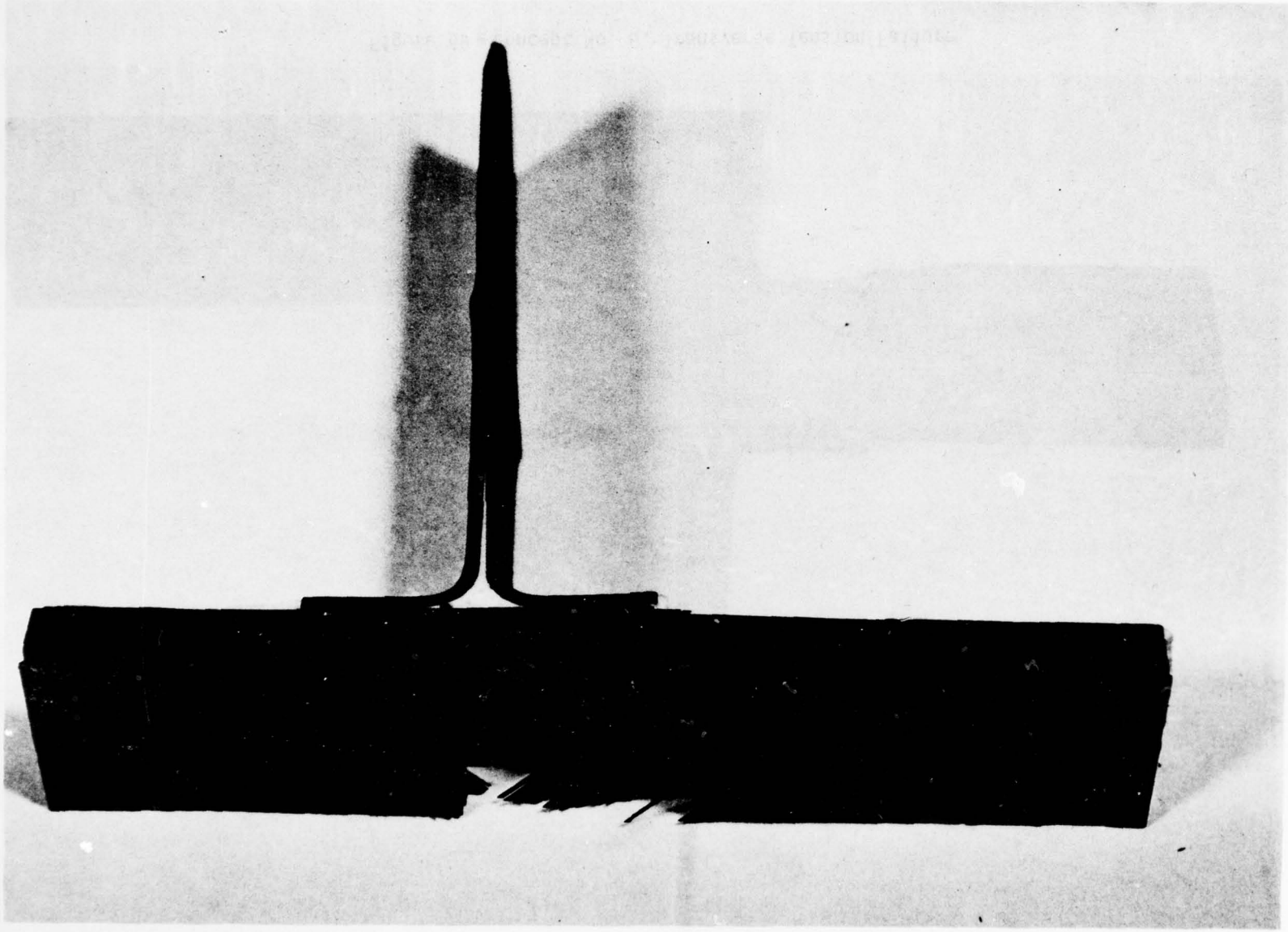

Figure 48 - Concept No. 3, Transverse Tension Failure

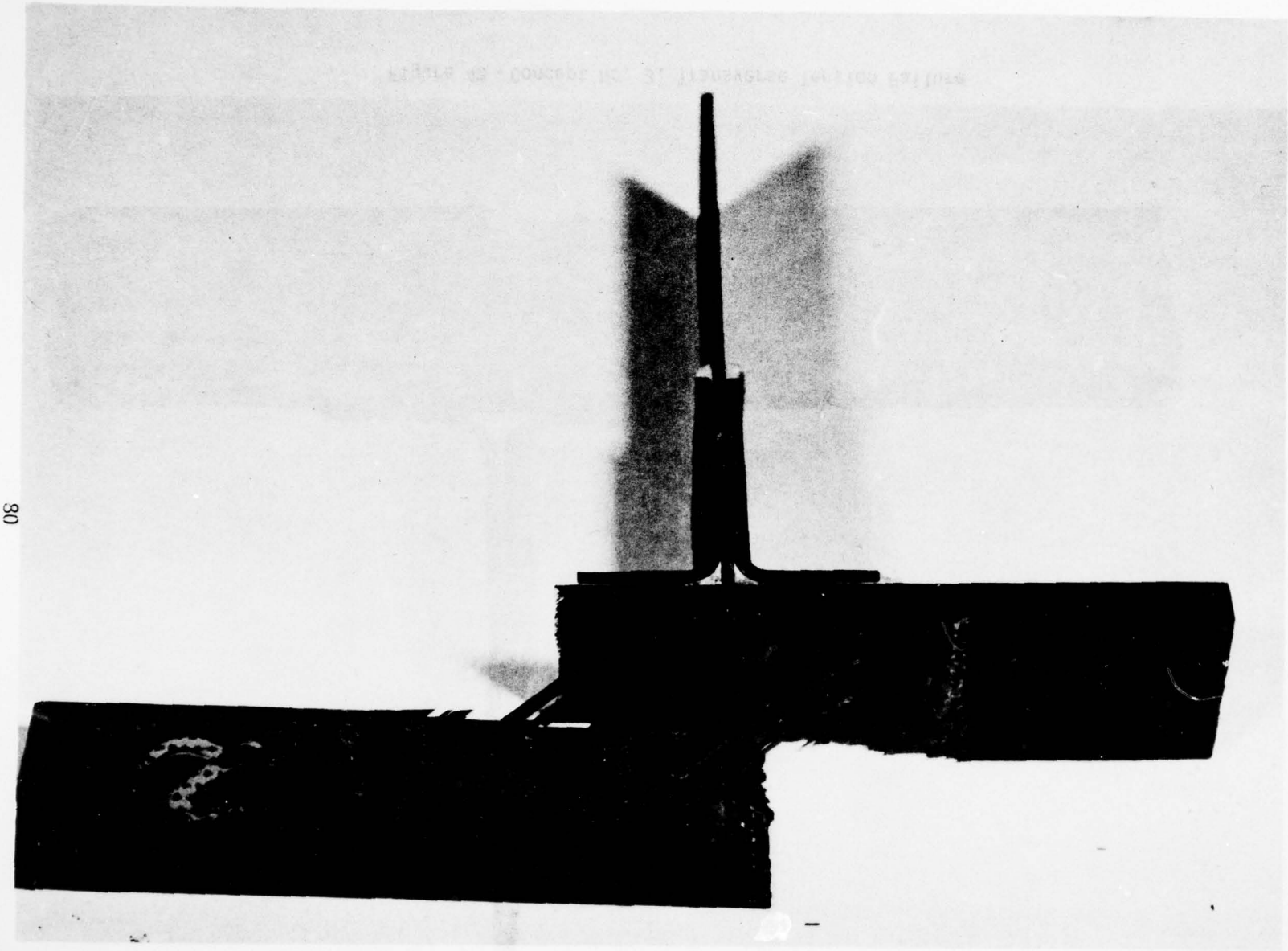

Figure 49 - Concept No. 6, Transverse Tension Failure

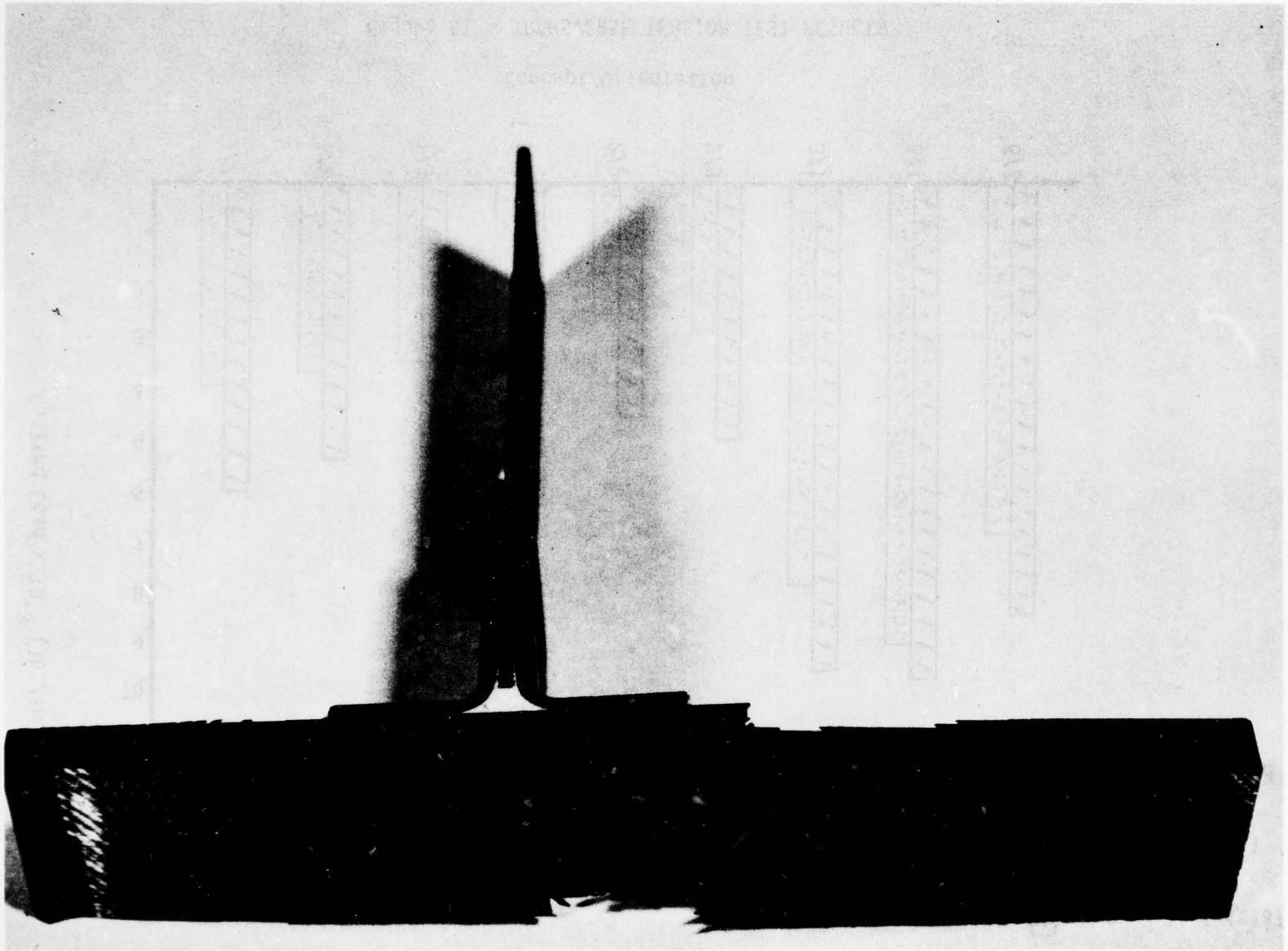

Figure 50 - Concept No. 6, Revision C - Transverse Tension Failure

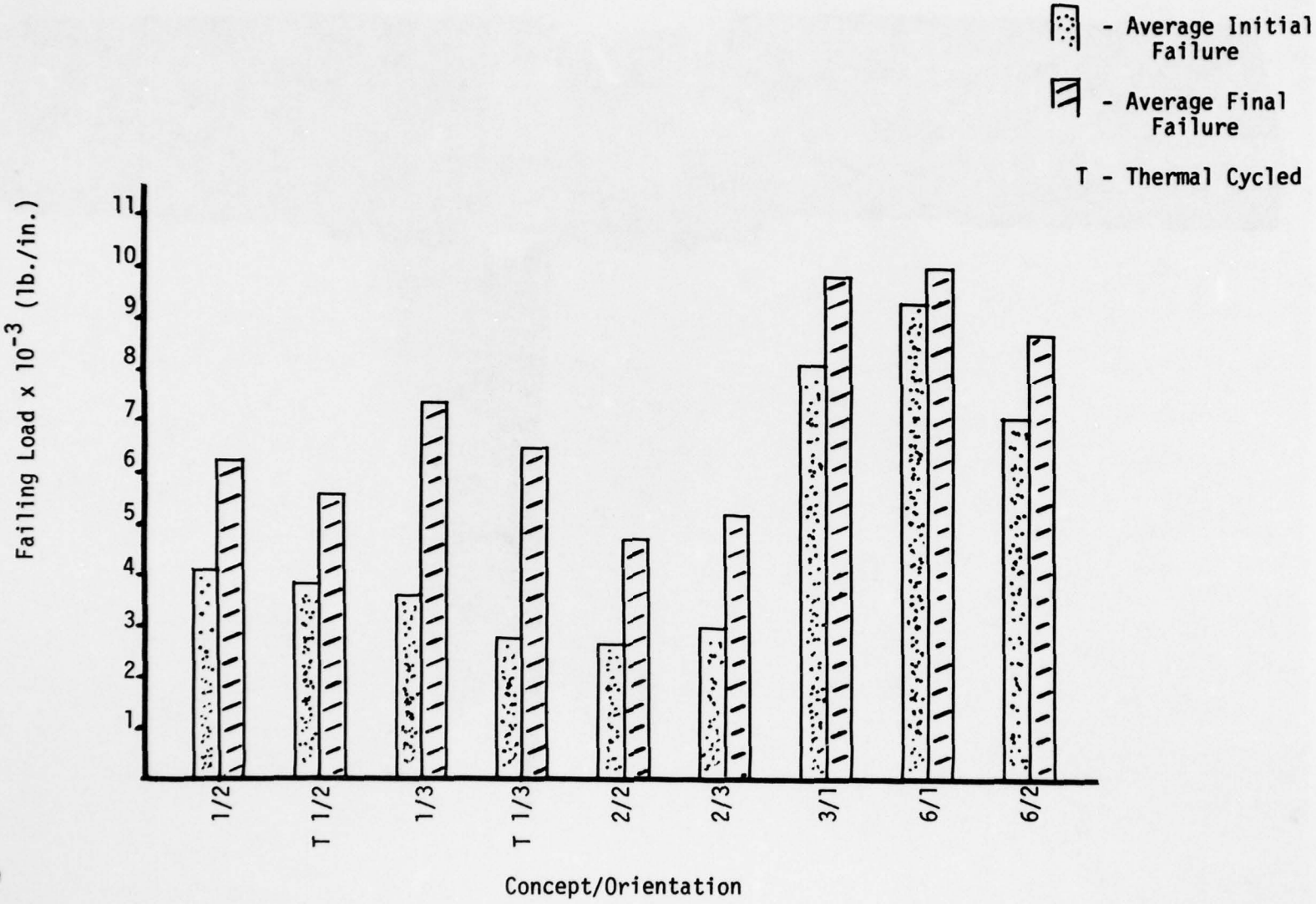

Figure 51 - TRANSVERSE TENSION TEST RESULTS

VI CONCLUSIONS

The conclusions from this effort can be divided into two distinct areas. These two areas are manufacturing and concept validation. In the manufacturing area, the following conclusions may be drawn:

1. The use of thin metal cauls does not guarantee a precise part profile. Therefore, substantial tooling should be used to manufacture any specimens of the type used for this program.

2. The overstuffing of root filler material in the fillet area does not reduce the amount of dimpling in the base opposite the upstanding web. This dimpling is apparently more involved with the wash of fibers from the base into the web. To alleviate this type of dimpling the web top and edges should be sealed during curing to eliminate wash out of fibers and resin from the web and from the base into the web.

3. The use of bleeder plies and separator sheets in the web should be avoided in order to assure a wrinkle free condition and to help increase the resin content in the web.

4. The use of a porous lower caul plate between the base and the bleeder plies beneath the base would be desirable to reduce the effects of dimpling.

5. The filler used in the fillet area should have strength multidimensionally in order to prevent premature cracking in this area.

6. The use of a diamond wheel saw blade should be used for all cutting operations. The polished surface which results from this type of cutting operation reduces the effects of cracks starting due to

machining flaws on the surface.

7. All tooling employed in this program, once the problems with each type are solved, can be used to produce composite specimens. This includes various types of hard autoclave type tooling as well as various types of elastomeric tooling.

8. Silicone rubber reusable vacuum bagging works satisfactorily provided care is taken in treating the inside of the bag with a coating which will protect it from the resin. The life of this silicone rubber bagging is approximately five cure cycles.

9. The Narmco 5208/T300 system, with its greater flow, is a more difficult material to work with compared to the Hercules 3501/AS system.

10. The use of stops to accurately control the web thicknesses in the hard autoclave tooling did not produce voidy parts.

In the concept validation area, the following conclusions may be drawn:

1. Simply supported flatwise tension testing is superior to the fixed-fixed variety of flatwise tension testing. The simply supported method improves test repeatability, ease of test set-up, and time required for test set-up. Furthermore, the end conditions for a simply supported specimen are the same for all tests, whereas, any fixed-fixed set-up will be influenced by the degree of fixity which will vary from one test to the next. Since the stresses which were simulated in the root area of the simply supported flatwise tension tests were the same as those simulated

AD-A071 715 AIR FORCE FLIGHT DYNAMICS LAB WRIGHT-PATTERSON AFB OH F/G 1/3
SKIN AND SPAR INTERFACE PROGRAM (SASIP).(U)
MAY 79 A GONSISKA, R T ACHARD

UNCLASSIFIED AFFDL-TR-79-3054 NL

2 OF 2
AD
A071715

END
DATE
FILMED
8-79
DDC

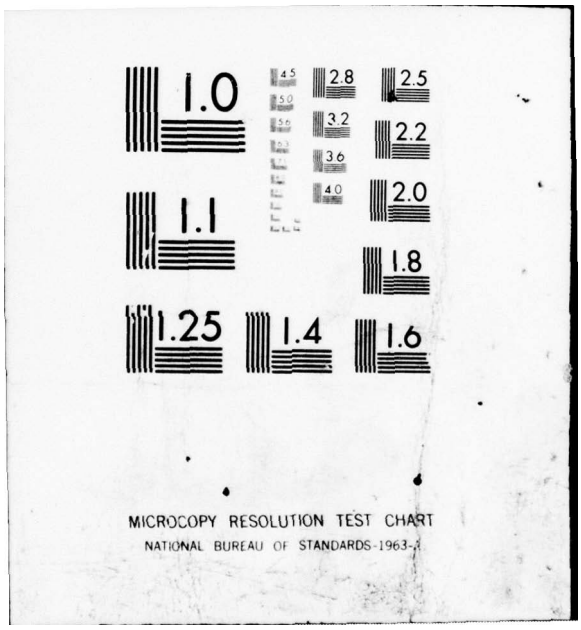
1.0
1.1
1.25
1.4
1.6
1.8
2.0
2.2
2.5
2.8
3.2
3.6
4.0
4.5
5.0
5.6
MICROCOPY RESOLUTION TEST CHART
NATIONAL BUREAU OF STANDARDS-1963-A

in the root area of the fixed-fixed flatwise tension tests, the two types of testing are directly comparable.

2. The loading speed used during the flatwise testing, although it may or may not affect the actual failure load or the types of failures encountered, does play an important role in the understanding of the failures. The slower the speed the better the various cracking mechanisms can be seen. If the tests are run at an accelerated rate, the failures occur so quickly that they may be interpreted as a single failure as opposed to several small cracks which when combined cause ultimate failure.

3. The deeper the penetration into the skin laminate the design goes to obtain the necessary plies to form the web, the poorer that concept will behave. Therefore, as was borne out by the testing, the bonded-on concepts are the best since they do not interrupt any of the skin lamina.

4. The chordwise loading does not appear to be a problem since the strength in this direction is adequate. Furthermore, the better concepts for the flatwise tension loading condition are also the better concepts for the chordwise loading condition since they have the most number of continuous plies.

APPENDIX A

VARIABLE EI BEAM ANALYSIS

(Reference 3)

A beam with variable EI's and loaded with a load at center:

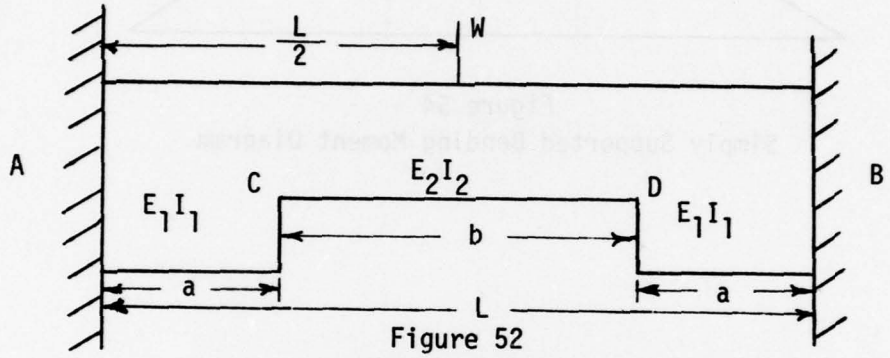

Figure 52
Beam Geometry

AB is a beam of span L and is fixed at supports A and B (Figure 52). It carries a concentrated load W at the center. The stiffness E_2I_2, at the middle portion CD of the beam is constant over the length b. The stiffness, E_1I_1 for the end portions AC, and DB is uniform over the length a.

The resultant bending moment diagram is shown in Figure 55 where M_α and M_β are the fixed end moments. The resultant bending moment is obtained by superposing the fixed end bending moment diagram (Figure 53) and the simply supported bending moment diagram (Figure 54).

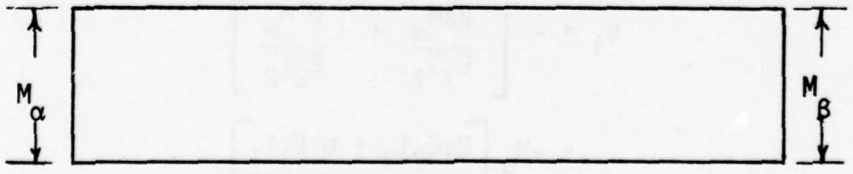

Figure 53
Fixed End Bending Moment Diagram

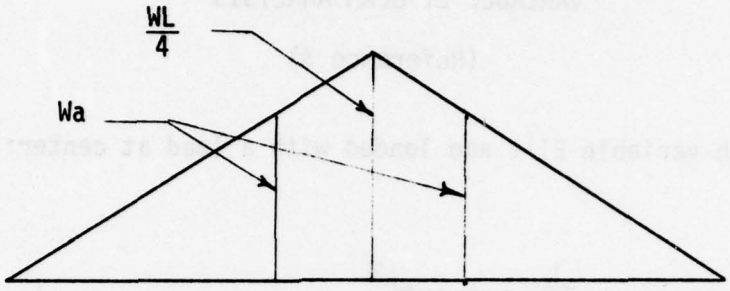

Figure 54
Simply Supported Bending Moment Diagram

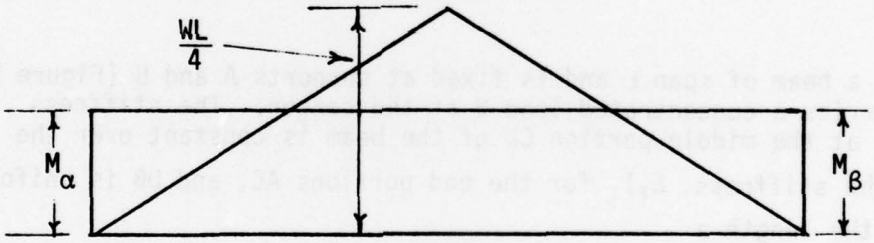

Figure 55
Resultant Bending Moment Diagram

For the case of fixed end moment, $M_\alpha = M_\beta$, and the change of slope θ_1 of the deflected beam from support A to support B is given by

$$\theta_1 = -\left[\frac{2aM_\alpha}{E_1I_1} + \frac{b\,M_\alpha}{E_2I_2}\right]$$

$$= -M_\alpha\left[\frac{2aE_2I_2 + b\,E_1I_1}{E_1I_1E_2I_2}\right]$$

Points of Contraflexure

Let the distance of the point of contraflexure from the left support be $\bar{a}$. Now there are three possibilities:

$$\text{i.e.,} \quad \bar{a} < a, \ \bar{a} = a \text{ or } \bar{a} > a$$

At the point of contraflexure simply supported bending moment = M_α

$$\frac{W}{8}\left[\frac{4a^2E_2I_2 + 4abE_1I_1 + b^2E_1I_1}{2aE_2I_2 + bE_1I_1}\right] = \frac{W\bar{a}}{2}$$

$$\bar{a} = \frac{l}{4}\left[\frac{4a^2E_2I_2 + 4abE_1I_1 + b^2E_1I_1}{2aE_2I_2 + bE_1I_1}\right] \qquad (2)$$

when $b = 0$, $E_1I_1 = E_2I_2$ i.e., beam is of uniform section

$$\bar{a} = \frac{a}{2} = \frac{L}{4}$$

Simplifying Formula 2

$$\bar{a} = \frac{L}{4}\left[\frac{4a^2 + \frac{E_1I_1}{E_2I_2}(4ab + b^2)}{2a + b\frac{E_1I_1}{E_2I_2}}\right]$$

Simplifying Formula 1

$$M_\alpha = \frac{W}{8}\left[\frac{4a^2 + \frac{E_1I_1}{E_2I_2}(4ab + b^2)}{2a + b\frac{E_1I_1}{E_2I_2}}\right]$$

The change of slope θ_2 of the deflected beam from the support A to the support B due to the simply supported bending moment is given by

$$\theta_2 = 2 \frac{Wa}{2} \times \frac{a}{2} \times \frac{1}{E_1 I_1} + 2 \left[\left(\frac{Wa}{2} + \frac{WL}{4} \right) \frac{b}{4 E_2 I_2} \right]$$

$$= \frac{Wa^2}{2E_1 I_1} + \frac{Wab}{4E_2 I_2} + \frac{WLb}{8E_2 I_2}$$

since $L = 2a + b$

$$\theta_2 = \frac{Wa^2}{2E_1 I_1} + \frac{Wab}{4E_2 I_2} + \frac{b(2a+b)W}{8E_2 I_2}$$

$$= \frac{W}{8} \left[\frac{4a^2 E_2 I_2 + 4abE_1 I_1 + b^2 E_1 I_1}{E_1 I_1 E_2 I_2} \right]$$

The change of slope θ_3 of the deflected beam from A to B due to the resultant moment can be expressed as:

$$\theta_3 = \theta_1 + \theta_2$$

For the fixed ended beam $\theta_3 = 0$. Therefore

$$\theta_1 + \theta_2 = 0$$

or
$$M_\alpha = \frac{W}{8} \left[\frac{4a^2 E_2 I_2 + 4abE_1 I_1 + b^2 E_1 I_1}{2aE_2 I_2 + bE_1 I_1} \right] \qquad (1)$$

when $b = 0$ $\quad E_1 I_1 = E_2 I_2$, and $L = 2a$

$$M_\alpha = \frac{W}{8} \cdot 2a = \frac{WL}{8}$$

VARIABLE EI ERROR PREDICTION DATA

Values of "a" used in these calculations are based on an $\ell = 5.33$.

Concept	Orientation	Case	E_aI_a	E_bI_b	$\bar{a}$	% Error
1	1	1	1.5E+04	9.3E+03	1.3850	4.0
1	1	2	1.5E+04	9.3E+03	1.3122	-1.6
1	1	3	1.5E+04	7.8E+03	1.4093	6.0
1	1	4	1.5E+04	7.8E+03	1.3255	-0.6
1	2	1	8.8E+03	6.2E+03	1.3687	2.7
1	2	2	8.8E+03	6.2E+03	1.3035	-2.2
1	2	3	8.8E+03	4.7E+03	1.4052	5.6
1	2	4	8.8E+03	4.7E+03	1.3233	-0.8
2	1	1	1.5E+04	9.0E+03	1.3885	4.3
2	1	2	1.5E+04	9.0E+03	1.3141	-1.5
2	1	3	1.5E+04	7.5E+03	1.4158	6.5
2	1	4	1.5E+04	7.5E+03	1.3291	-0.4
2	2	1	8.8E+03	7.0E+03	1.3734	3.0
2	2	2	8.8E+03	6.0E+03	1.3060	-2.1
2	2	3	8.8E+03	4.4E+03	1.4153	6.5
2	2	4	8.8E+03	4.4E+03	1.3288	-0.4
3	1	1	2.9E+04	2.0E+04	1.3755	3.2
3	1	2	2.9E+04	2.0E+04	1.3071	-2.0
3	1	3	2.9E+04	1.7E+04	1.3936	4.7
3	1	4	2.9E+04	1.7E+04	1.3169	-1.3
3	2	1	1.7E+04	1.3E+04	1.3632	2.2
3	2	2	1.7E+04	1.3E+04	1.3005	-2.5
3	2	3	1.7E+04	1.0E+04	1.3927	4.6
3	2	4	1.7E+04	1.0E+04	1.3164	-1.3

Table A-1

VARIABLE EI ERROR PREDICTION DATA (Table A-1 Con't)

Case

1 a = 2.472 b = full width of triangle = 0.387 E_bI_b = full laminate

2 a = 2.472 b = 1/2 width of triangle = 0.194 E_bI_b = full laminate

3 a = 2.472 b = full width of triangle E_bI_b = 0's degraded in laminate

4 a = 2.472 b = 1/2 width of triangle E_bI_b = 0's degraded in laminate

$$\% \text{ error} = \frac{1.333 - (2.667 - \bar{a})}{(2.667 - \bar{a})} \times 100$$

Table A-1 Con't

APPENDIX B

Test Data

APPENDIX B

TEST DATA

Concept No. 1 Orientation No. 2

Loading Condition	Room Temp - Dry			Thermal Cycled			Soaked		
	Specimen	Failure Initial (lb./in.)	Failure Final (lb./in.)	Specimen	Failure Initial (lb./in.)	Failure Final (lb./in.)	Specimen	Failure Initial (lb./in.)	Failure Final (lb./in.)
Flatwise Tension	S-2-1	338	625	S-15-10	306	487	S-2-5		534
	S-2-2	645	728	S-15-26		480	S-2-6	446	448
	S-2-7	659	705				S-2-24		497
	S-15-1		455						
	S-15-2		604						
	S-15-3	370	534						
Transverse Tension	S-2-3	3622	5995	S-15-4	2803	5903			
	S-2-4	3625	5985	S-15-21	4918	5172			
	S-2-8	3918	7280						
	S-2-9	4710	6296						
	S-2-10	4608	5946						
	S-2-21	5206	6967						
	S-2-22	4019	6450						
	S-2-23	4576	6623						
	S-2-25	4042	6946						
	S-2-26	4483	5931						

Table B-1

APPENDIX B (Con't)

TEST DATA

Concept No. 1 Orientation No. 2

Loading Condition: Room Temp - Dry

	Specimen	Failure Initial (lb./in.)	Failure Final (lb./in.)
Transverse Tension	S-2-27	5401	6803
	S-2-28	4200	7187
	S-2-29	4985	6915
	S-15-5	3249	5358
	S-15-6	3814	5069
	S-15-7	3599	5534
	S-15-8	3142	5523
	S-15-9	2686	5155

Table B-1 (Con't)

TEST DATA

Concept No. 1 Orientation No. 3

Loading Condition	Room Temp - Dry			Thermal Cycled			Soaked		
	Specimen	Failure Initial (lb./in.)	Failure Final (lb./in.)	Specimen	Failure Initial (lb./in.)	Failure Final (lb./in.)	Specimen	Failure Initial (lb./in.)	Failure Final (lb./in.)
Flatwise Tension	S-14-1		347	S-14-4	358	369	S-1-4		497
	S-14-2	374	410	S-14-21	457	548	S-1-6	323	449
	S-1-7		699				S-1-30	362	391
Transverse Tension	S-14-5	1809	6951	S-14-10	2585	5783			
	S-14-6	1978	6278	S-14-25	2985	7043			
	S-14-7	2231	7339						
	S-14-8	3722	6687						
	S-14-9	1696	5891						
	S-1-3	3866	7362						
	S-1-5	2860	6471						
	S-1-8	4573	6331						
	S-1-10	4090	8177						
	S-1-21	2791	6788						
	S-1-22	3594	7697						
	S-1-23	4796	6995						
	S-1-24	5346	8409						
	S-1-25	4106	8304						
	S-1-26	3360	7801						
	S-1-27	6436	7921						
	S-1-28		8082						
	S-1-29	3729	8121						

Table B-2

TEST DATA

Concept No. 2 Orientation No. 2

Loading Condition	Specimen	Room Temp - Dry Failure	
		Initial (lb./in.)	Final (lb./in.)
Flatwise Tension	S-8-1	236	282
	S-8-2	272	300
	S-8-3	170	242
Transverse Tension	S-8-4	2693	4622
	S-8-5	2439	4729
	S-8-6	2927	4808
	S-8-7	1974	4673
	S-8-8	3232	4619

Table B-3

TEST DATA

Concept No. 2 Orientation No. 3

Loading Condition	Specimen	Room Temp - Dry Failure	
		Initial (lb./in.)	Final (lb./in.)
Flatwise Tension	S-9-1	287	323
	S-9-2	239	323
	S-9-7	248	337
Transverse Tension	S-9-3	4294	4410
	S-9-4	2949	4971
	S-9-5	2237	5133
	S-9-6	2508	5818
	S-9-8	2564	5240

Table B-4

TEST DATA

Concept No. 3 Orientation No. 1

Loading Condition	Specimen	Room Temp - Dry Failure	
		Initial (lb./in.)	Final (lb./in.)
Flatwise Tension	S-24-7		1330
	S-24-1	831	1062
	S-24-4		950
	S-24-5		1032
	S-17B-1	520	707
	S-17B-3	591	1002
	S-17B-1C	619	934
	S-17B-2C	476	1051
	S-17B-3C	545	698
	S-17B-4C	559	810
	S-17B-5C	524	856
	S-18-1	977	1037
	S-18-2	948	1162
	S-18-3	518	864
	S-18-4	498	910
Transverse Tension	S-24-0		11284
	S-24-2		13265
	S-24-6		10446
	S-19-3	8324	9125
	S-19-4	8099	9176
	S-19-5	7663	8440
	S-19-6	8242	8600
	S-19-7		7180

Table B-5

TEST DATA

Concept No. 3 Orientation No. 2

Loading Condition	Specimen	Room Temp - Dry Failure	
		Initial (lb./in.)	Final (lb./in.)
Flatwise Tension	S-19-1		658
	S-19-2		537
Concept No. 5 Orientation			
Flatwise Tension	S-26-1		899
	S-26-2		1183
	S-26-3		844
	S-26-8	449	644

Table B-6

TEST DATA

Concept No. 6 Orientation No. 1

Loading Condition	Specimen	Room Temp - Dry Failure	
		Initial (lb./in.)	Final (lb./in.)
Flatwise Tension	S-23-3		799
	S-23-2		1025
	S-23-1		994
	S-22-3	409	1094
	S-22-2	542	911
	S-22-1	542	847
	S-25-1	648	897
	S-25-2	709	929
	S-25-3	511	1021
	S-25-4	516	881
Transverse Tension	S-25-5	9253	9806
	S-25-6		10277
	S-25-7		9654
Concept No. 6B			
Flatwise Tension	S-21-1	491	678
	S-21-3	405	861
	S-21-6	813	960
Concept No. 6C			
Flatwise Tension	S-21-4	517	851
	S-21-5	552	840
	S-21-7	855	937
	S-21-8	474	888

Table B-7

TEST DATA

Concept No. 6 Orientation No. 2

Loading Condition	Specimen	Room Temp - Dry Failure	
		Initial (lb./in.)	Final (lb./in.)
Flatwise Tension	S-10-7	406	756
	S-10-8	601	744
	S-10-9	182	925
	S-10-10	220	999
	S-20-1	443	664
	S-20-2	482	724
	S-20-5	554	604
	S-20-7	425	648
Transverse Tension	S-20-3		9156
	S-20-4	6555	9251
	S-20-6	7515	7521

Concept No. 7 Orientation No. 2

Flatwise Tension	S-11-1		580
	S-11-3		585
	S-11-5		664
	S-11-2b		511
	S-11-4b		417

Table B-8

APPENDIX C

Detail SASIP Drawings

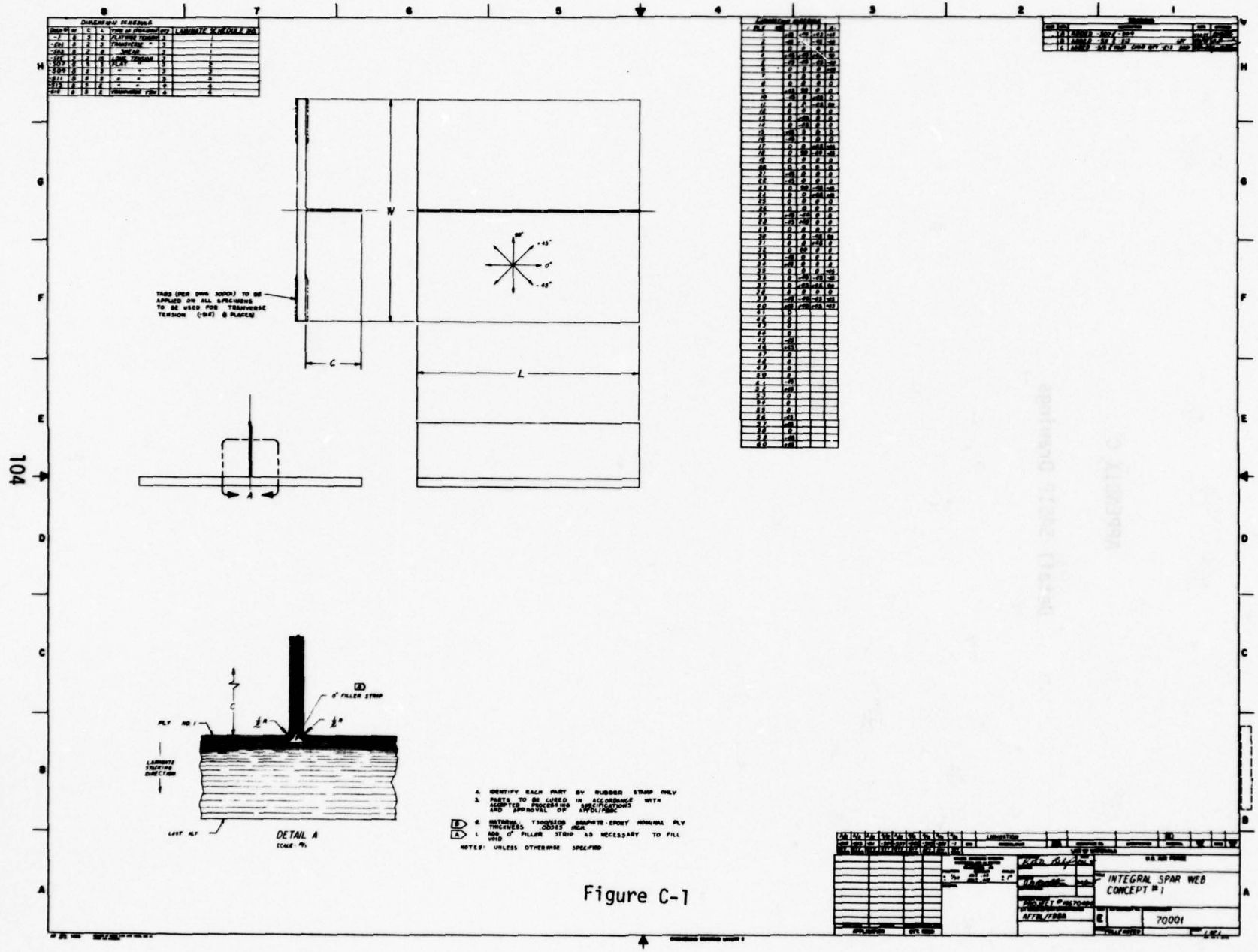
W
C
L
A
TABS (PER DWG 30001) TO BE APPLIED ON ALL SPECIMENS TO BE USED FOR TRANSVERSE TENSION (-90F) & PLACES)
0° FILLER STRIP
DETAIL A
INTEGRAL SPAR WEB CONCEPT #1
70001

Figure C-1

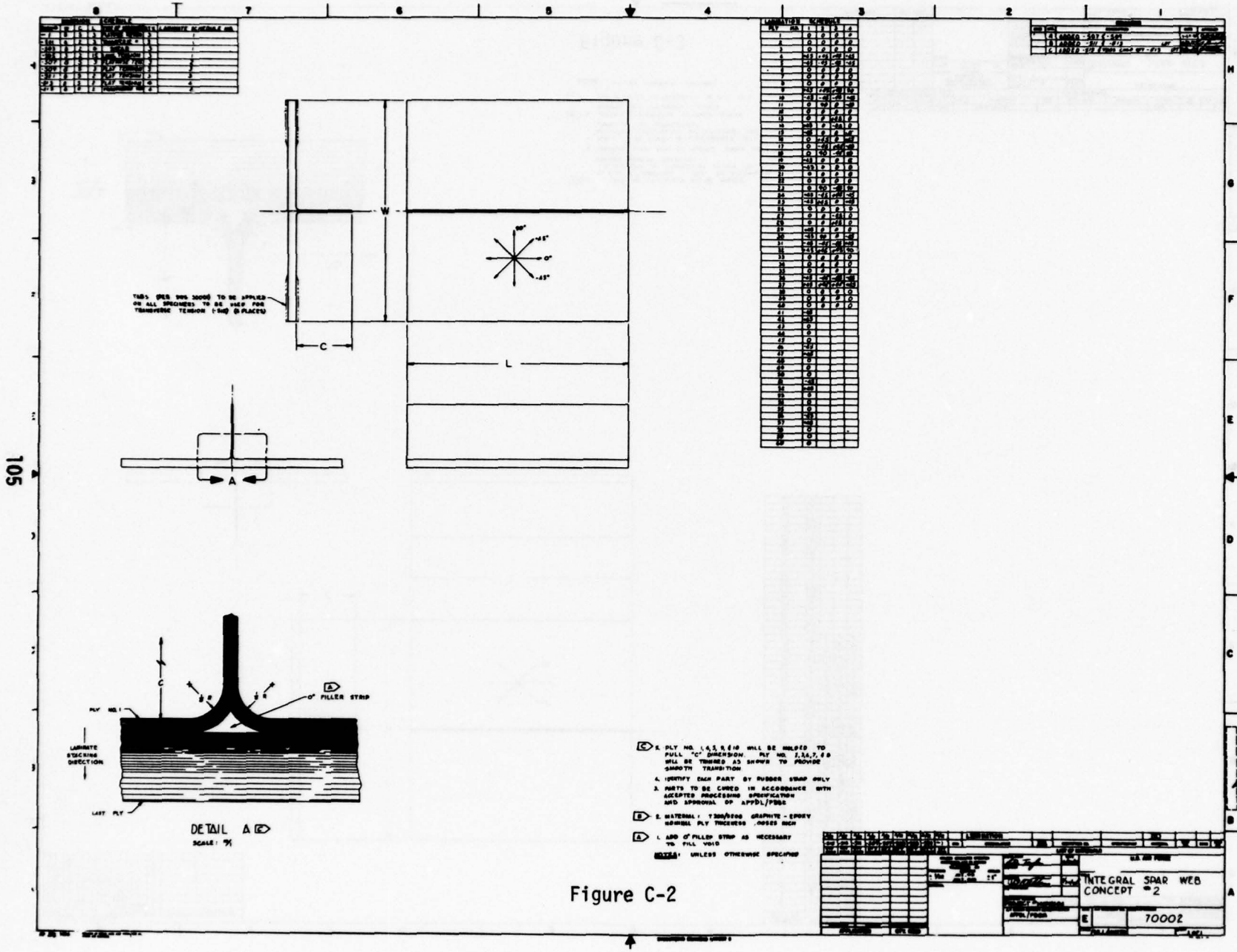

Figure C-2

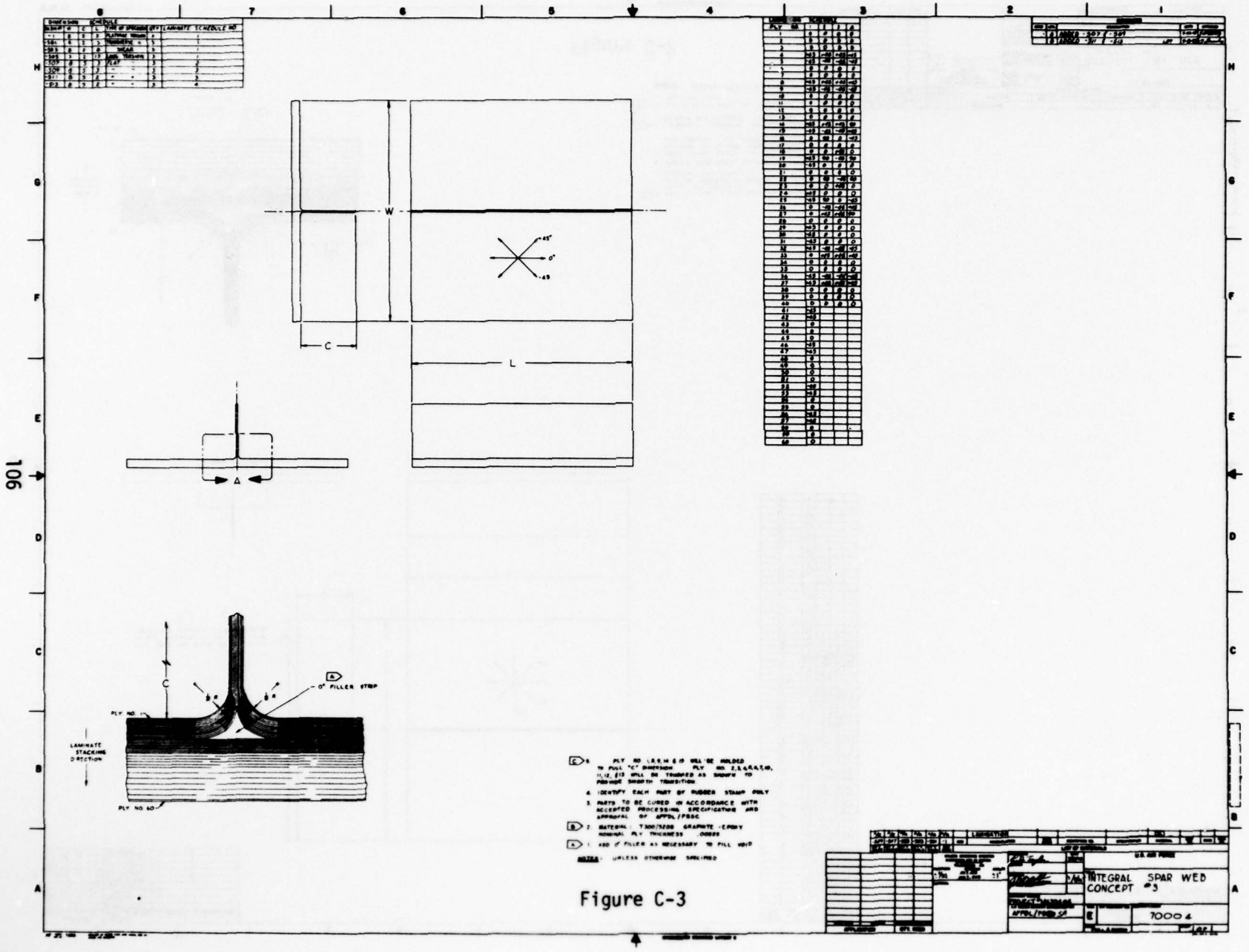
W
C
L
A
+45°
0°
-45
C
0° FILLER STRIP
PLY NO. 1
PLY NO. 60
LAMINATE STACKING DIRECTION
INTEGRAL SPAR WEB CONCEPT #3
7000 4

Figure C-3

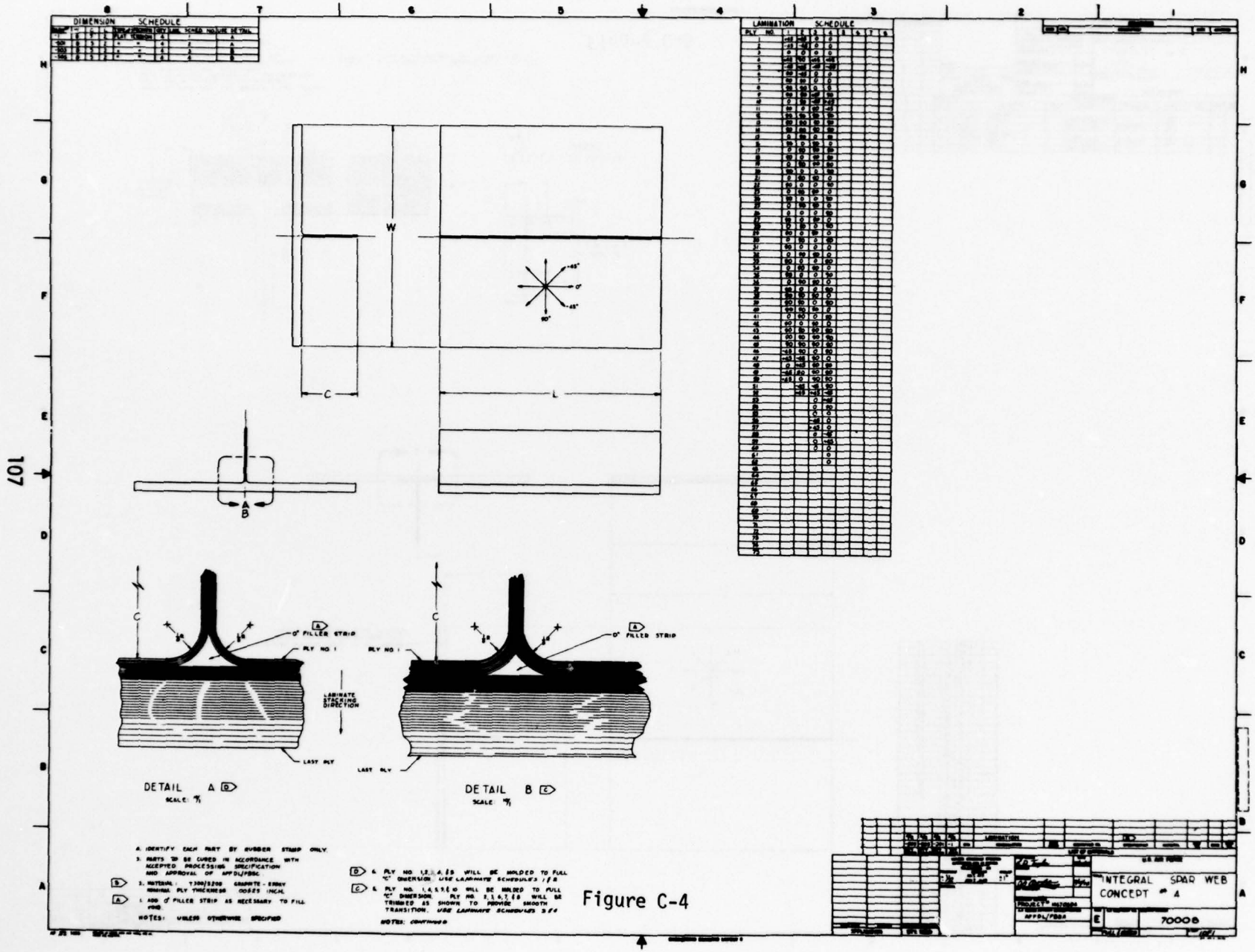
DIMENSION SCHEDULE
LAMINATION SCHEDULE
W
C
L
A
B
+45°
0°
-45°
90°
C
0° FILLER STRIP
PLY NO. 1
LAMINATE STACKING DIRECTION
LAST PLY
DETAIL A
SCALE: 1/1
DETAIL B
SCALE: 1/1
INTEGRAL SPAR WEB CONCEPT # 4
70008
107

Figure C-4

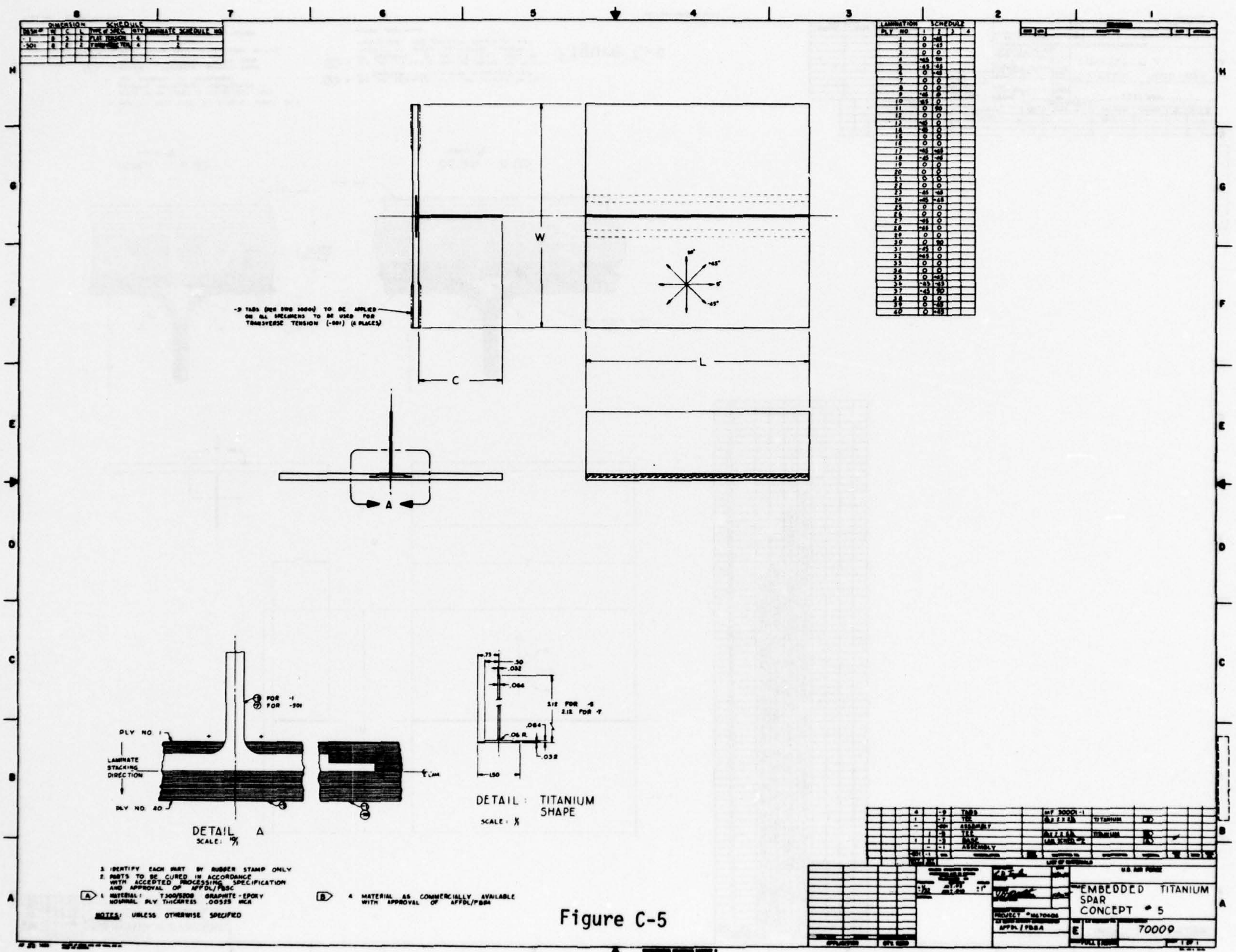
EMBEDDED TITANIUM SPAR CONCEPT # 5
70009
U.S. AIR FORCE
W
L
C
A
DETAIL A
DETAIL: TITANIUM SHAPE
PLY NO. 1
PLY NO. 40
LAMINATE STACKING DIRECTION
NOTES: UNLESS OTHERWISE SPECIFIED

Figure C-5

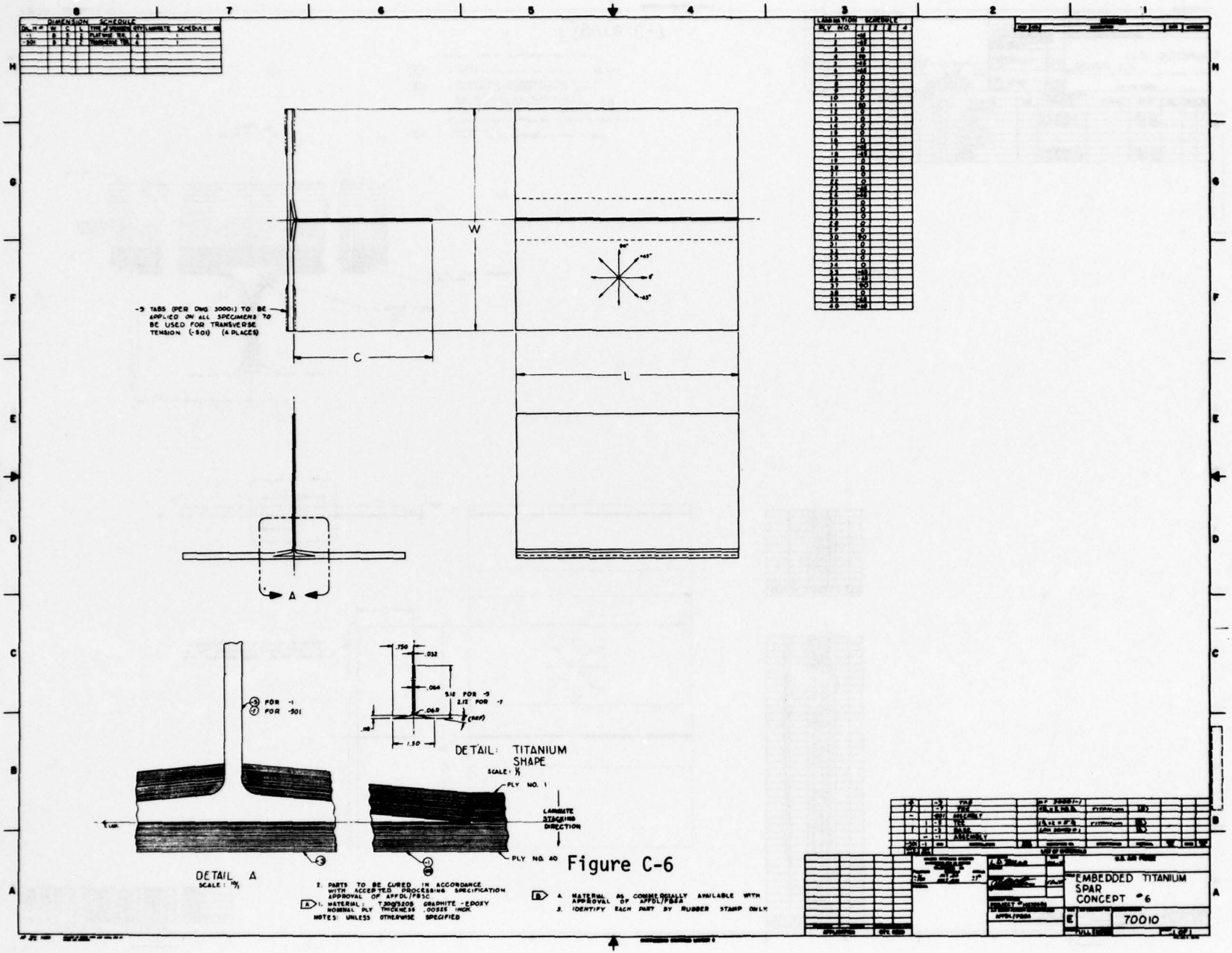
DIMENSION SCHEDULE
LAMINATE SCHEDULE
W
C
L
A
-9 TABS (PER DWG 30001) TO BE APPLIED ON ALL SPECIMENS TO BE USED FOR TRANSVERSE TENSION (-501) (4 PLACES)
DETAIL A
SCALE: 1/1
DETAIL: TITANIUM SHAPE
SCALE: 1/1
PLY NO. 1
PLY NO. 40
LAMINATE STACKING DIRECTION
NOTES: UNLESS OTHERWISE SPECIFIED
EMBEDDED TITANIUM SPAR CONCEPT #6
70010

Figure C-6

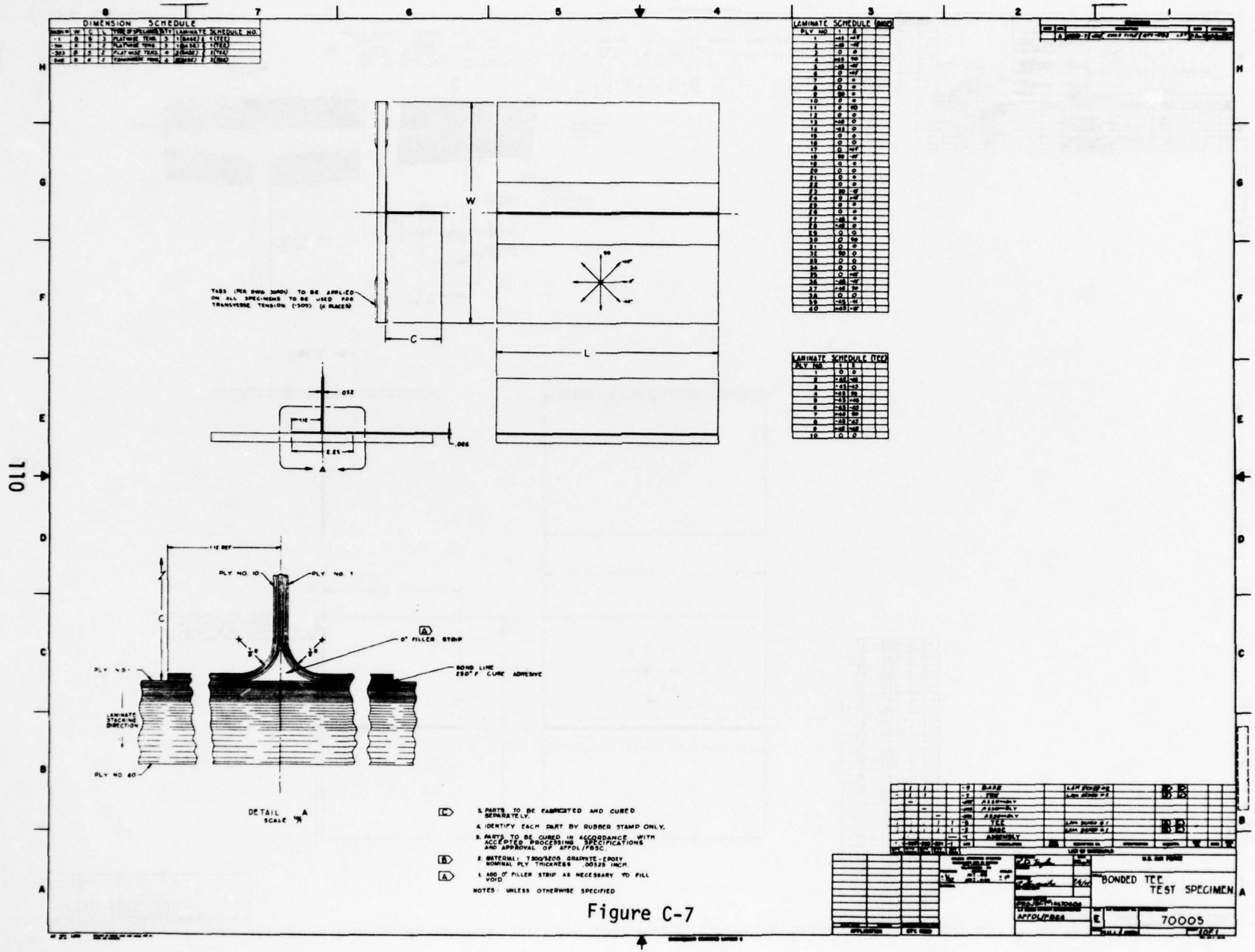
DIMENSION SCHEDULE
LAMINATE SCHEDULE (0/90)
LAMINATE SCHEDULE (TEE)
W
C
L
TABS (PER DWG 30000) TO BE APPLIED ON ALL SPECIMENS TO BE USED FOR TRANSVERSE TENSION (-509) (4 PLACES)
.052
.112
.086
A
PLY NO. 10
PLY NO. 1
PLY NO. 60
0° FILLER STRIP
BOND LINE 250°F CURE ADHESIVE
LAMINATE STACKING DIRECTION
DETAIL A
SCALE 4/1
5. PARTS TO BE FABRICATED AND CURED SEPARATELY.
4. IDENTIFY EACH PART BY RUBBER STAMP ONLY.
3. PARTS TO BE CURED IN ACCORDANCE WITH ACCEPTED PROCESSING SPECIFICATIONS AND APPROVAL OF AFFDL/FBSC.
2. MATERIAL: T300/5208 GRAPHITE-EPOXY NOMINAL PLY THICKNESS .00325 INCH.
1. ADD 0° FILLER STRIP AS NECESSARY TO FILL VOID.
NOTES: UNLESS OTHERWISE SPECIFIED
BONDED TEE TEST SPECIMEN
70005

Figure C-7

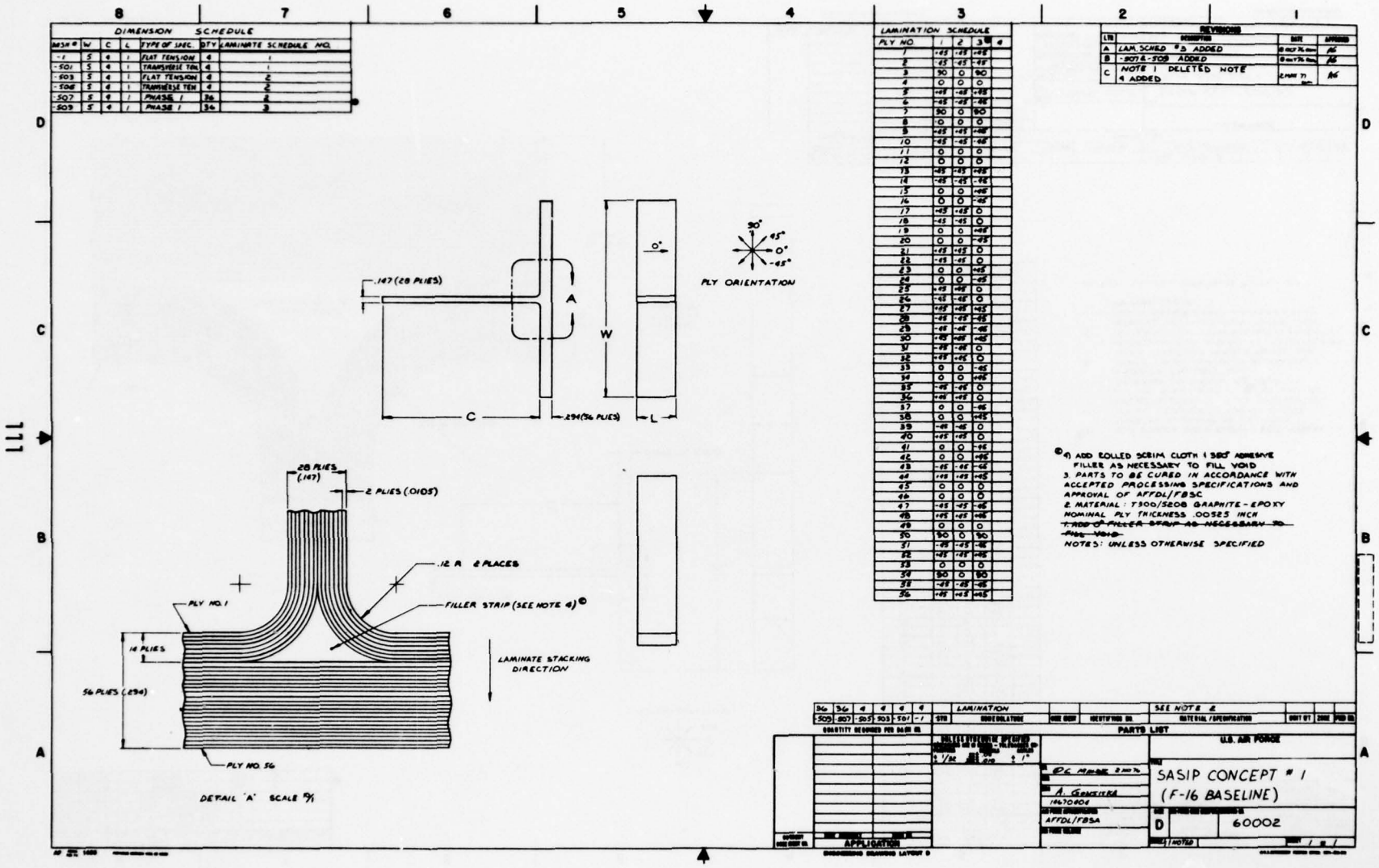
DIMENSION SCHEDULE
LAMINATION SCHEDULE
REVISIONS
.147 (28 PLIES)
.294 (56 PLIES)
PLY ORIENTATION
28 PLIES (.147)
2 PLIES (.0105)
.12 R 2 PLACES
PLY NO. 1
FILLER STRIP (SEE NOTE 4)©
16 PLIES
56 PLIES (.294)
PLY NO. 56
LAMINATE STACKING DIRECTION
DETAIL 'A' SCALE 5/1
NOTES: UNLESS OTHERWISE SPECIFIED
PARTS LIST
SASIP CONCEPT # 1
(F-16 BASELINE)
60002

Figure C-8

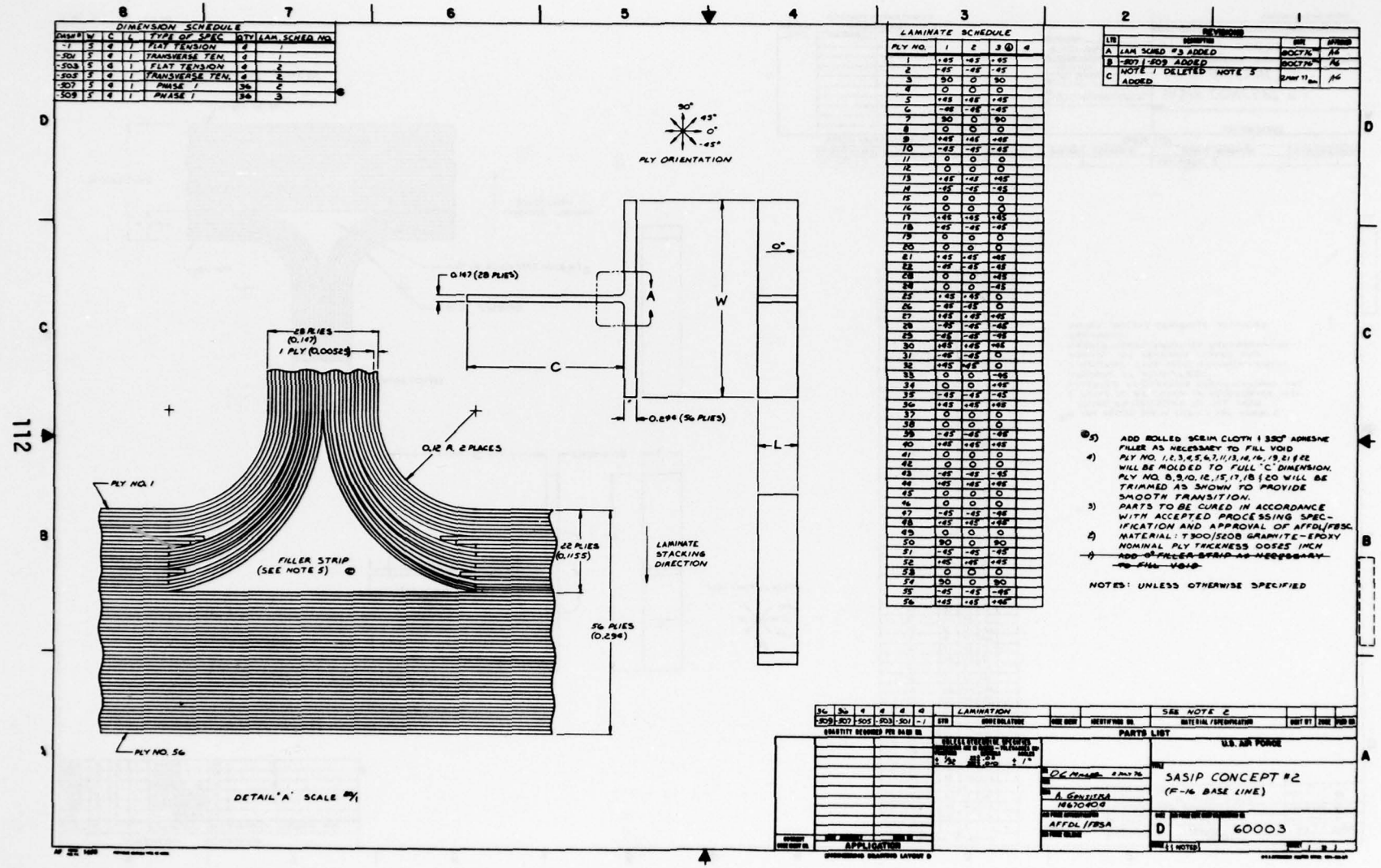
DIMENSION SCHEDULE
LAMINATE SCHEDULE
REVISIONS
PLY ORIENTATION
90°
45°
0°
-45°
0.147 (28 PLIES)
A
W
C
L
0.294 (56 PLIES)
28 PLIES (0.147)
1 PLY (0.0052)
0.12 R. 2 PLACES
PLY NO. 1
FILLER STRIP (SEE NOTE 5)
22 PLIES (0.1155)
56 PLIES (0.294)
LAMINATE STACKING DIRECTION
PLY NO. 56
DETAIL 'A' SCALE 8/1
NOTES: UNLESS OTHERWISE SPECIFIED
PARTS LIST
U.S. AIR FORCE
SASIP CONCEPT #2
(F-16 BASE LINE)
60003
APPLICATION
LAMINATION
AFFDL/FBSA

Figure C-9

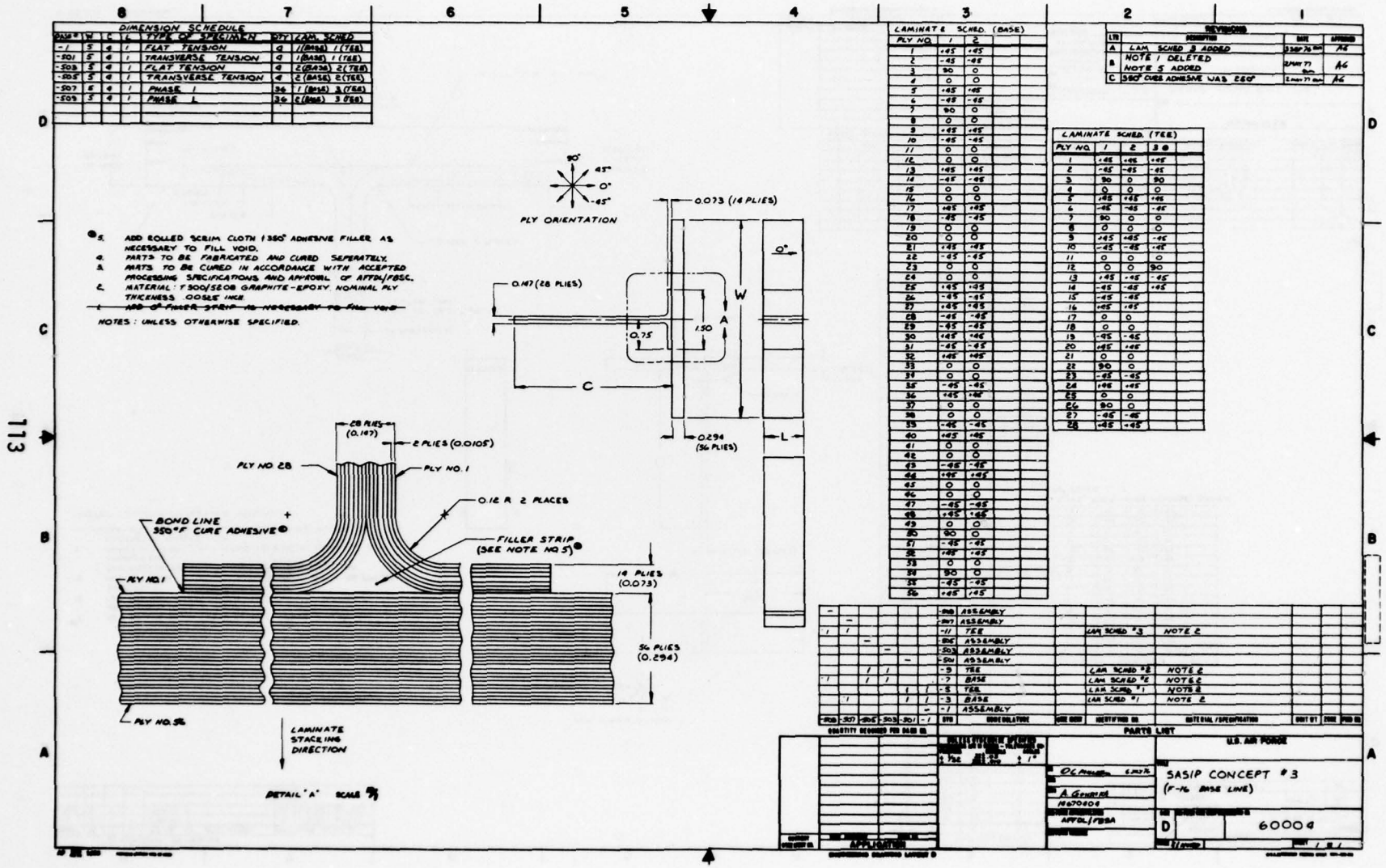
DIMENSION SCHEDULE
TYPE OF SPECIMEN
FLAT TENSION
TRANSVERSE TENSION
FLAT TENSION
TRANSVERSE TENSION
PHASE I
PHASE L
LAMINATE SCHED. (BASE)
LAMINATE SCHED. (TEE)
REVISIONS
A LAM. SCHED B ADDED
B NOTE 1 DELETED
NOTE 5 ADDED
C 350°F CURE ADHESIVE WAS 250°
PLY ORIENTATION
0.073 (14 PLIES)
0.147 (28 PLIES)
0.294 (56 PLIES)
0.75
1.50
W
A
C
L
NOTES: UNLESS OTHERWISE SPECIFIED.
4. ADD ROLLED SCRIM CLOTH 1 350° ADHESIVE FILLER AS NECESSARY TO FILL VOID.
3. PARTS TO BE FABRICATED AND CURED SEPERATELY.
2. PARTS TO BE CURED IN ACCORDANCE WITH ACCEPTED PROCESSING SPECIFICATIONS AND APPROVAL OF AFFDL/FBSC.
1. MATERIAL: T 300/5208 GRAPHITE-EPOXY. NOMINAL PLY THICKNESS .0026 INCH
ADD 0° FILLER STRIP AS NECESSARY TO FILL VOID
28 PLIES (0.147)
2 PLIES (0.0105)
PLY NO 28
PLY NO. 1
0.12 R 2 PLACES
BOND LINE 350°F CURE ADHESIVE
FILLER STRIP (SEE NOTE NO 5)
14 PLIES (0.073)
56 PLIES (0.294)
PLY NO. 56
LAMINATE STACKING DIRECTION
DETAIL "A" SCALE
PARTS LIST
U.S. AIR FORCE
SASIP CONCEPT #3
(F-16 BASE LINE)
60004

Figure C-10

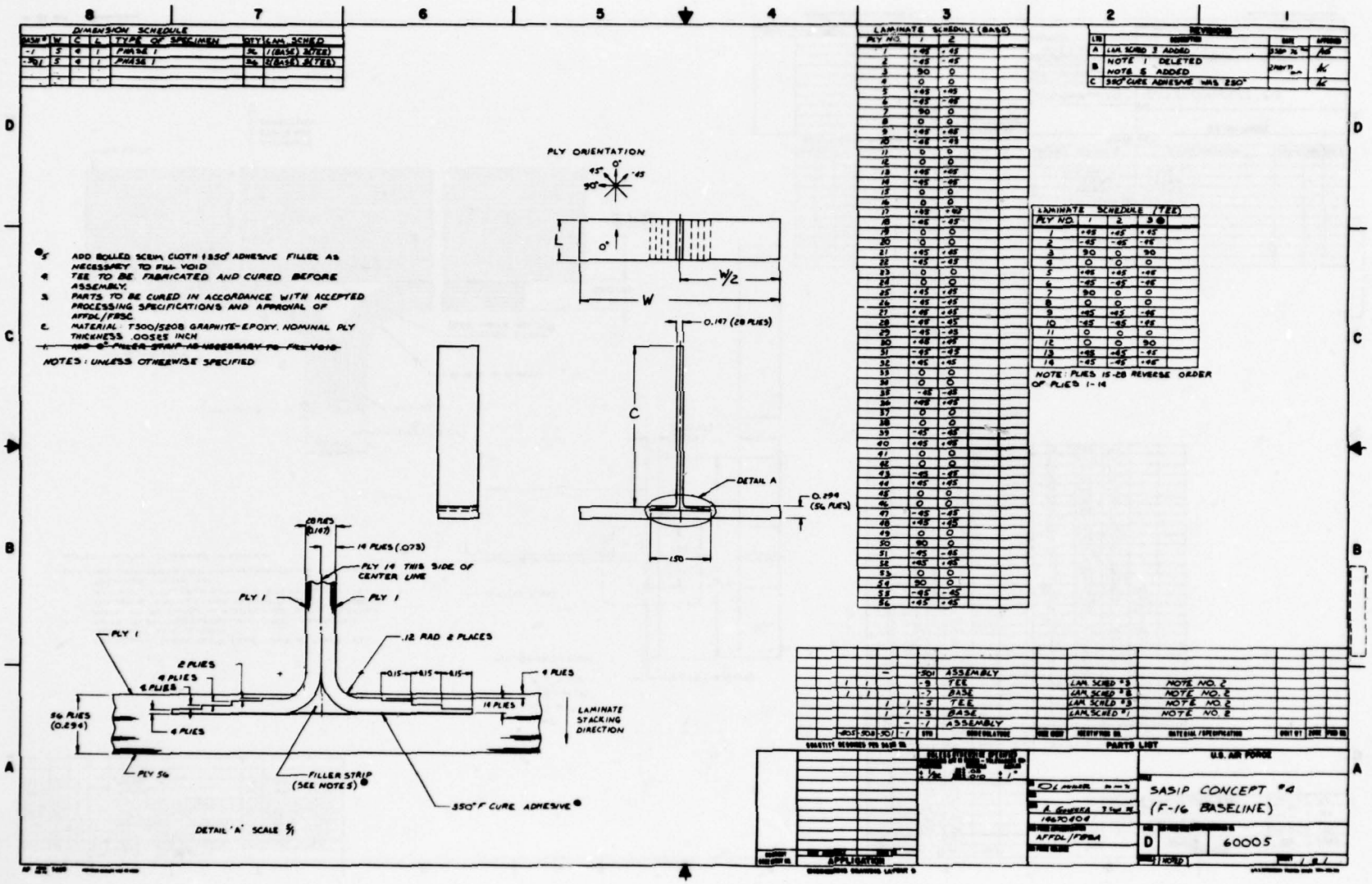
DIMENSION SCHEDULE
LAMINATE SCHEDULE (BASE)
LAMINATE SCHEDULE (TEE)
REVISIONS
PLY ORIENTATION
NOTES: UNLESS OTHERWISE SPECIFIED
NOTE: PLIES 15-28 REVERSE ORDER OF PLIES 1-14
DETAIL 'A' SCALE 5/1
PARTS LIST
SASIP CONCEPT #4
(F-16 BASELINE)
60005

Figure C-11

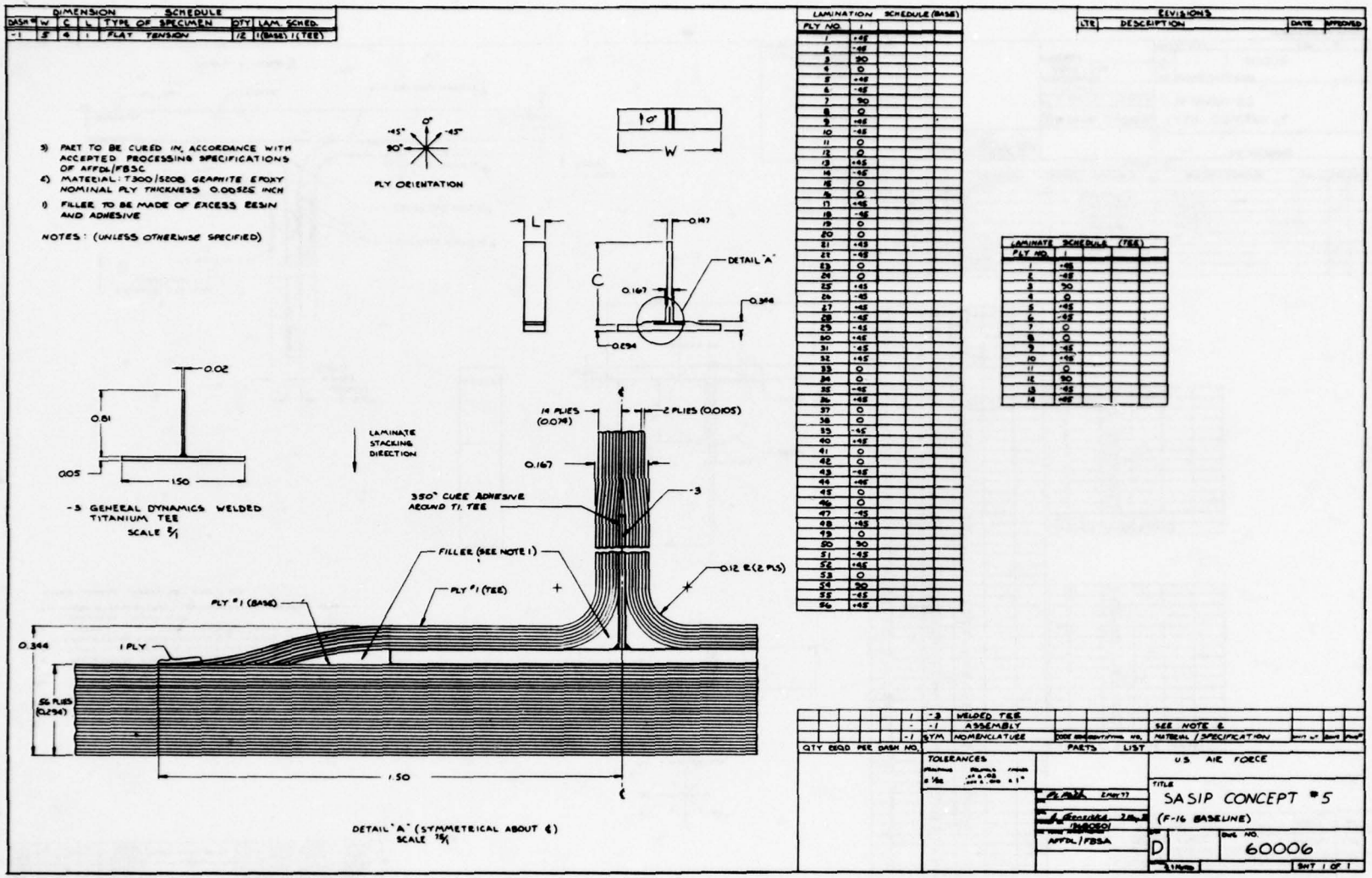
DIMENSION SCHEDULE
DASH # W C L TYPE OF SPECIMEN QTY LAM SCHED.
-1 5 4 1 FLAT TENSION 12 1(BASE) 1(TEE)
3) PART TO BE CURED IN ACCORDANCE WITH ACCEPTED PROCESSING SPECIFICATIONS OF AFFDL/FBSC
4) MATERIAL: T300/5208 GRAPHITE EPOXY NOMINAL PLY THICKNESS 0.0052S INCH
1) FILLER TO BE MADE OF EXCESS RESIN AND ADHESIVE
NOTES: (UNLESS OTHERWISE SPECIFIED)
PLY ORIENTATION
-45° 0° +45° 90°
10°
W
L
C
0.147
DETAIL "A"
0.167
0.344
0.294
0.02
0.81
0.005
1.50
-3 GENERAL DYNAMICS WELDED TITANIUM TEE
SCALE 2/1
LAMINATE STACKING DIRECTION
14 PLIES (0.074)
2 PLIES (0.0105)
0.167
350° CURE ADHESIVE AROUND TI. TEE
-3
FILLER (SEE NOTE 1)
0.12 R (2 PLS)
PLY #1 (BASE)
PLY #1 (TEE)
0.344
1 PLY
56 PLIES (0.294)
1.50
DETAIL "A" (SYMMETRICAL ABOUT ℄)
SCALE 15/1
LAMINATION SCHEDULE (BASE)
PLY NO. 1
1 +45
2 -45
3 90
4 0
5 +45
6 -45
7 90
8 0
9 +45
10 -45
11 0
12 0
13 +45
14 -45
15 0
16 0
17 +45
18 -45
19 0
20 0
21 +45
22 -45
23 0
24 0
25 +45
26 -45
27 +45
28 -45
29 -45
30 +45
31 -45
32 +45
33 0
34 0
35 -45
36 +45
37 0
38 0
39 -45
40 +45
41 0
42 0
43 -45
44 +45
45 0
46 0
47 -45
48 +45
49 0
50 90
51 -45
52 +45
53 0
54 90
55 -45
56 +45
LAMINATE SCHEDULE (TEE)
PLY NO. 1
1 -45
2 -45
3 90
4 0
5 +45
6 -45
7 0
8 0
9 -45
10 +45
11 0
12 90
13 -45
14 +45
REVISIONS
LTR DESCRIPTION DATE APPROVED
1 -3 WELDED TEE
- -1 ASSEMBLY
-1 SYM NOMENCLATURE
SEE NOTE 6
MATERIAL / SPECIFICATION
QTY REQD PER DASH NO.
PARTS LIST
TOLERANCES
US AIR FORCE
TITLE
SASIP CONCEPT #5
(F-16 BASELINE)
AFFDL/FBSA
SIZE D
DWG NO. 60006
SHT 1 OF 1

Figure C-12

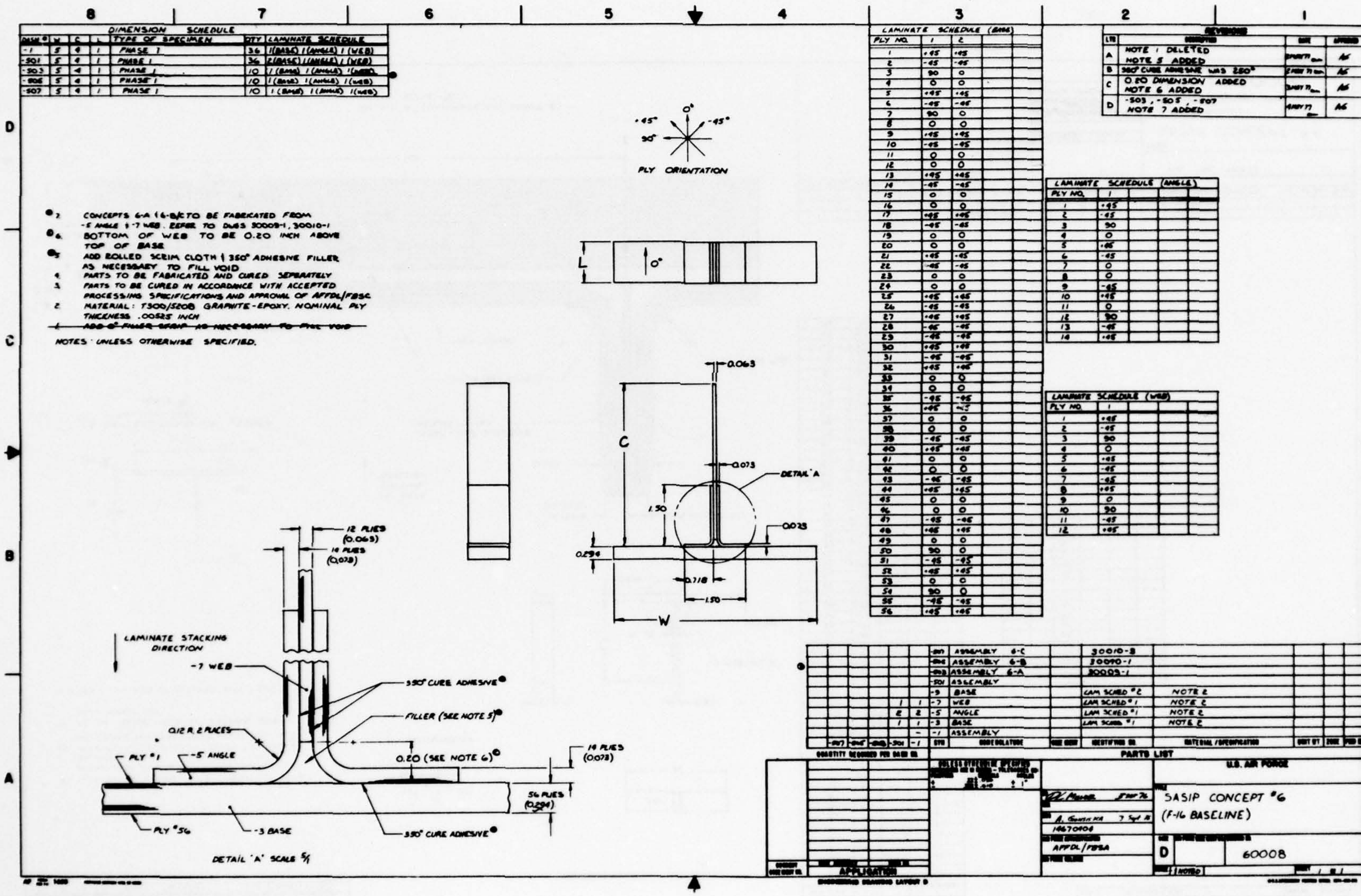

DIMENSION SCHEDULE

DASH #	W	C	L	TYPE OF SPECIMEN	QTY	LAMINATE SCHEDULE
-1	5	4	1	PHASE 1	36	1(BASE) 1(ANGLE) 1(WEB)
-501	5	4	1	PHASE 1	36	2(BASE) 1(ANGLE) 1(WEB)
-503	5	4	1	PHASE 1	10	1(BASE) 1(ANGLE) 1(WEB)
-505	5	4	1	PHASE 1	10	1(BASE) 1(ANGLE) 1(WEB)
-507	5	4	1	PHASE 1	10	1(BASE) 1(ANGLE) 1(WEB)

LAMINATE SCHEDULE (BASE)

PLY NO.	1	2		
1	+45	+45		
2	-45	-45		
3	90	0		
4	0	0		
5	+45	+45		
6	-45	-45		
7	90	0		
8	0	0		
9	+45	+45		
10	-45	-45		
11	0	0		
12	0	0		
13	+45	+45		
14	-45	-45		
15	0	0		
16	0	0		
17	+45	+45		
18	-45	-45		
19	0	0		
20	0	0		
21	+45	+45		
22	-45	-45		
23	0	0		
24	0	0		
25	+45	+45		
26	-45	-45		
27	+45	+45		
28	-45	-45		
29	-45	-45		
30	+45	+45		
31	-45	-45		
32	+45	+45		
33	0	0		
34	0	0		
35	-45	-45		
36	+45	[illegible]		
37	0	0		
38	0	0		
39	-45	-45		
40	+45	+45		
41	0	0		
42	0	0		
43	-45	-45		
44	+45	+45		
45	0	0		
46	0	0		
47	-45	-45		
48	+45	+45		
49	0	0		
50	90	0		
51	-45	-45		
52	+45	+45		
53	0	0		
54	90	0		
55	-45	-45		
56	+45	+45		

LAMINATE SCHEDULE (ANGLE)

PLY NO.	1			
1	+45			
2	-45			
3	90			
4	0			
5	+45			
6	-45			
7	0			
8	0			
9	-45			
10	+45			
11	0			
12	90			
13	-45			
14	+45			

LAMINATE SCHEDULE (WEB)

PLY NO.	1			
1	+45			
2	-45			
3	90			
4	0			
5	+45			
6	-45			
7	-45			
8	+45			
9	0			
10	90			
11	-45			
12	+45			

PARTS LIST

-507	-505	-503	-501	-1	SYM	NOMENCLATURE	IDENTIFYING NO.	MATERIAL / SPECIFICATION
					-507	ASSEMBLY 6-C	30010-3	
					-505	ASSEMBLY 6-B	30090-1	
					-503	ASSEMBLY 6-A	30009-1	
					-501	ASSEMBLY		
					-9	BASE	LAM SCHED #2	NOTE 2
			1	1	-7	WEB	LAM SCHED #1	NOTE 2
			2	2	-5	ANGLE	LAM SCHED #1	NOTE 2
			1	1	-3	BASE	LAM SCHED #1	NOTE 2
				–	-1	ASSEMBLY		

Figure C-13

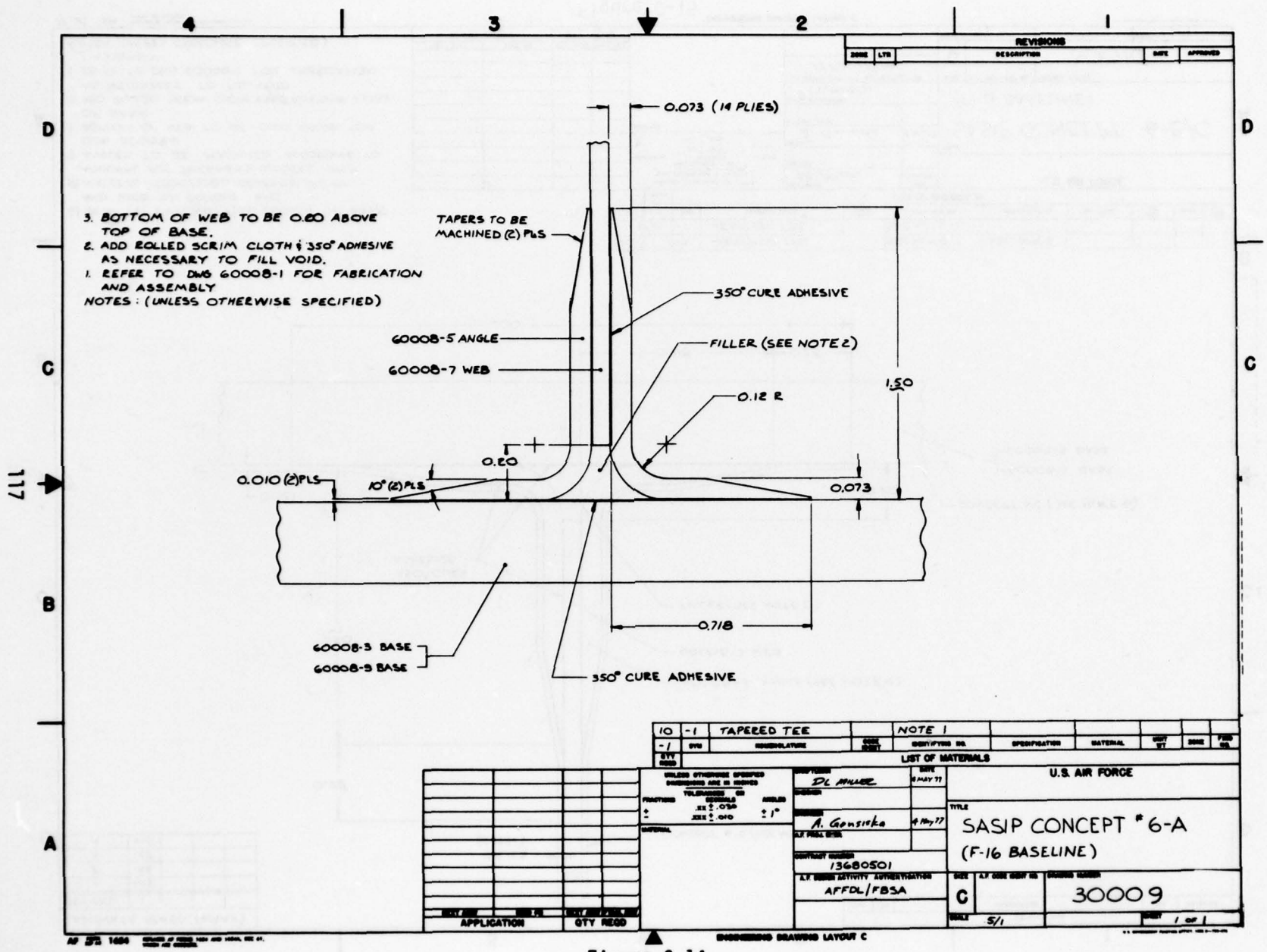
4
3
2
1
D
C
B
A
117
REVISIONS
ZONE
LTR
DESCRIPTION
DATE
APPROVED
0.073 (14 PLIES)
3. BOTTOM OF WEB TO BE 0.60 ABOVE TOP OF BASE.
2. ADD ROLLED SCRIM CLOTH & 350° ADHESIVE AS NECESSARY TO FILL VOID.
1. REFER TO DWG 60008-1 FOR FABRICATION AND ASSEMBLY
NOTES: (UNLESS OTHERWISE SPECIFIED)
TAPERS TO BE MACHINED (2) PLS
350° CURE ADHESIVE
60008-5 ANGLE
FILLER (SEE NOTE 2)
60008-7 WEB
1.50
0.12 R
0.60
0.010 (2) PLS
10° (2) PLS
0.073
0.718
60008-3 BASE
60008-9 BASE
350° CURE ADHESIVE
10 -1 TAPERED TEE NOTE 1
-1 QTY REQD NOMENCLATURE CODE IDENT IDENTIFYING NO. SPECIFICATION MATERIAL UNIT WT SIZE FSCM NO.
LIST OF MATERIALS
APPLICATION
QTY REQD
UNLESS OTHERWISE SPECIFIED DIMENSIONS ARE IN INCHES
TOLERANCES ON DECIMALS ANGLES
FRACTIONS ± XX ± .030 ± XXX ± .010 ± 1°
MATERIAL
DRAWN DL MAHLER 6 MAY 77
ENGINEER A. Gonsiska 6 May 77
A.F. PROJ. OFFICE
CONTRACT NUMBER 13680501
A.F. ISSUING ACTIVITY AUTHENTICATION AFFDL/FBSA
U.S. AIR FORCE
TITLE
SASIP CONCEPT * 6-A
(F-16 BASELINE)
SIZE C
A.F. CODE IDENT NO.
DRAWING NUMBER 30009
SCALE 5/1
SHEET 1 OF 1
ENGINEERING DRAWING LAYOUT C

Figure C-14

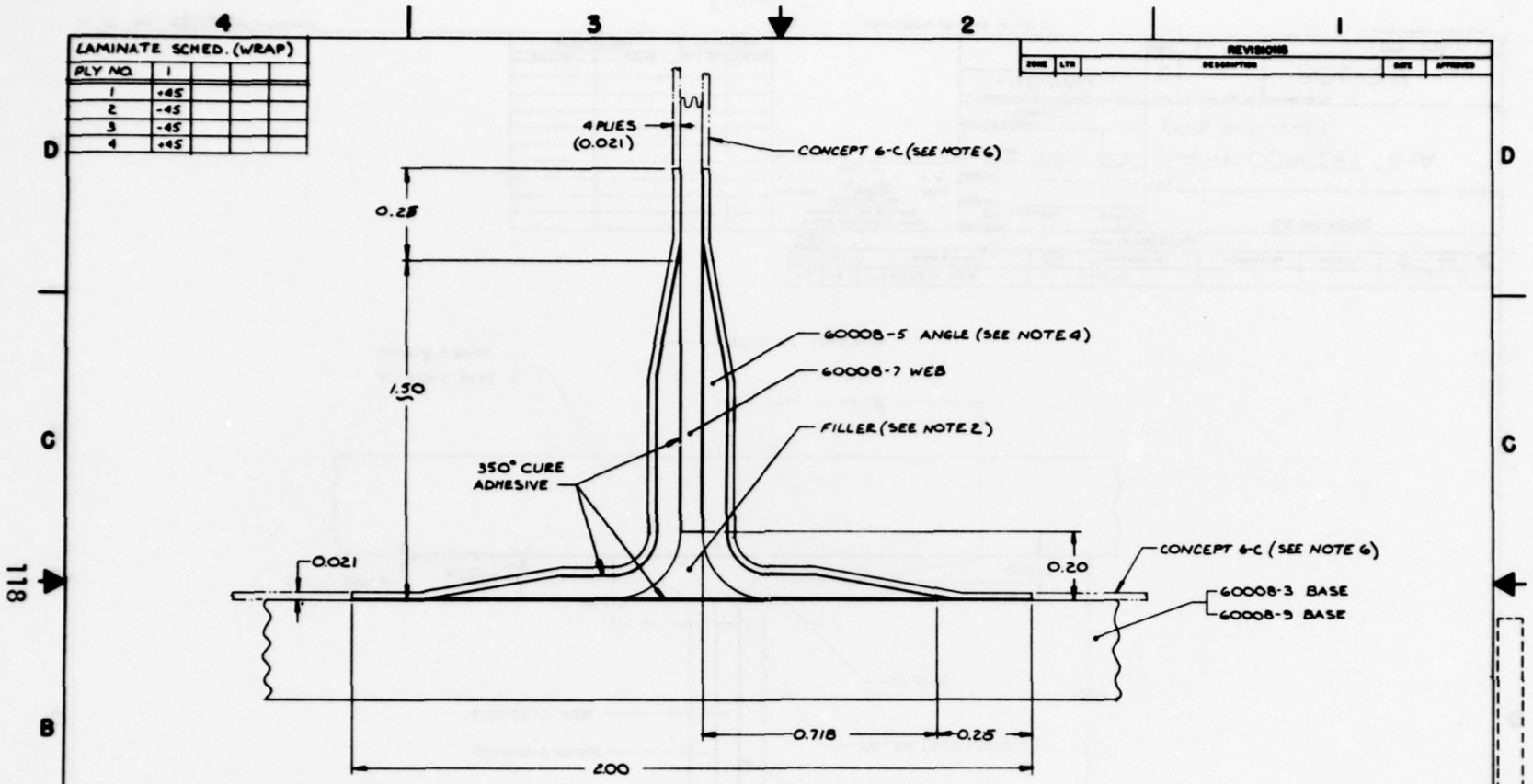

QTY REQD		DASH NO.	NOMENCLATURE	CAGE SHEET	IDENTIFYING NO.	SPECIFICATION	MATERIAL	UNIT WT	ZONE	FIND NO.
10		-3	WRAPPED TEE		SEE NOTE 1	SEE NOTE 6				
	10	-1	WRAPPED TEE		SEE NOTE 1					
-3	-1	SYM								

LIST OF MATERIALS

6) WRAP TO EXTEND FULL LENGTH OF BASE AND WEB ON CONCEPT 6-C
5) MATERIAL: T300/5208 GRAPHITE-EPOXY NOMINAL PLY THICKNESS 0.0052S INCH
4) ANGLES TO BE MACHINED ACCORDING TO DWG 30009-1
3) BOTTOM OF WEB TO BE 0.20 ABOVE TOP OF BASE
2) ADD ROLLED SCRIM CLOTH #350° ADHESIVE FILLER AS NECESSARY TO FILL VOID
1) REFER TO DWG 60008-1 FOR FABRICATION & ASSEMBLY
NOTES: (UNLESS OTHERWISE SPECIFIED)

APPLICATION	QTY REQD

UNLESS OTHERWISE SPECIFIED DIMENSIONS ARE IN INCHES
TOLERANCES ON DECIMALS: .XX ± .030, .XXX ± .010; FRACTIONS ± ; ANGLES ± 1°
MATERIAL

DRAWN: DL Miller 4 May 77
DESIGNED: A. Gonsiska 4 May 77
A.F. PROJ. ENGR.
CONTRACT NUMBER: 13680501
A.F. ISSUING ACTIVITY AUTHENTICATION: AFFDL/FBSA

U.S. AIR FORCE

TITLE: SASIP CONCEPT 6-B/C (F-16 BASELINE)

SIZE: C | A.F. CAGE SHEET NO. | DRAWING NUMBER: 30010
SCALE: 3/1 | SHEET 1 of 1

AF FORM 1684 — ENGINEERING DRAWING LAYOUT C

Figure C-15

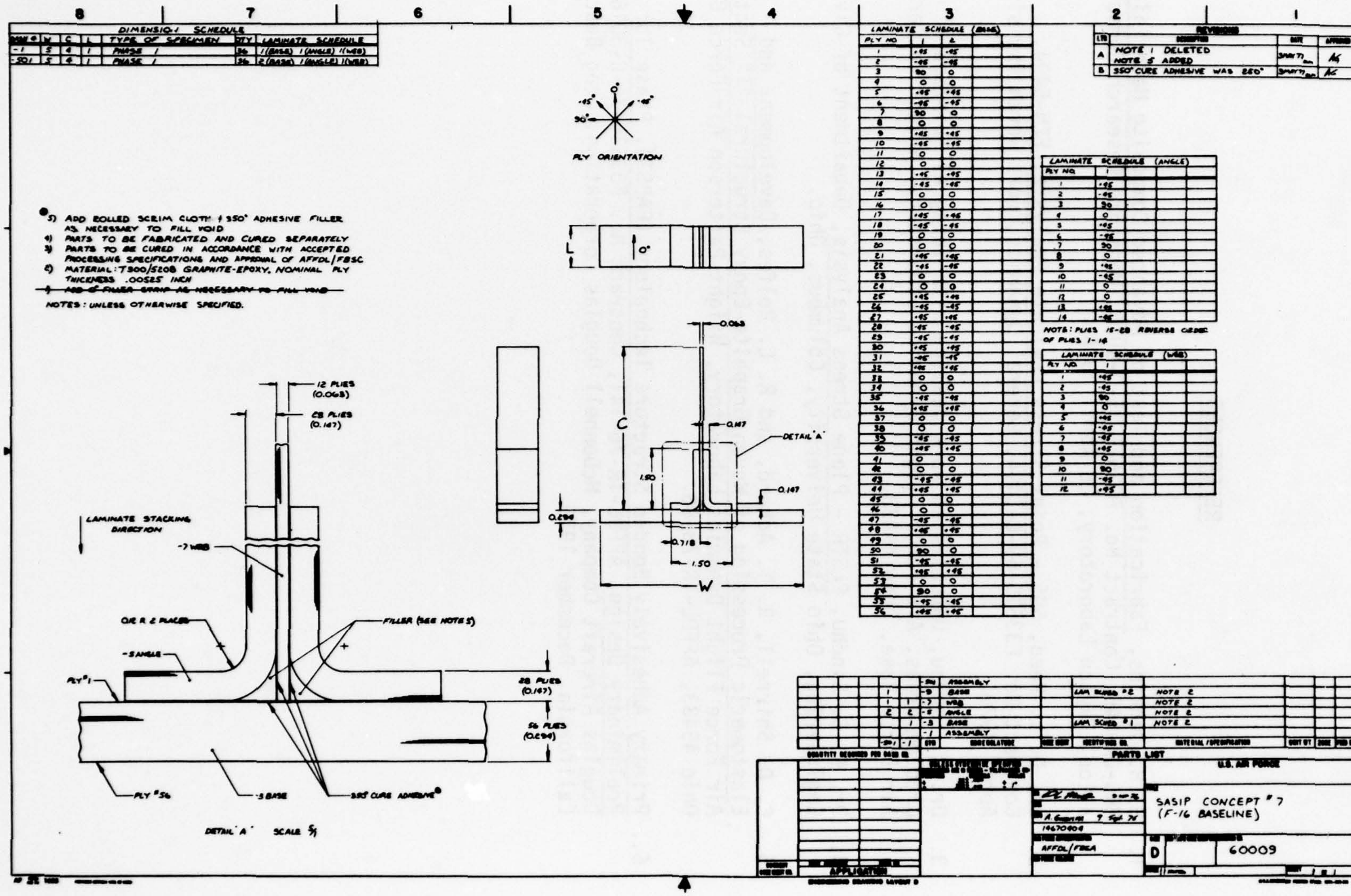

DIMENSION SCHEDULE
LAMINATE SCHEDULE (BASE)
LAMINATE SCHEDULE (ANGLE)
NOTE: PLIES 15-28 REVERSE ORDER OF PLIES 1-14
LAMINATE SCHEDULE (WEB)
REVISIONS
A NOTE 1 DELETED NOTE 5 ADDED
B 350° CURE ADHESIVE WAS 250°
PLY ORIENTATION
5) ADD ROLLED SCRIM CLOTH + 350° ADHESIVE FILLER AS NECESSARY TO FILL VOID
4) PARTS TO BE FABRICATED AND CURED SEPARATELY
3) PARTS TO BE CURED IN ACCORDANCE WITH ACCEPTED PROCESSING SPECIFICATIONS AND APPROVAL OF AFFDL/FBSC
2) MATERIAL: T300/5208 GRAPHITE-EPOXY, NOMINAL PLY THICKNESS .00525 INCH
NOTES: UNLESS OTHERWISE SPECIFIED.
LAMINATE STACKING DIRECTION
12 PLIES (0.063)
28 PLIES (0.147)
56 PLIES (0.294)
-7 WEB
-5 ANGLE
-3 BASE
FILLER (SEE NOTE 5)
350° CURE ADHESIVE
PLY #1
PLY #56
DETAIL 'A'
SCALE 5/1
PARTS LIST
U.S. AIR FORCE
SASIP CONCEPT #7 (F-16 BASELINE)
60009
APPLICATION

Figure C-16

REFERENCES

1. G. H. Jenkins, Fabrication and Test of Advanced Composite Materials, MRC-DA-545, Contract No. F33615-75-D-0018, Monsanto Research Corporation, Dayton Laboratory, 28 April 1976.

2. Dr. D. L. Reed, SQ5 - Point Stress Laminate Analysis, FZM-5494, Contract No. F33615-69-C-1494, General Dynamics, Fort Worth Division, April 1970.

3. Dr. R. Sandhu, Unpublished work dealing with Integral Skin/Spar problem areas, Air Force Flight Dynamics Laboratory, Wright-Patterson Air Force Base, Ohio 45433.

4. Dr. R. S. Sandhu, PLSTR - Plane Stress Analysis, Department of Civil Engineering, Ohio State University, Columbus, Ohio.

5. C. D. Shirrell, R. T. Achard, and R. L. Rolfes, Development and Elastomeric Processing of Woven Graphite-Epoxy Structural "T" Sections, Air Force Flight Dynamics Laboratory, Wright-Patterson Air Force Base, Ohio 45433, AFFDL-TR-78-88.

6. Primary Adhesively Bonded Structure Technology (PABST), Phase 1b: Preliminary Design, AFFDL-TR-76-141, Contract No. F33615-75-C-3016, Douglas Aircraft Company, McDonnell Douglas Corporation, Long Beach, California, December 1976.

*U.S.Government Printing Office: 1979 — 657-002/663